2015-04-29

Role of Protein Kinase Map4k4 in Energy Metabolism: A Dissertation

Laura V. Danai
University of Massachusetts Medical School

ROLE OF PROTEIN KINASE MAP4K4 IN ENERGY METABOLISM

A Dissertation Presented

By

LAURA V. DANAI

Submitted to the Faculty of the

University of Massachusetts Graduate School of Biomedical Sciences, Worcester

in partial fulfillment of the requirements for the degree of

DOCTOR OF PHILOSOPHY

APRIL 29, 2015

INTERDISCIPLINARY GRADUATE PROGRAM

ROLE OF PROTEIN KINASE MAP4K4 IN ENERGY METABOLISM

A Dissertation Presented By

Laura V. Danai

The signatures of the Dissertation Defense Committee signify

completion and approval as to style and content of the Dissertation

_____

Michael P. Czech, Ph.D., Thesis Advisor

_____

Christopher B. Newgard, Ph.D., Member of Committee

_____

David A. Guertin, Ph.D., Member of Committee

_____

Amy Walker, Ph.D., Member of Committee

_____

Marcus P. Cooper, MD., Member of Committee

The signature of the Chair of the Committee signifies that the written dissertation meets the requirements of the Dissertation Committee

_____

Heidi A. Tissenbaum, Ph.D., Chair of Committee

The signature of the Dean of the Graduate School of Biomedical Sciences signifies that the student has met all graduation requirements of the school.

_____

Anthony Carruthers, Ph.D.,
Dean of the Graduate School of Biomedical Sciences

Interdisciplinary Graduate Program
April 29, 2015

Acknowledgements

I'm very fortunate to be surrounded by family, friends, and colleagues that are supportive and encouraging and from whom I constantly learn so much.

Thanks to Mike Czech, my graduate mentor, for giving me the opportunity to join his lab, for giving me intellectual freedom that promotes independent thinking, and for always having his door open, ready to discuss and encourage.

Thanks to all past and present Czech lab members for their support, ideas, and discussions. Special thanks to my two lab mentors, Adilson Guilherme and Joseph V. Virbasius. They have been extremely patient, taught me innumerable scientific lessons, and challenged me to be a better scientist. Thanks to Rachel Roth-Flach for her constant willingness to discuss and make suggestions and for working with me on several projects. Thanks to Marina DiStefano, Ozlem Senol-Cosar, and Joseph Virbasius for making lab so fun.

Thanks to my thesis advisory committee for making time to meet with me, for their experimental suggestions, and for their career advice. Thanks to Heidi, my chair, for challenging me when necessary and for her guidance and advice. Thanks to Amy for all the lipid synthesis/Srebp-1 discussions and openness to talk anywhere. Thanks to Dave for giving me the opportunity to come to his lab meetings and present, for all the helpful suggestions, and for the advice on future endeavors.

Lastly, thanks to my family. Thanks to my parents for their unconditional support and love and my husband for everything.

Abstract

Systemic glucose regulation is essential for human survival as low or chronically high glucose levels can be detrimental to the health of an individual. Glucose levels are highly regulated via inter-organ communication networks that alter metabolic function to maintain euglycemia. For example, when nutrient levels are low, pancreatic α-cells secrete glucagon, which signals to the liver to promote glycogen breakdown and glucose production. In times of excess nutrient intake, pancreatic β-cells release insulin. Insulin signals to the liver to suppress hepatic glucose production, and signals to the adipose tissue and the skeletal muscle to take up excess glucose via insulin-regulated glucose transporters. Defects in this inter-organ communication network including insulin resistance can result in glucose deregulation and ultimately the onset of type-2 diabetes (T2D).

To identify novel regulators of insulin-mediated glucose transport, our laboratory performed an siRNA-mediated gene-silencing screen in cultured adipocytes and measured insulin-mediated glucose transport. Gene silencing of Mitogen-activated protein kinase kinase kinase kinase 4 (Map4k4), a Sterile-20-related serine/threonine protein kinase, enhanced insulin-stimulated glucose transport, suggesting Map4k4 inhibits insulin action and glucose transport. Thus, for the first part of my thesis, I explore the role of Map4k4 in cultured adipose cells and show that Map4k4 also represses lipid synthesis independent of its effects on glucose transport. Map4k4 inhibits lipid synthesis in a Mechanistic target of rapamycin complex 1 (mTORC1)- and Sterol regulatory

element-binding transcription factor 1 (Srebp-1)-dependent mechanism and not via a c-Jun NH_2-terminal kinase (Jnk)-dependent mechanism. For the second part of my thesis, I explore the metabolic function of Map4k4 *in vivo.* Using mice with loxP sites flanking the Map4k4 allele and a ubiquitously expressed tamoxifen-activated Cre, we inducibly ablated Map4k4 expression in adult mice and found significant improvements in metabolic health indicated by improved fasting glucose and whole-body insulin action. To assess the role of Map4k4 in specific metabolic tissues responsible for systemic glucose regulation, we employed tissue-specific knockout mice to deplete Map4k4 in adipose tissue using an adiponectin-cre transgene, liver using an albumin-cre transgene, and skeletal muscle using a Myf5-cre transgene. Ablation of Map4k4 expression in adipose tissue or liver had no impact on whole body glucose homeostasis or insulin resistance. However, we surprisingly found that Map4k4 depletion in Myf5-positive tissues, which include skeletal muscles, largely recapitulates the metabolic phenotypes observed in systemic Map4k4 knockout mice, restoring obesity-induced glucose intolerance and insulin resistance. Furthermore these metabolic changes were associated with enhanced insulin signaling to Akt in the visceral adipose tissue, a tissue that is nearly devoid of Myf5-positive cells and does not display changes in Map4k4 expression. Thus, these results indicate that Map4k4 in Myf5-positive cells, most likely skeletal muscle cells, inhibits whole-body insulin action and these effects may be mediated via an indirect effect on the visceral adipose tissue. The results presented here provide evidence for Map4k4 as a potential therapeutic target for the treatment of insulin resistance and T2D.

Table of Contents

List of Figures and Tables

List of Common Abbreviations

Type II diabetes – T2D

Thiazolidinediones –TZDs

Triglycerides – TG

Fatty acid – FA

Body mass index – BMI

Peroxisome Proliferator-Activated Receptor – Pparγ

Insulin receptor – InsR

Insulin receptor substrate – Irs

Phosphatidylinositol-4,5-biphosphate 3-kinase – PI3K

Protein kinase b – Akt

Solute carrier family 2 (facilitated glucose transporter) member 4 – Glut4

Mechanistic target of rapamycin complex 1 – mTORC1

Ribosome protein S6 kinase – S6k

Eukaryotic translation initiation factor 4E binding protein – 4E-bp

c-Jun NH_2-terminal kinase – Jnk

Sterol regulatory element binding transcription factor 1 – Srebp-1

Glycogen synthase – Gs

Small interfering RNA – siRNA

Mitogen-activated protein kinase kinase kinase kinase – Map4k4

Tumor necrosis factor alpha – Tnf-α

List of Third Party Copyrighted Material

Chapter I, Figure 1.5 (A) modified from: Tang X., Guilherme A., Chakladar A., Powelka A.M., Konda S., Virbasius J.V., Nicoloro S.M., Straubhaar J., and Czech M.P. (2006). An RNA interference-based screen identifies MAP4K4/NIK as a negative regulator of PPARgamma, adipogenesis, and insulin-responsive hexose transport. Proc Natl Acad Sci 103(7):2087-92.

Chapter I, Figure 1.5 (B) modified from: Puri V., Virbasius J.V., Guilherme A., and Czech M.P. (2008). RNAi screens reveal novel metabolic regulators: RIP140, MAP4K4, and the lipid droplet associated fat specific protein (FSP) 27. Acta Physiol (Oxf). 192(1):103-15.

CHAPTER I: INTRODUCTION

Whole-body glucose homeostasis

Controlled glucose homeostasis is essential for the survival of mammals (1). Hyperglycemia (elevated blood glucose) can result in ketoacidosis, neuropathy, nephropathy, and eye complications that can lead to blindness (1, 2). Conversely, because neurons rely primarily on glucose as a fuel source, hypoglycemia (low blood glucose levels) can result in compromised brain function, coma, and death (3). Due to the dire consequences that occur if blood glucose is deregulated, blood glucose levels are maintained within a narrow range (approximately 5mM) by an elaborate physiological system that involves multi-organ communication and regulation in response to nutrient conditions and hormonal signals (2, 4).

Appropriate glucose homeostasis is maintained primarily by the actions of glucagon and insulin, hormones that are released by the pancreas in response to nutritional status. These two hormones act on many organs including the liver, the adipose tissue, and the skeletal muscle to change cellular functions that aid in glucose control (2). In fasting conditions, circulating glucose levels decrease, stimulating pancreatic α-cells to release glucagon (5). Glucagon signals to the liver to produce glucose via breakdown of glycogen (glycogenolysis) and synthesis of glucose from pyruvate and other substrates (gluconeogenesis), thus restoring glucose levels (5). In the post-prandial state, a glucose

surge that results from digestion of dietary sources including carbohydrates, promotes pancreatic β-cells to secrete insulin. Insulin promotes glucose uptake in the muscle and adipose tissue while suppressing hepatic glucose production (2). The net effect of insulin action on these three organs helps return blood glucose to basal levels. Thus, in healthy individuals, blood glucose concentrations are tightly regulated and maintained within a narrow range (approximately 5mM) despite variations in glucose utilization or availability of exogenous glucose. Failure to control circulating glucose levels results in diabetes, defined as displaying fasting glucose levels higher than 7mM and Hemoglobin A1C values higher than 6.5% (6). Type I diabetes is characterized by immune cells attacking and destroying β-cells, resulting in loss of insulin-secreting cells. Type II diabetes (T2D), on the other hand, is more common and a frequent complication of obesity that also results in gradual loss of insulin-secreting cells (7).

Chronic over-nutrition and a sedentary lifestyle promote adipose tissue expansion, which results in obesity. Adipose tissue expansion promotes inflammation that compromises adipose tissue function, resulting in insulin resistance (8-10). Insulin resistance is manifested as reduced insulin-mediated glucose disposal and unrepressed hepatic glucose production, resulting in deregulation of blood glucose levels and hyperglycemia (11). To maintain glucose homeostasis, β-cells compensate by secreting more insulin (12, 13). Chronic obesity-induced insulin resistance can ultimately lead to β-cell failure (β-cell exhaustion and death), resulting in the onset of T2D (12, 14). Therefore, T2D is a condition with defects in both insulin secretion and insulin action.

T2D is predicted to affect approximately 9% of the population worldwide, and the number of afflicted individuals is projected to increase as the incidence for T2D-predisposing conditions including obesity continue to rise (7). It is of paramount importance to therapeutically manage T2D, as this disease is commonly associated with other more costly and deadly co-morbidities including cancer, cardiovascular disease, retinopathy, and nephropathy (7). To that extent, to improve glycemic control, current therapies aim to increase insulin secretion or suppress hepatic glucose production; however, most patients inevitably require further intervention (15). Thiazolidinediones (TZDs) are potent insulin-sensitizing drugs that target Peroxisome Proliferator Activated Receptor (Pparγ) and address the underlying pathophysiology in T2D; however, these drugs are in limited use due to contra-indications, including cardiovascular side effects (16, 17). Thus, discovering novel proteins that can be targeted with drug therapies to improve peripheral insulin sensitivity would prove useful in the treatment for T2D.

Insulin signaling pathway

Insulin is an anabolic hormone that activates metabolic pathways to promote cellular growth. A post-prandial glucose surge induces β-cell insulin secretion into the bloodstream to reach peripheral target tissues where it binds to the α-subunits of the insulin receptor (InsR) (18). Binding of insulin to the InsR causes a conformational change that brings the β-InsR subunits in proximity, promoting autophosphorylation and

further increasing receptor kinase activity (Figure 1.1) (19, 20). The InsR is a unique receptor-tyrosine kinase, as it does not directly bind to downstream effectors; instead, InsR activation leads to rapid tyrosine phosphorylation and recruitment of scaffold proteins known as Insulin receptor substrate (Irs) proteins (21). Phosphorylated tyrosine residues on these Irs proteins, in turn, promote the recruitment and activation of Phosphatidylinositol-4,5-biphosphate 3-kinase (PI3K) (18). Enhanced PI3K activity results in the transient increase of phosphatidylinositol (3,4,5)-triphosphate (PIP_3) in the plasma membrane (22). PIP_3 binds to the pleckstrin homology (PH) domain of various proteins, including Protein kinase b (Pkb/Akt) and 3-Phosphoinositide-dependent protein kinase-1 (Pdk1), effectively recruiting these proteins to the plasma membrane (23). At the plasma membrane, Pdk1 and Mechanistic target of rapamycin complex 2 (mTORC2) phosphorylate Akt, resulting in maximal Akt activation (24). Insulin via Akt activation will then initiate signaling cascades that promote anabolic processes including cellular growth, glucose uptake, lipid metabolism, glycogenesis, and cell survival.

Figure 1.1 Canonical insulin signaling pathway.

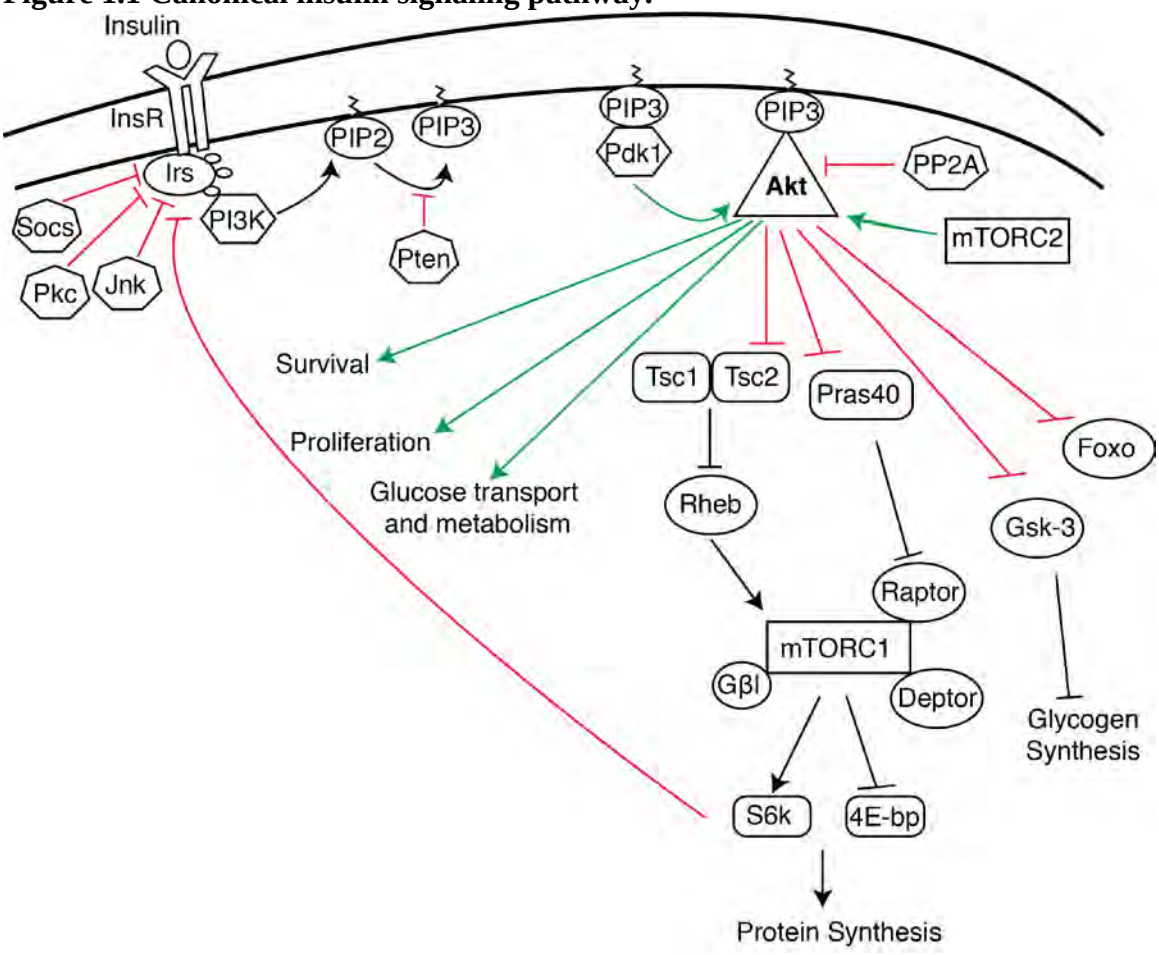

Figure 1.1 Canonical insulin signaling pathway. Binding of insulin to the insulin receptor (InsR) promotes InsR autophosphorylation and recruitment of Insulin Receptor Substrate (Irs) proteins. Tyrosine phosphorylated Irs proteins further recruit and promote the activation of Phosphatidylinositol-4,5-biphosphate 3-kinase (PI3K). Activated PI3K elevates Phosphatidylinositol (3,4,5)-triphosphate (PIP_3) levels, recruiting Protein Kinase B (Akt) to the cell surface. At the cell surface, Akt is phosphorylated and activated by 3-Phosphoinositide-dependent protein kinase-1 (Pdk1) and Mechanistic Target of Rapamycin (mTORC2, also known as Pdk2). Activated Akt will then initiate a plethora of anabolic signaling pathways that protein synthesis, lipid synthesis, glucose transport and metabolism, glycogen synthesis, proliferation, and survival.

Insulin promotes glucose disposal via enhancement of the PI3K and Akt signaling pathway (25). Skeletal muscle and adipose tissue express Solute carrier family 2 (facilitated glucose transporter) member 4 (Slc2a4 or Glut4), an insulin-responsive glucose transporter (26). Under basal conditions, Glut4 is concentrated in specialized intracellular vesicles (27). Insulin stimulation promotes Glut4 vesicle translocation and fusion with the plasma membrane, increasing the concentration of Glut4 on the cell surface by 10-15 fold, effectively allowing glucose to enter the cell to be metabolized (27). Whole-body Glut4 heterozygous mice (-/+) display a decrease in Glut4 expression in adipose tissue and muscle, resulting in hyperglycemia and hyperinsulinemia (28). Therefore, the ability of insulin to regulate glucose transport in the adipose and muscle is a critical mechanism in maintaining whole-body glucose homeostasis.

Insulin signaling to Akt also activates Mechanistic target of rapamycin complex 1 (mTORC1), a protein kinase that promotes cellular growth and proliferation via modulation of protein and lipid synthesis (11, 29). To enhance mTORC1 activation, Akt phosphorylates and inhibits two negative regulators of mTORC1, Proline-Rich Akt substrate of 40 kDa (Pras40) and Tuberous sclerosis complex 2 (Tsc2) (29). Akt-induced phosphorylation of Pras40 prevents Pras40 from binding to mTORC1 and thus relieves mTORC1 inhibition (30-33). Similarly, Tsc2 forms a complex with Tsc1 that acts as a GTPase-activating protein (GAP) to suppress Ras homolog enriched in brain (Rheb), a small G-protein that promotes mTORC1 signaling (34, 35). Activated Akt phosphorylates Tsc2 on several residues, preventing formation of the Tsc1/Tsc2 complex, therefore

increasing GTP-bound Rheb and allowing for mTORC1 activation (36-38). mTORC1 promotes protein synthesis via direct phosphorylation of Ribosome protein S6 kinase (S6k) and Eukaryotic translation initiation factor 4E binding protein (4E-bp), resulting in activation of translation and ribosome biogenesis (39). mTORC1 phosphorylation of S6k promotes S6k kinase activity, leading to increased activation of downstream targets including Ribosomal protein S6, a component of the 40S ribosomal subunit, to promote translation (39, 40). 4E-bp is a cap-dependent translational repressor and mTORC1 phosphorylation inhibits its activity (41). 4E-bp binds Eukaryotic translation initiation factor-4E (eIF4E), which is a rate-limiting initiation factor of translation, thus 4E-bp phosphorylation promotes dissociation from eIF4E and allows cap-dependent translation to initiate (41). A role for mTORC1 in lipid synthesis has also been clearly established; however, the mechanisms of action require further studies (42). Overall, insulin signaling to Akt relays the fed nutritional status of the animal to promote activation of anabolic processes via Akt and mTORC1 activation.

Since the insulin signaling pathway promotes cellular growth, perturbations in this signaling pathway can lead to pathological conditions. Therefore, fine-tuning of the insulin-signaling pathway includes negative feedback mechanisms that are established to prevent chronic activation and uncontrolled growth (43, 44). Irs proteins can be phosphorylated at serine sites to prevent their association with the InsR and downstream effectors (45). Chronic serine phosphorylation of Irs proteins is therefore hypothesized to attenuate insulin signaling and promote insulin resistance (46). Protein kinase c (Pkc),

S6k1, and c-Jun NH_2-terminal kinase (Jnk) are among the kinases proposed to promote Irs serine phosphorylation including at amino acid 307 to negatively regulate insulin signaling; however, evidence *in vivo* is lacking (47). Mice with a knock-in mutation of Irs-1 serine 307 to alanine, for example, cannot be serine phosphorylated at this site and therefore are predicted to display enhanced insulin sensitivity (48). However, when challenged with high-fat feeding, these animals are unexpectedly more insulin resistant than controls, demonstrating that negative-feedback mechanisms in the insulin-signaling pathway are complex *in vivo (48)*. Other negative regulators of the insulin-signaling pathway have also been studied. Protein tyrosine phosphatases such as Protein tyrosine phosphatase 1B (Ptb1B) can also inhibit insulin signaling by dephosphorylating the InsR, effectively suppressing Irs recruitment function and insulin signaling (49). Suppressor of cytokine signaling proteins (Socs) can also inhibit insulin action via various mechanisms including competing with Irs proteins to bind InsR and targeting Irs proteins for proteosomal degradation, resulting in reduced in insulin signaling to Akt (50-52). Another major negative regulator of the insulin-signaling pathway is Phosphatase and tensin homolog (Pten), a lipid phosphatase that converts PIP_3 to Phosphatidylinositol 4,5-biphosphate (PIP_2), thereby preventing Akt translocation to the plasma membrane and its full activation by Pdk1 and mTORC2 (53, 54). Pten is often mutated in cancers, enhancing Akt activation (53, 54). Thus, insulin signaling to Akt initiates anabolic pathways that need to be highly regulated to prevent uncontrolled growth.

Perturbations in this control of insulin signaling are a feature of insulin resistance, which frequently develops as a complication of obesity. Chronic over-nutrition and a sedentary lifestyle promote AT expansion, which can lead to low-grade inflammation and impaired ability of the adipose tissue to store lipids, leading to ectopic lipid deposition (55, 56). Obesity-induced inflammation occurs in various tissues including adipose tissue, skeletal muscle, liver, and hypothalamus (57). Pro-inflammatory cytokines can activate Jnk signaling, thus promoting Irs serine phosphorylation and suppression of insulin signaling to Akt (58-60). Lipid deposition in skeletal muscle and liver can result in increased levels of toxic lipid metabolites including ceramides and diacylglycerol (61, 62). These lipid metabolites can also activate signaling pathways such as Pkc and Jnk, which promote Irs serine phosphorylation and disruption of the insulin-signaling pathway, thus contributing to insulin resistance (11, 61). Ceramides can also inhibit insulin signaling to Akt by increasing Protein phosphatase 2A (Pp2a) activity, a phosphatase that dephosphorylates Akt, as well as by enhancing Pkc activity, which phosphorylates Akt and prevents its translocation to the plasma membrane, effectively reducing insulin signaling to Akt (63). Therefore ectopic lipid deposition results in heightened levels of toxic lipid metabolites that inhibit insulin signaling to Akt and promotes systemic insulin resistance.

Inter-organ communication in the control of glucose homeostasis

Although adipose tissue dysfunction plays a significant role in obesity-associated insulin resistance, it has also become clear that control of whole body homeostasis in animals

involves complex interactions among peripheral tissues both in the flow of nutrients as well as endocrine signals. Nutrient and hormonal signaling can also affect the central nervous system (CNS), which can impact feeding behaviors and energy metabolism (64, 65); however, this will not be discussed in the present work. Instead I will focus on the metabolic and hormonal network involving the organs most relevant to this thesis: pancreas, adipose tissue, liver, and skeletal muscle.

Pancreas

The endocrine pancreas is responsible for the secretion of glucagon and insulin, two important hormones responsible for the maintenance of appropriate blood glucose levels. The Islets of Langerhans comprise approximately 1-2% of the entire pancreas; these clusters of cells are composed of β-cells (insulin-secreting) surrounded by α-cells (glucagon-secreting), δ- cell (somatostatin-secreting) and pancreatic peptide-cells (PP-cells) (66). These islets are responsible for sending hormonal signals that orchestrate systemic glucose metabolism.

In fasting conditions, α-cells secrete glucagon to stimulate catabolic pathways that restore glucose levels. α-cells are equipped with K_{ATP} channels that are active under low glucose levels, opening voltage-dependent T- and N-type Ca^{2+} channels, triggering action potentials, Ca^{2+} influx, and glucagon secretion via exocytosis (67). Due to the high vascularization of the pancreas, glucagon readily diffuses into the circulation, where it stimulates the liver to enhance glucose production (68). Genetic mouse models with deficiencies in glucagon secretion display hypoglycemia, as the liver lacks the activation

signals necessary to promote hepatic glucose production (5). Prohormone Convertase 2 (PC2) post-translationally cleaves preproglucagon, resulting in the maturation of preproglucagon hormone (69, 70). PC2-*null* mice therefore display hypoglucagonemia and an inability to promote hepatic glucose production, resulting in hypoglycemia (71). Hypoglycemic conditions are restored following administration of exogenous glucagon, demonstrating that glucagon secretion is essential in maintaining euglycemic conditions (72).

A glucose surge, on the other hand, inhibits glucagon release and promotes insulin secretion. Glucagon release is inhibited via various mechanisms including direct effects of glucose on the secretory function of α-cells (73-75), intra-islet paracrine factors including Zn^{2+} and insulin (67, 76, 77), and central nervous system signaling (78-80). Insulin is secreted in a biphasic manner to release the appropriate insulin concentrations needed to stabilize glucose levels (81). During the first phase of insulin secretion, glucose enters β-cells via rapid facilitated diffusion and is quickly metabolized, increasing the ATP:ADP ratio and causing K_{ATP} channels to close (82). The closure of K_{ATP} channels increases the intracellular concentration of positive ions, leading to depolarization of the β-cell and activation of voltage-gated Ca^{2+} channels (82). The activation of voltage-gated Ca^{2+} channels increases intracellular Ca^{2+} concentrations, triggering the export of insulin-storing granules via exocytosis (82). During the second wave of insulin secretion, insulin must be synthesized, processed, and secreted, therefore this wave of secretion usually occurs approximately 30 minutes after initial glucose surge (83). Furthermore, recent

evidence suggests that this wave of insulin secretion may be independent of K_{ATP} channels (84); thus, future studies will address the molecular mechanisms employed by the second wave of insulin secretion. After secretion, insulin travels in the circulation to peripheral tissues including liver, skeletal muscle, and adipose tissue, signaling via InsR to promote anabolic processes including glucose uptake, lipid synthesis, and glycogenesis that remove and store glucose from the blood.

Because of this vital role of insulin in reducing blood glucose, obesity-induced insulin resistance results in hyperglycemic conditions that in turn lead to a compensatory increase in insulin secretion (12, 13). During the β-cell compensatory response, enhanced β-cell expansion (via proliferation and neogenesis) and increased insulin biosynthesis promote elevated circulating insulin levels in an attempt to restore glucose homeostasis (12). Much research has been devoted to understanding the molecular mechanisms governing β-cell expansion, as patients that are unable to sustain this compensatory response develop T2D (12, 14). Continuous nutrient overload and chronic low-grade inflammation promote β-cell dysfunction via various mechanisms including oxidative stress (85, 86), endoplasmic reticulum (ER) stress (87, 88), toxic effects of high glucose and lipid levels (glucolipotoxicity) (75, 89), and amyloid accumulation (90, 91). Obesity is associated with chronic low-grade inflammation that enhances the circulatory levels of pro-inflammatory cytokines (92-94). Pancreatic inflammation can also be associated with obesity (93, 95), and local inflammatory stimuli such as Interleukin-1 beta (IL-1β) can signal to promote β-cell dysfunction and death (96, 97). Chronic over nutrition can also

be detrimental to β-cells, as excess glucose and lipids can promote mitochondrial overstimulation, leading to elevated levels of reactive oxygen species (ROS) (98). β-cells are highly sensitive to ROS levels due to low expression of antioxidant enzymes (99); thus, enhanced ROS concentrations can further stimulate inflammatory pathways and promote DNA damage, resulting in β-cell death. Therefore, obesity-associated chronic low-grade inflammation and lipotoxicity are detrimental to β-cell function and promote the onset of β-cell failure and T2D.

Adipose tissue

The adipose tissue is a key metabolic organ that plays a pivotal role in maintaining metabolic homeostasis mainly due to its capacity to take-up, store, and release lipids according to the physiological energy demands of the organism (55, 56, 100-102). Human lipodystrophic syndromes and mouse genetic models lacking adipose tissue have confirmed the metabolic importance of adipose tissue in both humans and rodents (103-105). Despite extreme leanness, these subjects often display systemic insulin resistance, dyslipidemia, and severe hepatic steatosis due to decreased adipose lipid-buffering capacity that usually prevents lipotoxic damage to other tissues (106). Therefore, proper adipose tissue function is essential in maintaining metabolic homeostasis.

In times of excess energy, insulin activates metabolic pathways that enhance glycolysis (conversion of glucose to acetyl-CoA), synthesis of FA (lipogenesis), and formation of TG (esterification) (107, 108). Akt activation in the adipocyte promotes Glut4 translocation to the plasma membrane to enhance glucose transport (Figure 1.2, A) (26).

Although the molecular mechanisms by which insulin promotes Glut4 translocation to the cell surface are still not fully understood, Akt can phosphorylate and inhibit TBC1 domain family 4 (Tbc1d4, also known as As160) (Figure 1.2, A) (109, 110). Tbc1d4/As160 is a negative regulator of Glut4 trafficking; thus, inhibited Tbc1d4/As160 allows Glut4 to translocate to the plasma membrane promoting glucose flux into adipocyte (Figure 1.2, A) (111). Glucose can be converted to acetyl-CoA via glycolysis, which can be synthesized into FA (*de novo* lipogenesis) or be converted to glycerol-3-phosphate, the backbone of a TG molecule (108). Insulin also promotes FA uptake from Very low-density lipoprotein (Vldl) and chylomicrons by increasing Lipoprotein lipase (Lpl) expression – a lipase that facilitates uptake of lipoprotein-derived FAs – on the surface of endothelial cells (112, 113). Lastly, insulin also promotes lipid synthesis via enhanced transcription and maturation of lipogenic transcription factor Sterol regulatory element-binding transcription factor 1 (Srebp-1) (Figure 1.2, A) (114, 115), and hyperglycemic conditions promote Carbohydrate-responsive element-binding protein (Chrebp) activation (116). These two transcription factors, in turn, control the expression of a plethora of lipogenic enzymes necessary for all steps of lipid synthesis (114, 117-120). Thus, insulin promotes the uptake of glucose and FAs, which will be converted and safely stored as TG.

Figure 1.2 Adipose signaling to maintain whole-body glucose homeostasis.

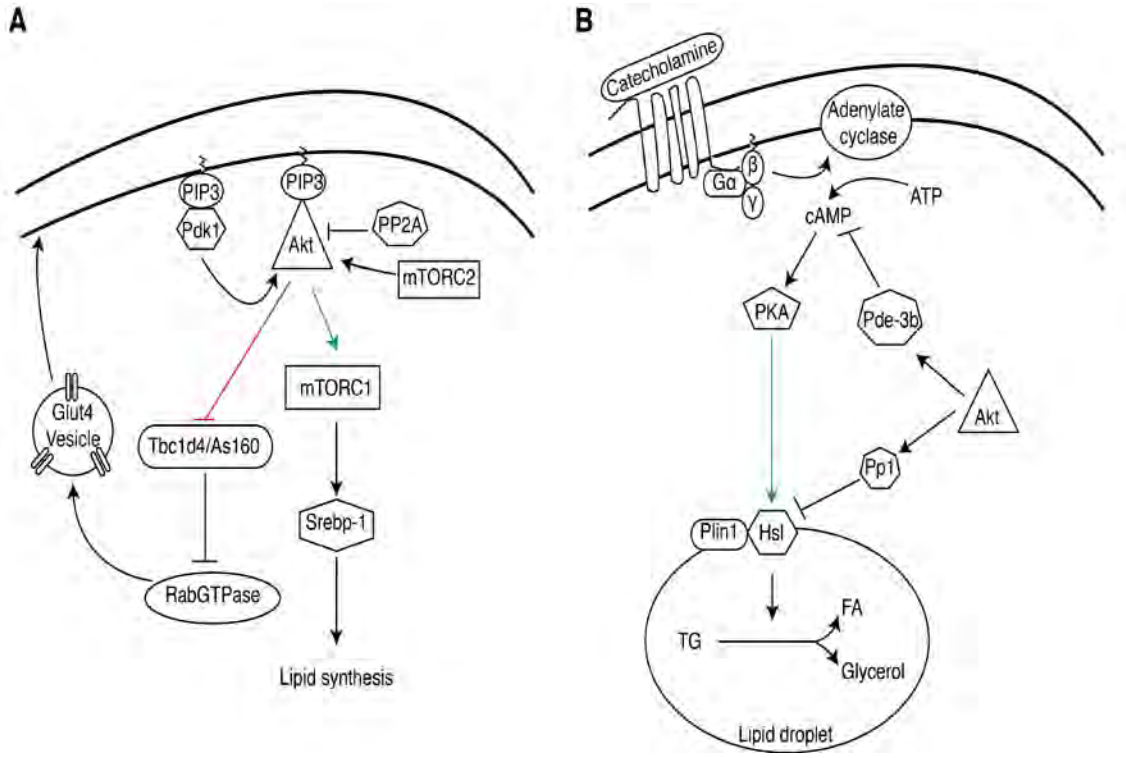

Figure 1.2 Adipose signaling to maintain whole-body glucose homeostasis. (A) Effects of insulin signaling to Akt in adipose cells. Activated Akt promotes glucose transport via inhibition of TBC1 domain family 4 (Tbc1d4, also known as As160). Inhibited Tbc1d4/As160 promotes Glucose Transport Type 4 (Glut4) vesicles translocation to the cell surface to allow glucose flux into the cell. **(B) Fasting-induced lipolysis in adipose cells.** Catecholamines signal via G protein-coupled receptor to activate adenylate cyclase and increase cAMP levels. Elevated cAMP levels promote Protein Kinase A (Pka) activation, which triggers Hormone-sensitive Lipase (Hsl) and Perilipin 1 (Plin1) activation, promoting the catalysis of triglycerides.

Various animal models have revealed the importance of adipose tissue insulin-stimulated glucose disposal and lipid synthesis. Transgenic animals that overexpress Glut4 in adipocytes display enhanced glucose uptake (even in the absence of insulin stimulation) and improved glucose homeostasis, highlighting the importance of adipose-mediated glucose uptake in regulating circulating glucose levels (121, 122). Furthermore, animal models that enhance adipose lipid-buffering capabilities, either via adiponectin overexpression or forced expression of an adipose-specific dominant-active Pparγ transgene, also display improved metabolic parameters due to enhanced lipid sequestration, despite enhanced adiposity (123, 124). These animal models suggest that the ability of adipose tissue to sequester lipids protects peripheral organs from lipotoxicity and metabolic abnormalities.

In fasting conditions, glucose uptake and lipid synthesis are suppressed while lipolysis is activated (125). Catecholamines signal in adipose cells to stimulate lipolysis, the breakdown of triglycerides to release FAs into the circulation for other metabolically active tissues to utilize as oxidative fuel (Figure 1.2, B) (126-130). Catecholamines bind to β-adrenergic receptors that are present in adipocytes, promoting adenylate cyclase activity and production of cAMP (Figure 1.2, B) (127-130). cAMP subsequently binds and sequesters the regulatory subunits of Protein Kinase A (Pka), allowing the catalytic subunits to phosphorylate and activate downstream effectors such as Hormone-sensitive lipase (Hsl) and Perilipin 1 (Plin1) (Figure 1.2, B) (131, 132). Activation of Hsl and Plin1 results in catalysis of TGs into FA and glycerol, which are subsequently released into the

circulation (Figure 1.2, B) (133). As an anabolic hormone, insulin inhibits this catalytic process (134). Insulin activates Akt, which activates phosphodiesterase 3B (Pde-3b), an enzyme that hydrolyzes cAMP, effectively lowering cAMP levels and reducing Pka activation (Figure 1.2, B) (135, 136). Akt also phosphorylates protein phosphatase 1 (Pp1), a phosphatase that dephosphorylates and inactivates Hsl (Figure 1.2, B) (137-139). Deregulated adipose lipolysis can therefore lead to excess FAs in the circulation resulting in ectopic lipid deposition and insulin resistance (140).

Besides its key lipid-buffering metabolic functions, the adipose is an endocrine organ that generates and secretes a plethora of bioactive factors (more than 600 molecules have been discovered) that can regulate a wide range of physiological processes including blood pressure, glucose and lipid metabolism, inflammation, atherosclerosis, appetite, and energy balance in various distant targets including liver, skeletal muscle, pancreas, and the cardiovascular system (141-143). The two most well studied adipokines (adipose-secreted factors) are leptin and adiponectin. The circulating concentrations of leptin reflect adipose tissue energy stores, with increasing leptin concentrations indicating increased adipose mass (144, 145). Leptin signals to other tissues to regulate processes such as satiety, appetite, food intake, energy expenditure, and fertility (146). Thus, mutations in the leptin gene result in extreme obesity both in rodents and humans (147). For example, the *ob/ob* mouse model harbors a missense mutation in the leptin gene that disrupts leptin secretion and causes obesity due to incessant food intake and reduced energy expenditure (144, 145, 148). Adiponectin is another well-known adipokine that

promotes insulin sensitivity (149-151). Unlike leptin, adiponectin secretion negatively correlates with adipose size (*i.e.,* more adipose tissue results in less adiponectin secretion) (152, 153). Adiponectin inhibits hepatic glucose production, promotes muscle glucose uptake, increases fatty-acid oxidation, promotes insulin secretion, and dampens inflammation (154). Thus, decreased adiponectin secretion, as occurs in Adiponectin-KO mice, results in exaggerated metabolic dysfunction with extreme hyperinsulinemia and glucose intolerance (155-157). Furthermore, adipose cells also generate lipokines (lipids secreted from adipose) via *de novo* lipogenesis, that enhance local and systemic glucose metabolism (158). Palmitoleate (C16:1n7) is a lipokine that is suggested to suppress hepatic steatosis and thus promote systemic insulin sensitivity (159). Therefore, the endocrine function of adipose tissue is critical maintaining whole-body glucose homeostasis.

These vital functions of adipose tissue can be compromised in obesity. Obesity-induced insulin resistance is associated with a dysfunctional adipose tissue – deregulated lipolysis, reduced insulin-stimulated glucose transport, altered adipokine secretion, and suppressed lipid synthesis (55, 56, 160). Increased food intake and decreased energy expenditure promote adipose tissue expansion and immune cell infiltration (8-10). Various obesity-related mechanisms have been proposed to contribute to the initiation of adipose tissue inflammation including lipotoxicity (161), ER stress (162, 163), adipocyte cell death (164), and hypoxia (165). The adipose tissue is composed of various cell types including adipocytes, fibroblasts, immune cells, and the vasculature. In a lean and healthy state,

macrophages in the adipose tissue are anti-inflammatory and promote insulin sensitivity by secreting Interleukin 10 (IL-10) (166). IL-10 attenuates pro-inflammatory cytokine signaling by inhibiting Nuclear factor kappa-light-chain-enhancer of activated B-cells (NF-κB), a key regulator of inflammatory gene expression (167). Obesity increases the number of adipose tissue macrophages and shifts the balance to a pro-inflammatory state (M1-macrophages), releasing pro-inflammatory cytokines such as Tumor necrosis factor-alpha (Tnf-α) (168). Pro-inflammatory cytokines, in turn, promote adipose dysfunction by enhancing lipolysis and repressing lipid synthesis, creating a vicious feed-forward cycle whereby immune cells secrete inflammatory cytokines that promote adipose tissue dysfunction, and adipose tissue dysfunction promotes adipose tissue immune cell infiltration and proliferation. Pro-inflammatory cytokines can also activate signaling pathways such as Jnk, which promote Irs serine phosphorylation and dampen insulin signaling to Akt, resulting in detrimental effects on glucose homeostasis (47). Lastly, adipokine production is altered in obesity, releasing pro-inflammatory adipokines that attract immune cells into the adipose tissue and promote insulin resistance (141). Therefore, proper adipose tissue function (lipolysis, lipogenesis, and adipokine secretion) is essential in maintaining whole-body glucose homeostasis.

Liver

The liver is a critical organ that maintains blood glucose homeostasis via uptake, storage, and output of glucose (169). The liver also performs *de novo* lipogenesis to synthesize TG and package these into Vldl vesicles that will be transported to the adipose tissue for storage (170). While glucagon promotes the breakdown of glycogen to produce glucose,

insulin promotes glycogen formation and lipid synthesis; thus, proper liver function is essential in maintaining whole-body metabolic homeostasis.

In fasting conditions, the liver produces glucose to maintain optimal systemic blood glucose levels (171). Two proteins are well recognized to be necessary for the transcriptional regulation of hepatic glucose production, cAMP response element-binding protein (Creb) and Forkhead box protein O1 (Foxo1) (5, 172). In fasting animals, α-cells secrete glucagon resulting in liver G-protein-coupled receptor (Gpcr) activation and increased adenylate cyclase activity, elevating cAMP levels (Figure 1.3, A) (5, 172). cAMP then activates Pka, which subsequently phosphorylates and activates Creb (173). Creb phosphorylation recruits transcriptional co-activators, Creb-binding protein (CBP), E1A binding protein p300 (p300), Creb-regulated transcription coactive 2 (Crtc2), and Pparγ-coactivator 1a (Pgc-1α), thus promoting the transcription of essential gluconeogenic genes including Phosphoenolpyruvate carboxykinase (Pepck) and Glucose-6-phosphatase (G6pc) (172). Furthermore, activated Akt negatively regulates Foxo1 transcription factors via direct phosphorylation, which causes cytoplasmic sequestration of Foxo1 proteins (174-176). Thus, in the absence of insulin in fasting conditions, Foxo1 transcription factors translocate to the nucleus to enhance gluconeogenic gene expression (174-176). Glucagon also signals in the liver to 1) inhibit glycolysis by decreasing the expression of Fructose 2,6-biphosphate (F-2,6-Bp), which decreases phosphofructokinase-1 (Pfk1) concentrations (177-179), 2) decrease glycogen formation by lowering glycogen synthase (Gs) expression (180, 181), and 3) promote

amino acid uptake (alanine, glycine, and proline), which can be converted to glucose via the gluconeogenic pathway (5).

Figure 1.3 Liver signaling to maintain glucose homeostasis.

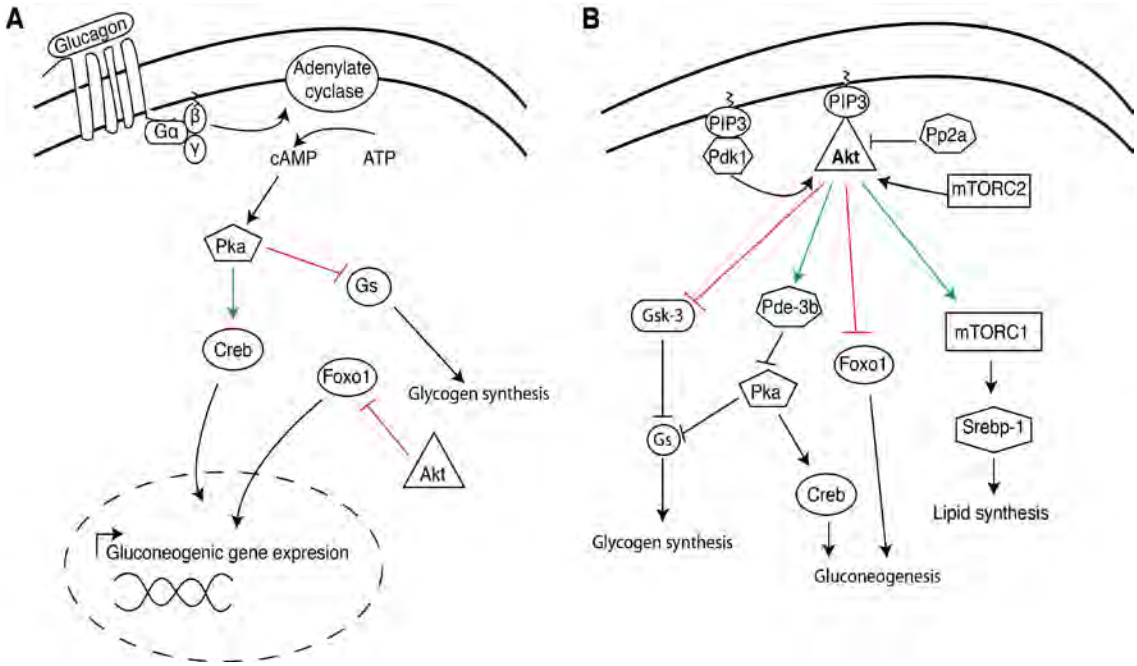

Figure 1.3 Liver signaling to maintain glucose homeostasis. (A) Glucagon signaling to promote hepatic glucose production. Glucagon signaling increases adenylate cyclase activity, resulting in elevated cAMP levels. Heightened cAMP levels promote Pka activation; resulting in cAMP response element-binding protein (Creb) phosphorylation and nuclear recruitment to promote gluconeogenic gene expression. In the absence of insulin, Forkhead box protein O1 (Foxo1) transcription factors are also able to translocate to the nucleus to promote gluconeogenic gene expression. **(B) Insulin signaling to Akt in the liver.** Activated hepatic Akt promotes glycogen and lipid synthesis and suppresses gluconeogenesis. To promote glycogen synthesis, Akt directly phosphorylates and inhibits Glycogen Synthase Kinase 3 (Gsk-3), thus relieving Gsk-3-induced inhibition of Glycogen Synthase (Gs). Activated Akt activates Phosphodiesterase 3b (Pde-3b), thus lowering cAMP levels, reducing Pka activation and Creb-induced gene expression. Akt also phosphorylates Forkhead Box Protein O1 (Foxo1), which promotes Foxo1 cytosolic retention and reduces gluconeogenic gene expression. Activated Akt also promotes lipid synthesis via Mechanistic Target of Rapamycin (mTORC1) and Sterol regulatory element-binding transcription factor 1 (Srebp-1) activation.

After feeding, a glucose surge promotes β-cell insulin secretion. Insulin binds to the hepatic InsR where it elicits a wide range of cellular responses including glycogen formation, suppression of glucose production, and lipid synthesis (Figure 1.3, B) (182). Insulin promotes glycogen formation by suppressing Pka activity and inhibiting Glycogen synthase kinase-3 (Gsk-3), resulting in increased Gs activity (183-185). Gs is a tetrameric enzyme that catalyzes the formation of glycogen from glucose (186). Pka and Gsk-3 can both phosphorylate and inhibit Gs, resulting in reduced glycogen formation (184, 187, 188). Insulin signaling to Akt activates Pde-3b, lowering cAMP levels and Pka activity, and promoting glycogen formation (136). Akt also phosphorylates and inhibits Gsk-3 activity, allowing for Gs activation and glycogen formation (189). To suppress gluconeogenesis, insulin promotes the lowering of cAMP levels, resulting in reduced Creb activation (173). Insulin also phosphorylates Foxo1 proteins, promoting their binding to cytosolic 14-3-3 proteins, resulting in Foxo1 nuclear exclusion (190). The end result of insulin signaling is therefore to suppress gluconeogenic gene expression. Insulin can also promote other processes including lipid synthesis via Akt activation, similar to the adipose tissue (191). Enhanced Akt signaling results in mTORC1 activation, which in turn promotes Srebp-1c cleavage and activation (42, 192). Srebp-1c is an important lipogenic transcription factor that resides in the ER, and proteolytic cleavage allows the NH_2-terminus to translocate to the nucleus and bind to the sterol response elements (SRE) of various lipogenic genes including Acetyl-CoA carboxylase (Acc), Fatty acid synthase (Fasn), Stearoyl-CoA desaturase-1 (Scd-1), Pparγ, and Elongation of long chain fatty acids family member 6 (Elovl6) (42, 193). Newly produced TGs are then secreted

via Vldl particles for the adipose tissue to store (170). Due to the major effects on glucose production and lipid synthesis, proper hepatic insulin signaling is critical in maintaining whole-body glucose homeostasis.

Obesity can promote peripheral insulin resistance and the liver is unique in that it becomes selectively insulin resistant (194). While insulin fails to suppress hepatic glucose production, allowing blood glucose levels to rise, hepatic lipid synthesis is protected, resulting in excessive lipid accumulation (18, 115). Hepatic steatosis can be ameliorated, however, via liver specific deletion of Scap proteins (195). Scap proteins transport Srebp-1 to the Golgi to be proteolytically cleaved depending on the stimuli, thus Scap is required for Srebp-1 processing (196). Liver-Scap KO mice have reduced nuclear Srebp-1 and decreased lipogenic gene expression, resulting in less hepatic steatosis and better metabolic homeostasis (195).

Skeletal Muscle

The skeletal muscle accounts for approximately 40% of body mass in a lean individual and functions to promote movement, maintain posture, stabilize joints, and generate heat (197). To properly function, the skeletal muscle requires energy; thus, in the post-prandial state, it is the major site for glucose disposal, taking approximately 75% of ingested glucose via insulin-stimulated glucose uptake (198, 199). Therefore, insulin action on skeletal muscle can have profound effects on systemic glucose control.

During fasting conditions and energy-demanding processes such as exercise, epinephrine signals in the skeletal muscle to promote glycogen breakdown (Figure 1.4, A). Epinephrine signaling enhances adenylate cyclase activity and increases cAMP levels (200). cAMP promotes Pka activation, resulting in phosphorylation and increased activity of phosphorylase kinase (Phk) (200). Phk, in turn phosphorylates phosphorylase b, converting it into the active form phosphorylase a, which promotes the cleavage of glucose from glycogen (200). Glycogen breakdown, therefore, releases glucose, which is then rapidly oxidized by the muscle for energy. Furthermore, during glycogen breakdown, hexokinase (Hk) activity is inhibited by Glucose 6-phosphate (G-6-P), resulting in reduced glucose uptake and glucose phosphorylation (201). Muscle glycogen breakdown is therefore essential in providing energy as well as preventing removal of glucose from the circulation in fasting conditions.

Figure 1.4 Muscle signaling to maintain glucose homeostasis.

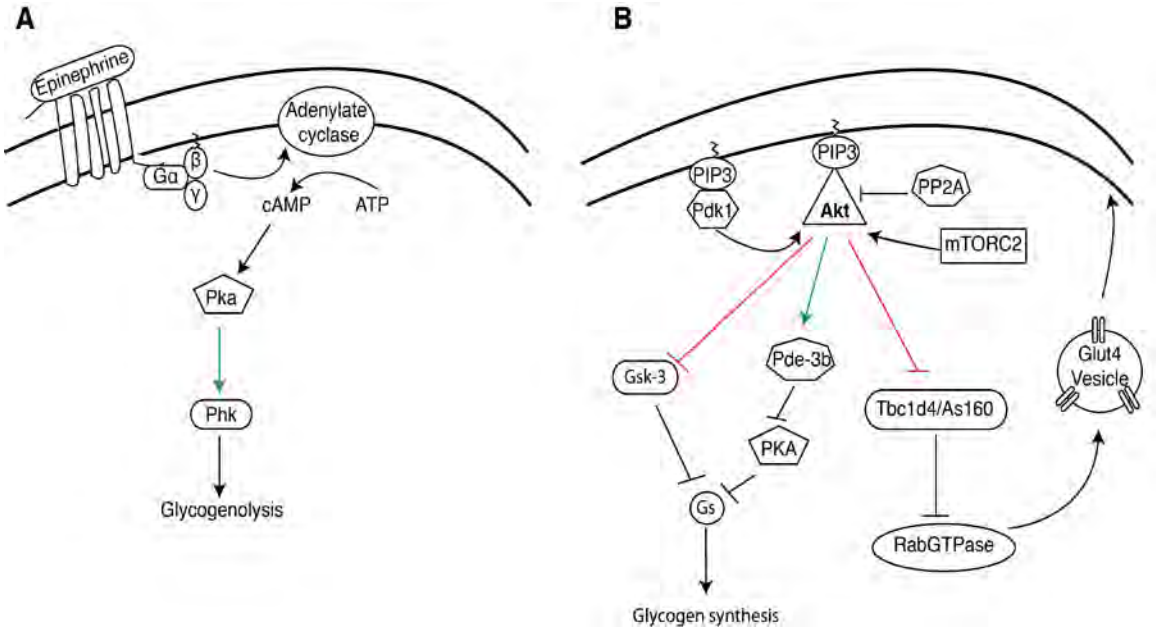

Figure 1.4 Muscle signaling to maintain glucose homeostasis. (A) Epinephrine signaling to promote glycogenolysis. Epinephrine stimulates adenylate cyclase activity, effectively increasing cAMP levels and promoting Pka activation. Activated Pka phosphorylates Phosphorylase kinase (Phk), thus promoting cleavage of glucose from glycogen. **(B) Insulin signaling to Akt promotes glucose transport and glycogen synthesis.** Activated Akt promotes Glut4 translocation to the cell surface, thus promoting glucose influx. Activated Akt also promotes glycogen synthesis by phosphorylating and inhibiting Gsk-3 as well as by reducing Pka activity. Both Gsk-3 and Pka inhibit Gs and glycogen synthesis.

In the post-prandial state, secreted insulin binds to the skeletal muscle InsR and signals via Akt to promote Glut4 translocation in a similar manner to the adipose tissue (Figure 1.4, B) (26). Skeletal muscle glucose transport is mediated by Glucose transporter 1 (Glut1), which is basally expressed at the plasma membrane, and Glut4, which translocates to the cell surface upon insulin stimulation (26). As expected, enhanced skeletal muscle glucose transport observed in either muscle-specific Glut4-transgenic (122, 202, 203) or muscle-specific Glut1-transgenic mice (204) significantly improves whole-body glucose homeostasis, reinforcing the importance of skeletal muscle glucose transport in whole-body metabolism. Glucose disposal in the skeletal muscle occurs via glucose oxidation (glycolysis and TCA cycle) and glycogen formation (205). Insulin signaling to Akt promotes glycogen formation in a similar manner as the liver, via phosphorylation and inhibition of Gsk-3 and reduced Pka activity (189). Both of these proteins phosphorylate and inhibit Gs, thus insulin signaling to Akt relives Gs suppression and allows for glycogen formation (206).

The skeletal muscle also has endocrine functions as it secretes myokines, which are muscle-derived molecules that can exert autocrine, paracrine, and endocrine effects (207). Although our knowledge on myokines is still limited, they can have profound effects on insulin sensitivity. For example, Fibroblast growth factor 21 (Fgf-21) can be secreted from the skeletal muscle and improve metabolic functions by increasing circulating adiponectin levels (208). Interleukin-6 (IL-6) can also be secreted from the skeletal muscle, mostly after muscle contraction, and although the role of Il-6 in whole-

body glucose homeostasis is controversial, IL-6 may have autocrine functions during exercise to promote muscle glucose uptake (207). Other myokines include irisin, which is secreted after exercise and induces white-to-brown adipose conversion to promote insulin sensitivity (209), Follistatin-like 1 (Fstl1), which has been shown to be cardioprotective (207), and brain-derived neurotrophic factor (Bdnf), which may have autocrine roles to enhance skeletal muscle fatty-acid oxidation (210). Many of the above mentioned myokines are critical in maintaining insulin sensitivity, however, inter-organ communication networks, including myokine secretion, is altered in obesity contributing to metabolic dysfunction (207).

Elevated circulating FAs can promote muscle insulin resistance (211). Lipid infusion into lean human subjects results in decreased PI3K activation, reduced insulin-stimulated glucose uptake and insulin resistance (211). FAs can promote insulin resistance via various mechanisms including ectopic lipid accumulation (both ceramides and diacylglycerides), oxidative stress, chronic low-grade inflammation, and mitochondrial dysfunction (85, 211). All of these processes can result in suppression of the insulin-signaling pathway, reducing insulin-stimulated glucose uptake and contributing to hyperglycemic conditions and metabolic dysfunction.

Map4k4

Insulin action on the skeletal muscle and the adipose tissue is essential in regulating systemic glucose levels (26, 122). Insulin signaling to Akt promotes Glut4 translocation to the cell surface, allowing glucose to enter the cell to restore euglycemia. Since T2D is

associated with defects in insulin action, including glucose-uptake, understanding the mechanisms by which insulin regulates Glut4 trafficking may have profound effects in the treatment of insulin resistance and T2D. Thus, previous colleagues in the Czech laboratory performed a siRNA screen aimed at identifying novel regulators (including kinases) of insulin-mediated glucose uptake (Figure 1.5, A) (212). In a lean and healthy mammal, the skeletal muscle is responsible for approximately 75% of insulin-mediated glucose disposal (13). However, mice with muscle-specific ablation of the InsR (MIRKO), despite reduced glucose uptake and insulin signaling, do not display major metabolic abnormalities (213). On the other hand, enhanced adipose glucose uptake observed in adipose-specific Glut4 transgenic mice, results in improved glucose tolerance and insulin sensitivity (121, 122). Previous colleagues in the Czech laboratory therefore performed the siRNA screen in cultured 3T3-L1 adipocytes (212). Using siRNA-mediated gene silencing, the expression of 249 protein kinases expressed in cultured adipocytes was reduced and the effects on basal and insulin-stimulated deoxyglucose uptake assessed (Figure 1.5, A) (212). Interestingly, Mitogen-activated protein kinase kinase kinase kinase (Map4k4) silencing significantly increased insulin-stimulated glucose uptake, thus identifying Map4k4 as a novel negative regulator of glucose transport and insulin action in adipocytes (Figure 1.5, A) (212).

Figure 1.5 Protein Kinase Map4k4.

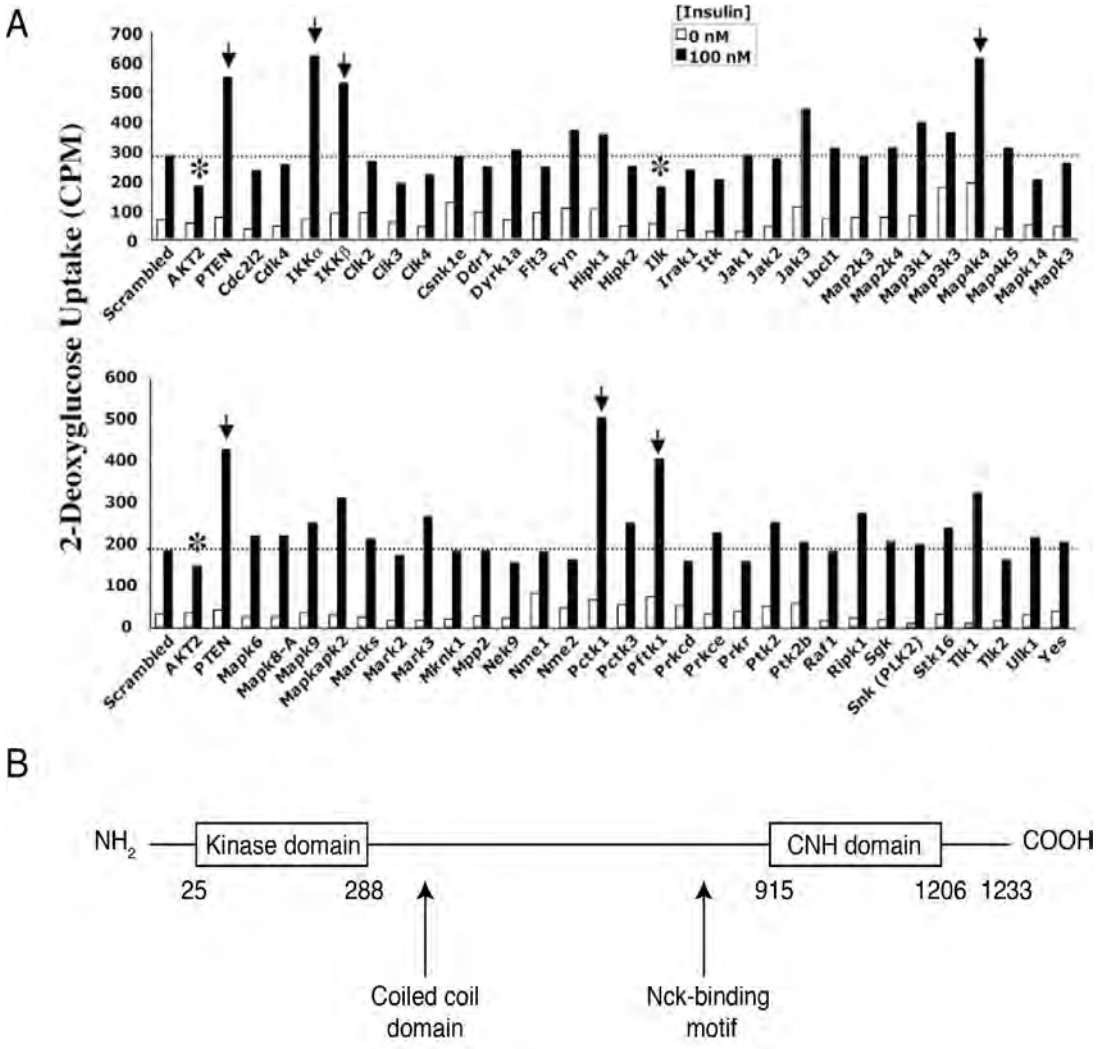

Figure 1.5 (A) Map4k4 identified as repressor of glucose transport. siRNA-based screen to identify novel regulators of insulin action. Cells were transfected with respective siRNA. 72hrs post-transfection, cells were stimulated with insulin and glucose transport assayed with ^{3}H-deoxyglycose. Adapted from Tang *et al.*, 2006. **(B) Map4k4 predicted domain structure.** Map4k4 contains 1233 amino acids. The kinase domain of Map4k4 is in the NH_2 terminus, while the Citron homology (CNH) domain is in the COOH terminus.

Map4k4 (also known as Hepatocyte progenitor kinase-like/germinal center kinase-like kinase (HGK) and Nck-interacting kinase (NIK)) is a serine/threonine protein kinase that was first identified as an interacting partner of the adaptor protein Nck (214). Map4k4 is located on chromosome 1 (1B) in mice (chromosome 2 in humans) and encodes a protein containing 1288 amino acids with 33 exons, although alternative splicing resulting in different isoforms has been reported (215). Structurally, Map4k4 contains a SH3 domain, citron-homology domain (CNH), and two putative caspase cleavage sites, however the function of these structures has not been thoroughly studied (Figure 1.5, B) (216).

Ste20-related protein kinases

Based on homology and signature sequence in subdomain VIII (GTP(Y/F/C)WMAPE), Map4k4 and 27 other mammalian serine/threonine protein kinases belong to the Ste20-related protein kinase family (217). In *Saccharomyces cerevisiae*, Ste20p is a protein involved in a wide variety of processes including pheromone response and migration (216). All related mammalian kinases also have diverse and wide-ranging functions including ion transport, cell cycle, cytoskeletal organization, and programmed cell death (217, 218).

Based on the location of the catalytic domain, Ste20-related kinases are further subdivided into two groups—in p21-activated kinases (PAKs), the catalytic domain is in the -COOH-terminus, whereas in germinal center-like kinases (GCKs), the catalytic domain in the NH_2-terminus (217). Because the catalytic domain of Map4k4 is in the

NH_2-terminus, Map4k4 is a member of the GCK family and belongs to subgroup IV based on the most shared sequence with Traf2 and Nck-interacting protein (Tnik) and Mishapen-like kinase 1 (Mink), 92% and 87%, respectively (219).

Biological functions

In keeping with the yeast Ste20p cellular functions, Map4k4 is implicated in various physiological cellular processes including migration, inflammation, and cellular metabolism (220). Although the molecular targets and signaling pathways for Map4k4 are still under investigation, a conserved role for Map4k4 in cellular migration has been established. In *Caenorhabditis elegans*, Map4k4 (MIG-15) regulates neuroblast migration (221, 222), while in *Drosophila melanogaster* Map4k4 (Misshapen) regulates dorsal closure, neuronal targeting, and cell invasion (223-225). In mammals, whole-body Map4k4-*null* mice display early embryonic lethality due to the failure of mesodermal cells to migrate away from the primitive streak (214). Consistent with a role for Map4k4 in promoting cellular motility increased Map4k4 expression in cancerous tissue correlates with worse prognosis due to increased likelihood of metastasis (226-228). The molecular targets of Map4k4 to promote cellular motility are still under investigation, however a role for Map4k4 in regulating both F-actin polymerization dynamics via Actin-related protein (Arp) 2/3 complex phosphorylation and microtubule and focal adhesion dynamics via ADP-ribosylation factor 6 (Arf6) activation has been reported (229, 230).

Map4k4 is also reported to inhibit insulin action and cellular metabolism. Our laboratory identified Map4k4 as a negative regulator of glucose uptake and insulin action in cultured adipocytes (212). Consistent with a role for Map4k4 as a repressor of insulin action, Map4k4 has been suggested to be a cellular mediator of inflammatory cytokines such as Tnf-α (231-233). For example, Map4k4 depletion in macrophages *in vivo* attenuates systemic inflammation and prolongs survival after a Lipopolysaccharides (LPS) challenge (231). In C2C12 muscle cells, Map4k4 inhibits muscle differentiation (234), and in mature human myotubes, Map4k4 depletion protects from Tnf-α-induced insulin resistance (232). Finally, in cultured β-cells, Map4k4 silencing protects cells from reduced insulin secretion caused by Tnf-α (233). Thus, these studies suggest Map4k4 may suppress insulin action and Map4k4 inhibition *in vivo* may ameliorate obesity-induced metabolic dysfunction. A recent publication, however, suggests Map4k4 may function to suppress, rather than promote, inflammation (235). Using a T-cell specific cre line to generate T-cell specific Map4k4 knockout mice, knockout mice develop systemic inflammation due to stabilization of Tnf receptor-associated factor 2 (Traf2) and IL-6 overproduction (235). Future studies will be required to assess the cell-type specific functions of Map4k4 and their role in metabolic disease.

Project Goals

Controlled glucose homeostasis is an elaborate physiological process that requires inter-organ communication. Our laboratory is particularly interested in understanding novel regulators of adipocyte function as these signaling nodes can significantly contribute to systemic glucose control and alternations in these pathways promote metabolic disease. To identify such signaling nodes, previous colleagues in the Czech laboratory used a siRNA-based screen in cultured adipocytes and identified the protein kinase Map4k4 as a negative regulator of insulin action. Furthermore, they found that the metabolic consequences of Map4k4 depletion in adipocytes included increased glucose transport. Therefore the experiments performed in this thesis are aimed at **dissecting the role of Map4k4 in the adipocyte, identifying key signaling pathways downstream of Map4k4, and defining how the actions of Map4k4 in these signaling pathways may regulate whole-body metabolism.** We are specifically interested in Map4k4 as it is a potential novel therapeutic target for the treatment of metabolic disease, where there is a need for new therapies.

Two main questions are addressed in this thesis:

1. Does Map4k4 affect adipocyte-specific functions? If so, what are the specific signaling mechanisms involved?
2. What is the role of Map4k4 in regulation of whole-body glucose and lipid metabolism? Do the actions of Map4k4 contribute to the metabolic dysfunction associated with obesity and insulin resistance?

To answer these questions, the studies reported in this thesis utilize both *in vitro* and *in vivo* models to investigate the role of Map4k4. In cultured adipocytes, I found that Map4k4 represses lipid synthesis independent of glucose transport, and these effects are mediated via mTORC1- and Srebp-1-dependent mechanisms (Chapter II) (236). Contrary to initial expectations, I found that Map4k4 does not repress lipid synthesis via the Jnk signaling cascade. I also showed that Map4k4 is not an upstream regulator of Jnk, and further demonstrated that prior work placing Map4k4 as an upstream positive regulator of Jnk was based on artifactual overexpression (Chapter II) (236). Based on the effects observed *in vitro*, where Map4k4 suppresses glucose transport and lipid synthesis, I assessed the role of Map4k4 *in vivo* and tested whether Map4k4 deletion would protect obese mice from metabolic disease. In fact, I found that Map4k4 deletion improved glucose tolerance in high-fat diet fed mice. Consistent with the *in vitro* studies in cultured adipocytes in Chapter II, where Map4k4 signals to inhibit insulin action, I also found that systemic Map4k4 depletion in adult mice improves whole-body insulin sensitivity (Chapter III). I generated multiple tissue-specific Map4k4 KO mice and observed that Map4k4 ablation in Myf5-positive cells, which include skeletal muscles, recapitulates the improved systemic insulin sensitivity observed in systemic Map4k4-ablated mice, while ablation of Map4k4 in adipocytes or hepatocytes had no such effect (Chapter III). Therefore, Map4k4 regulates signaling nodes in Myf5-positive cells that alter whole-body metabolism. Thus, Map4k4 may serve as a novel drug target in the treatment for T2D.

CHAPTER II:

Map4k4 suppresses lipogenic transcription factor Srebp-1 and adipose lipid synthesis independent of the Jnk signaling cascade.

This chapter is derived from the article of the same name that appeared in publication in the Journal of Lipid Research:

Laura V. Danai, Adilson Guilherme, Kalyani V. Guntur, Juerg Straubhaar, Sarah M. Nicoloro, and Michael P. Czech, J Lipid Res. 2013. 54(10):2697-2707.

Author Contributions

- **Figure 2.1 A. Microarray and normalization.** The Gene Chip microarray studies were performed by Sarah M. Nicoloro, Czech Lab. Juerg Straubhaar analyzed the data from these microarrays.

- **Figure 2.2 D-E. ^{14}C-acetate incorporation into lipids.** These experiments were performed by Adilson Guilherme, Czech Lab.

- **Figure 2.3 A-C. ^{14}C-acetate incorporation into lipids.** These experiments were performed by Adilson Guilherme, Czech Lab.

- Figure 2.4 D. The initial observations assessing Map4k4 function in TNF-α signaling were performed by Kalyani Guntur.

- The rest the experiments presented in this chapter were performed by Laura V. Danai.

- This manuscript was written by Laura V. Danai with helpful suggestions from Adilson Guilherme, Joseph V. Virbasius, and Michael P. Czech.

Summary

Adipose tissue lipogenesis is paradoxically impaired in human obesity, promoting ectopic triglyceride (TG) deposition, lipotoxicity, and insulin resistance. We previously identified Mitogen-activated protein kinase kinase kinase kinase 4 (Map4k4), a Sterile 20 protein kinase reported to be upstream of c-Jun NH_2-terminal kinase (Jnk) signaling, as a novel negative regulator of insulin-stimulated glucose transport in adipocytes. Using full-genome microarray analysis we uncovered a novel role for Map4k4 as a suppressor of lipid synthesis. We further report that Map4k4 suppresses adipocyte lipogenesis independently of Jnk. While Map4k4 silencing in adipocytes enhances the expression of lipogenic enzymes, concomitant with increased conversion of ^{14}C-glucose and ^{14}C-acetate into TG and fatty acids (FA), Jnk1 and Jnk2 depletion causes the opposite effects. Furthermore, high expression of Map4k4 fails to activate endogenous Jnk, while Map4k4 depletion does not attenuate Jnk activation by Tnf-α. Map4k4 silencing in cultured adipocytes elevates both the total protein expression and cleavage of Srebp-1 in a rapamycin-sensitive manner, consistent with Map4k4 signaling via Mechanistic target of rapamycin complex 1 (mTORC1). We show Map4k4 depletion requires Srebp-1 upregulation to increase lipogenesis and further show that Map4k4 promotes Ampk (AMP-protein kinase) signaling and the phosphorylation of mTORC1 binding partner Raptor (Ser 792) to inhibit mTORC1. Our results indicate that Map4k4 inhibits adipose lipogenesis by suppression of Srebp-1 in an Ampk- and mTOR-dependent but Jnk-independent mechanism.

Introduction

Obesity can promote adipose dysfunction, which paradoxically results in decreased adipose lipid synthesis and contributes to ectopic lipid deposition and whole body insulin resistance (105). Lipodystrophic human subjects and mouse models demonstrate that deficits in adipose lipid synthesis (lipogenesis) correlate with excess lipid deposition and whole-body insulin resistance, highlighting the importance of adipose lipogenesis in metabolic dysfunction (103, 105, 237, 238). The expression and activity of the lipogenic transcription factors peroxisome proliferator-activated receptor gamma **(**Pparγ), sterol-regulated element binding protein-1 (Srebp-1), and carbohydrate responsive element-binding protein (Chrebp, also known as Mlxipl) are suppressed in the adipose tissue of obese humans, resulting in decreased expression of lipogenic enzymes and decreased adipose fatty acid (FA) and triglyceride (TG) synthesis; however, the mechanisms that lead to this inhibition are still unclear (237-244). Therefore, understanding this deregulation is fundamental in developing strategies that enhance adipose lipogenesis and lipid sequestration, thus preventing the ectopic lipid deposition and insulin resistance that occurs during obesity.

Srebp-1 and Srebp-2 are transcription factors important for regulating the expression of genes involved in the synthesis and uptake of cholesterol, FA, TG, and phospholipids (117). These factors reside in the endoplasmic reticulum (ER) and upon demand for lipid synthesis are transported to the Golgi apparatus to be post-translationally cleaved, allowing the functional NH_2-terminal fragment to translocate into the nucleus and

regulate lipogenic gene expression (117). Srebp transcription factors have distinctive specificities: Srebp-2 mainly controls expression of genes involved in the cholesterol biosynthetic pathway, while Srebp-1 mainly controls lipogenic gene expression; however, overlap in function has been reported (117, 196). Srebp-1 is an important regulator of lipogenesis as it controls the expression of lipogenic genes including solute carrier family 2 (facilitated glucose transporter) member 4 (Slc2a4 or Glut4) (245), ATP citrate lyase (Acly) (246), acetyl-Coenzyme A carboxylase alpha (Acaca) (247), fatty acid synthase (Fasn) (248, 249), stearoyl-Coenzyme A desaturase 1 (Scd-1) (250), glycerol-3-phosphate acyltransferase (Gpat) (251), and Pparγ (252, 253). As a regulator of anabolic processes, Srebp-1 is positively regulated by mechanistic target of rapamycin (mTORC1) (254-257) and negatively regulated by AMP-protein kinase (Ampk) (258-260). Although the mechanism by which mTORC1 promotes Srebp-1 activity is not fully understood, increased Pparγ function in response to mTORC1 activation may contribute to increased Srebp-mediated adipose lipogenesis (254, 261-266).

In an attempt to find novel modulators of insulin action, our laboratory performed an siRNA screen to identify regulators of insulin-stimulated glucose transport in adipose cells. Depletion of Mitogen-activated protein kinase kinase kinase kinase 4 (Map4k4) significantly enhanced glucose transport, thus Map4k4 was discovered as novel negative regulator of glucose transport. Map4k4 is a serine/threonine protein kinase related to *Saccharomyces cerevisiae* Sterile 20 (Ste 20) protein kinases. Previous work suggests Map4k4 is a pro-inflammatory kinase that activates c-Jun NH_2-terminal kinase (Jnk)

protein kinase (267-269). This would be in keeping with a role for Map4k4 as a Ste20-like protein kinase, upstream of the MAP kinase-signaling pathway (216, 217, 270). Map4k4 has also been reported to inhibit mTORC1, resulting in decreased Pparγ protein levels (261). Interestingly, Map4k4 expression increases in the adipose tissue of obese subjects, while adipose lipogenesis decreases (271). We therefore aimed to test the role of Map4k4 in adipose lipogenesis and whether its actions require mTORC1 or the Jnk signaling pathway. These studies extend our previous understanding of Map4k4 function and demonstrate that Map4k4 suppresses lipogenesis in an mTORC1-dependent and Jnk-independent manner.

Materials and methods

Materials and Chemicals – Bovine insulin, FA-free BSA, D-glucose, sodium pyruvate, and sodium acetate were purchased from Sigma. Tnf-α was purchased from Calbiochem. ^{14}C-U-glucose (250 μCi/mL) and ^{14}C-acetate (250 μCi/mL) were purchased from Perkin Elmer. Flag-Jnk1 and Flag-Jnk2 were developed by R. Davis (University of Massachusetts Medical School) (Addgene plasmid 13798 and 13801, respectively) (272, 273).

Cell Culture – 3T3-L1 fibroblasts were grown and differentiated into adipocytes as previously described (274). Briefly, 3T3-L1 fibroblasts were grown to confluence in complete media (high glucose (25mM) DMEM containing 10% fetal bovine serum, 50 units/mL penicillin and 50 μg/mL of streptomycin). Two days after confluence, differentiation media (0.25 μM dexamethasone, 0.5 mM 1-methyl-3-isobutylxanthine,

and 10^{-7} M insulin) was added. On the fourth day after differentiation media was added, adipocytes were either infected with 40 μL of 1.43 X 10^{12} particles/mL of adenovirus (AdCMV-HA-Control or AdCMV-HA-Map4k4, University of Massachusetts Medical School Viral Vector Core Facility, the CMV driven adenoviral vector expresses Map4k4 with an NH_2-terminal triple HA epitope tag) or washed with PBS, trypsinized, and transfected by electroporation (Bio-Rad Gene Pulser II – 0.18 kV, 960 microfarads) with siRNA (Scrambled, Map4k4, Jnk1/2, Srebp1/2 from Dharmacon). A green fluorescent protein (GFP)-expressing control virus or Map4k4 D152N-expressing virus were also used and added at a dose of 40 μL of 1.43 X 10^{12} particles/mL for 72hr. These adenoviruses were gifts from Diane L. Barber (Department of Cell and Tissue Biology, University of California, San Francisco, CA. Transfection of HEK 293T cells was achieved using Lipofectamine 2000 (Invitrogen) following the manufacturer's protocol. Briefly, cells were plated at a density of 2.5 X 10^5 cells per 6-well plate a day before transfection. 1 μg of DNA was used for each transfection and empty vector was used to achieve equal amounts of DNA between conditions. Knockdown experiments in HEK 293T cells were achieved using Lipofectamine RNAi Max (Invitrogen), following the manufacturer's protocol.

RNA Isolation, Real Time PCR, Affymetrix Gene Chip Analysis– Total RNA was extracted from adipocytes using TriPure isolation reagent (Roche) following manufacturer's instructions. cDNA was synthesized using iScript cDNA Synthesis Kit (BioRad) and quantitative RT-PCR was performed using iQ SybrGreen supermix and

analyzed as previously described (275, 276). 36B4 (Rplp0) and Hprt served as housekeeping internal controls.

For Affymetrix Gene Chip analysis, RNA was isolated from three independent experiments and hybridized to three different murine genome MOE430-2 microarrays. RNA quality was measured using the Agilent 2100 Bioanalyzer. Differentially expressed mRNAs were identified using a random-variance t-test.

siRNA Duplexes – siRNA sequences were purchased from Dharmacon RNAi Technologies (Thermo Scientific). Scramble control (CAGUCGCGUUUGCGACUGGUU), Map4k4 (GACCAACUCUGGCUUGUUAUU), Jnk1 (GGAGUUAGAUCAUGAAAGAUU), Jnk2 (GGAAAGAGCUAAUUUACAAUU), Srebp1 (Srebf1) SMARTpool (GGGCAGCUCUGUACUCCUU; GUACACUUCUGGAGACAUC; CAAACAAGCUGACCUGGAU; GCAAGGCCAUCGACUACAU), Srebp2 (Srebf2) SMARTpool (GAGGAAGGCCAUUGAUUAC; GGUGCAACCUCAGAUCAUU; GAAAGUUCCUAUCAAGCAA; CCAGUGCUCUAGAGUAUUU)

Immunoblotting –For studies on Jnk signaling, cells were treated with 50 ng/mL Tnf-α for 15 minutes. Cells were washed twice in cold PBS and collected in RIPA buffer supplemented with protease and phosphatase inhibitors (Thermo Scientific). Total cell lysates were resolved by SDS-PAGE and electro-transferred to nitrocellulose membranes. Membranes were incubated with indicated antibodies overnight at 4°C. Blots were washed with TBST (0.1% Tween 20 in Tris-Buffered saline), incubated with horseradish

peroxidase anti-mouse or anti-rabbit secondary antibody and visualized using enhanced chemiluminescent substrate kit (Perkin Elmer). Densitometry analyses were performed using ImageJ. For experiments on insulin signaling, 3T3-L1 adipocytes were washed twice with PBS and 2 mL of low glucose DMEM (2.5% FA free BSA, 1% (v/v) Pen/Strep, 0.5mM D-Glucose, 0.5mM Sodium Acetate, 2mM sodium pyruvate) was added in all wells. 1 μM insulin was added to corresponding wells for 1.5 hr. Phospho-Jnk and Jnk, DYKDDDDDK Tag, HA, phospho-4E-bp and total 4E-bp, phospho-S6 and total S6 antibodies were purchased from Cell Signaling. Phospho-cJun and cJun antibodies were purchased from Santa Cruz. Actin and Flag M2 antibodies were purchased from Sigma and Map4k4 antibody was purchased from Bethyl (#A301-503A).

Srebp Immunoblotting- Srebp-1 antibody was purchased from Millipore (Clone 2121) and Srebp-2 was purchased from Cayman Chemical (#10007663). A minimum of 30μg of protein lysates (2% SDS, 150 mM NaCl and 5mM EDTA) was resolved by SDS-PAGE (8%) and electrotransferred to nitrocellulose membranes. Membranes were incubated with indicated antibodies overnight at 4°C (1:1000). Blots were washed with TBST (0.1% Tween 20 in Tris-Buffered saline), incubated with horseradish peroxidase anti-mouse (for Srebp-1) or anti-rabbit secondary antibody (for Srebp-2) (1hr) and visualized using enhanced chemiluminescent substrate kit (Perkin Elmer). It is important to note that a non-specific band is recognized by Srebp-2 that could be mistaken as the cleaved Srebp-2 protein. Srebp-1 antibody occasionally recognizes a non-specific band circa 75 KDa.

In Vitro Protein Kinase Assay –Map4k4 kinase assays were performed by lysing cells (20mM Tris (pH 7.5), 150mM NaCl, 1 mM EDTA, 1 % Triton X-100, 2.5 mM sodium pyrophosphate, 1mM β-glycerophosphate, 1mM Sodium Orthovanadate and 1 μg/mL leupeptin) and precipitating Map4k4 with HA antibody (Cell Signaling) and protein A agarose beads. Precipitates were washed 4 times and mixed with 40 μL kinase buffer (20mM Hepes pH 7.4, 10mM $MgCl_2$, 20mM β-glycerophosphate, 10mM NaF, 0.2mM Sodium Orthovanadate, 1mM DTT), 5 μg unphosphorylated MBP (Millipore), 250 μM ATP, and 1μCi/reaction ATP. Kinase reactions were performed at 30°C for 30 minutes and terminated with addition of SDS sample buffer and heating the samples to 95°C for 5 minutes. Reaction mixtures were resolved by SDS-PAGE and transferred to a nitrocellulose membrane for autoradiogram and western blot analysis.

Radiolabeled Glucose and Acetate Conversion to TG and FA – The incorporation of the various radioactive substrates into TG and FA was measured as previously described *(277)*. In brief, adipocytes were washed twice with PBS and 1 mL of labeling media (2.5% FA free BSA, 1% (v/v) Pen/Strep, 0.5mM D-Glucose, 0.5mM Sodium Acetate, 2mM sodium pyruvate, 2 μCi/mL ^{14}C-U-glucose or ^{14}C-acetate) was added. Final concentration of 1μM insulin was added to insulin-stimulated conditions. Cells were incubated at 37°C in a humidified incubator (5% CO_2) for 4.5 h before lipid extraction. All metabolic processes were stopped by washing cells twice with cold PBS and lysing cells by the addition of modified Dole's extraction mixture (80 mL isopropanol, 20 mL hexane, 2 mL of 1N H_2SO_4) (278). Triglycerides were extracted with hexane, washed, and the solvent was evaporated. Incorporation of ^{14}C-glucose or ^{14}C-acetate into FA of

TG was determined by evaporating the solvent from the neutral lipids, adding 1 mL KOH-ethanol (20 mL of 95% ethanol, 1 mL water, 1 mL saturated KOH), and heating samples to 80°C for 1 hr. Sulfuric acid was added to the mixture to ensure complete saponification. Addition of hexane allowed hydrophobic separation, which was evaporated and counted by liquid scintillation. Incorporation data were normalized to cell number.

Thin Layer Chromatography – TG and FA were separated by TLC using hexane: ethyl ether: acetic acid (200:50:4). Autoradiography was performed with TG and FA standards. The silica gel from each radiolabeled spot was subsequently scraped and quantified by liquid scintillation.

Results

Map4k4 depletion enhances metabolic gene expression

We have previously shown that Map4k4 depletion enhances Pparγ protein expression and TG accumulation in cultured adipocytes (212, 261). To further investigate the effects of Map4k4 depletion, we used Affymetrix Mouse MOE430-2 microarrays to compare gene expression between scrambled-siRNA versus Map4k4-siRNA treated mature 3T3-L1 adipocytes. KEGG Gene Set Enrichment Profiles using scrambled siRNA versus Map4k4 siRNA-treated adipocytes indicated that the most upregulated genes upon Map4k4 depletion are enriched in metabolic pathways (Pathway 01100), valine, leucine and isoleucine degradation (Pathway 00280), peroxisome biosynthesis (04146), glycolysis (Pathway 00010), pyruvate metabolism (Pathway 00620), fatty acid metabolism (Pathway 00071), insulin signaling pathway (Pathway 04910), and the TCA cycle

(Pathway 00020)(Figure 2.1, A). We further validated the mRNA expression of several lipogenic genes upon Map4k4 depletion in cultured adipocytes (Figure 2.1, B). These analyses suggest that Map4k4 suppresses lipid metabolism-related processes in cultured adipocytes.

Figure 2.1 Map4k4 depletion enhances metabolic gene expression.

A

Gene List	Pathway	P-value
H6pd, Acacb, Hsd3b7, Alg9, Nt5m, Acly, Ppcs, Acaca, Sephs1, Mpi, Pgd, Acat1, Pcca, Acad, Acadvl, Acaa1a, Acads, Aco2, Ak2, Alas1, Pnpla3, Atp6v0e, Auh, Bcat2, Bckdhb, Chkb, Cox8b, Dbt, Dld, Fasn, Gda, Glul, Got1, Gstz1, Hk2, Hmbs, Hmgcl, Hpd, Hyal2, Ldha, Ldhb, Rdh11, Me1, Ndufs4, Ndufv1, Nos3, Ogdh, Pfkl, Pfkm, Pgam1, Plcb4, Pts, Dhrs3, Scp2, St3gal4, St3gal2, Aldh4a1, Chpt1, Itpk1, Atp6v0a2, Tkt, Tpi1, Uck1, Uqcrc1, Ndufs8, Ndufs1, Ccbl2, Coq3, Hadhb, Sc5d, Dlat, Impdh1, Mgll, Papss2, Chsy1, Gcdh, Ptdss2, Pdhx, Agpat3, Dhrs4, Pmm1, Itpkb, Pon2, Acsl5, Coq5, Acaa2, Pla2g6, Ivd, Apip, Pfkp, Suclg1, Mlycd, Pigo, Dhodh, Pdxp, Pole3, Ptges, Ndufa3, Pla2g12a, Cyc1, Uqcrfs1, Alg14, Ndufb7, Pi4k2b, Pgp, Aldh3b1, Idh3a, Ndufa5, Pdhb, Pcyt2, Cmbl, Cox11, Ndufa11, Ndufab1, Cox10, Pgm2, Gbe1, Gale, Pank1, Grhpr, Gpt, Nt5c2, Agl, Mccc2, Dlst, Ptges2, Hadha	Metabolic Pathways	2.22e-16
Acat1, Pcca, Acaa1a, Acads, Auh, Bcat2, Bckdhb, Dbt, Dld, Hmgcl, Hadhb, Acaa2 Ivd, Mccc2, Hadha	Valine, leucine and isoleucine degradation	1.00e-13
Acaa1a, Abcd1, Crat, Hmgcl, Phyh, Pex11a, Pex16, Pex19, Pxmp2, Scp2, Dhrs4, Acsl5, Pex3, Mlycd, Far1, Nudt12, Pex11c, Gstk1	Peroxisome	1.90e-13
Dld, Hk2, Ldha, Ldhb, Pfkl, Pfkm, Pgam1, Tpi1, Dlat, Pfkp, Aldh3b1, Pdhb, Pgm2	Glycolysis	6.75e-10
Acacb, Acaca, Acat1, Dld, Ldha, Ldhb, Me1, Dlat, Acyp1, Pdhb, Grhpr	Pyruvate metabolism	8.30e-10
Acat1, Acadl, Acadvl, Acaa1a, Acads, Cpt2, Hadhb, Gcdh, Acsl5, Acaa2, Hadh	FA metabolism	3.34e-09
Acacb, Acaca, Araf, Calm3, Fasn, Gys1, Hk2, Pparg1c, Prkar2a, Prkar2b, Sorbs1, Slc2a4, Sos2, Cblb, Ppp1r3d, Eif4e2, Rps6kb2, Rps6kb1	Insulin signaling pathway	3.74e-09
Acly, Aco2, Dld, Ogdh, Dlat, Suclg1, Idh3a, Pdhb, Dlst	TCA cycle	4.64e-09

B

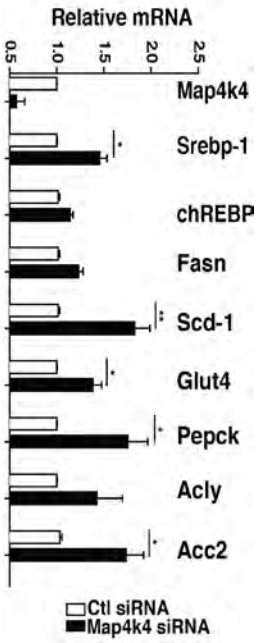

Figure 2.1 Map4k4 depletion enhances metabolic gene expression. (A) KEGG gene set enrichment profile of differentially expressed genes upon Map4k4 depletion (P<.05, fold change 1.3) in murine 3T3-L1 mature adipocytes. The table shows the pathways that were most significantly upregulated by Map4k4 depletion. The gene list contains genes involved in each pathway and the genes in green further represent genes that were significantly upregulated within the specific pathway upon Map4k4 depletion. **(B)** RT-qPCR analysis of metabolic genes upon Map4k4 depletion in mature cultured adipocytes.

Map4k4 functions as a repressor of triglyceride synthesis in cultured adipocytes

To further assess the role of Map4k4 as a negative regulator of TG synthesis in adipocytes, we depleted Map4k4 in mature 3T3-L1 adipocytes using siRNA or elicited increased Map4k4 expression using adenovirus vectors, and measured the conversion of ^{14}C-glucose into neutral lipids. Consistent with the hypothesis that Map4k4 inhibits lipid synthesis, Map4k4 depletion resulted in approximately 50% increased incorporation of the ^{14}C-radiolabel into neutral lipids compared to scrambled control (Figure 2.2, A). Conversely, Map4k4 overexpression significantly reduced ^{14}C-radiolabel incorporation into TG by ~29% compared to the adenovirus HA-control (Ad: HA-control) (Figure 2.2, A). To determine whether Map4k4 was suppressing glycerol-3-phosphate (G-3-P) formation or *de novo* lipogenesis, we measured ^{14}C-radiolabel incorporation into both FA of TG (Figure 2.2, B) and glyceride-glycerol (Figure 2.2, C). We determined that Map4k4 inhibited both glyceride-glycerol formation and *de novo* lipid synthesis in mature adipocytes as seen by increased incorporation of the radiolabel into both molecules upon Map4k4 depletion and decreased incorporation upon Map4k4 overexpression (Figure 2.2, B-C). We also confirmed that these observed changes in neutral lipid synthesis and *de novo* lipogenesis reflect changes in TG and FA, respectively, by TLC analysis (data not shown).

Figure 2.2 Map4k4 represses triglyceride synthesis in cultured adipocytes.

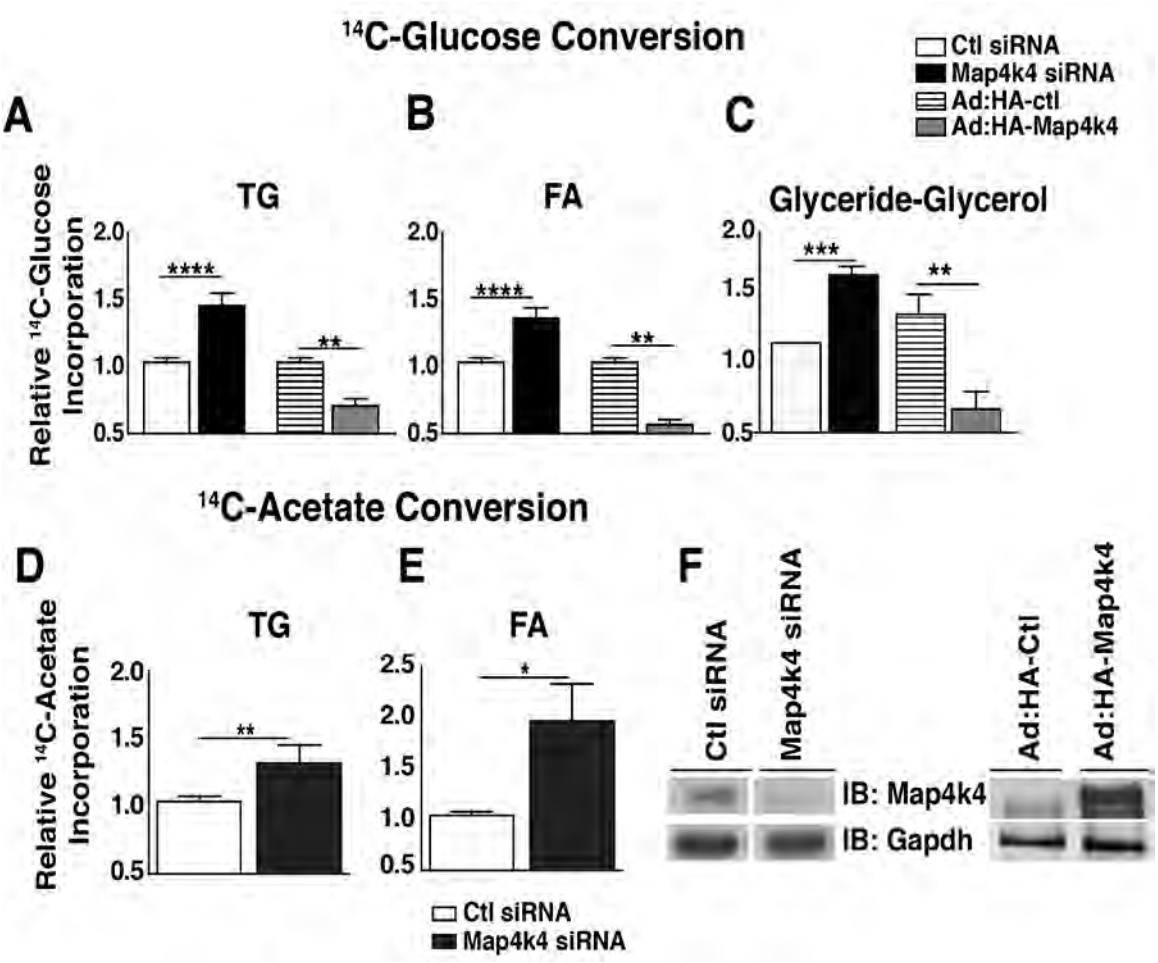

Figure 2.2 Map4k4 represses triglyceride synthesis in cultured adipocytes. (A-C) ^{14}C-glucose conversion into TG **(A),** FA **(B),** and glyceride-glycerol **(C)** is shown. Cells were transfected by electroporation with scrambled (7.5 μM) or Map4k4 (7.5 μM) siRNA (N=9) or were infected with control virus (Ad: HA-Ctl) or HA-Map4k4 adenovirus (Ad: HA-Map4k4) (N=4). 72 hrs. post-transfection, cells were incubated with ^{14}C-glucose for 4hr and triglycerides extracted. **(D-E)** ^{14}C-acetate conversion into TG **(D)** and FA **(E)** is shown; lipids were extracted as **(A). (F)** Representative immunoblots depicting Map4k4 protein expression upon siRNA transfection or adenoviral overexpression. Samples were noncontiguous on the same gel. The data are represented as the average +/- SE and were compared to appropriate controls by Student's T-test. ****P<. 0001, **P<. 01.

We have previously reported that Map4k4 silencing increases Glut4 expression and glucose uptake (212), possibly providing the substrate for both glyceride-glycerol and fatty acid synthesis. To distinguish whether Map4k4 regulates lipid synthesis independent of glucose flux, we used either control or Map4k4 siRNA-transfected adipocytes and measured ^{14}C-acetate incorporation into TG. ^{14}C-acetate incorporation into TG is a measure of *de novo* lipogenesis as the radiolabel bypasses glucose transport and metabolism and provides the substrate for FA synthesis. Consistent with Map4k4 inhibiting lipid synthesis, Map4k4 depletion significantly increased ^{14}C-acetate incorporation into TG and its constituent FA (Figure 2.2, D-E). Representative protein immunoblots confirmed Map4k4 knockdown or overexpression at the protein level (Figure 2.2, F). These results indicate that Map4k4 is a negative regulator of glucose flux, *de novo* FA synthesis, and TG synthesis in cultured adipocytes.

Map4k4 silencing does not enhance lipid synthesis via Jnk signaling

Map4k4 has been proposed to be a pro-inflammatory kinase and upstream positive regulator of the Jnk signaling cascade (267-269). Because the role of adipose Jnk in lipid synthesis has not been clearly established, we tested whether Map4k4 repressed lipogenesis via Jnk. We hypothesized that if Map4k4 was an upstream activator of Jnk, then Jnk depletion would enhance lipid synthesis compared to scrambled control, similar to Map4k4 depletion. 3T3-L1 adipocytes were electroporated with scrambled siRNA or siRNA against Map4k4 or Jnk1 and Jnk2, and ^{14}C-acetate incorporation into FA and TG was used to assess the role of these kinases in TG synthesis and *de novo* lipogenesis.

Consistent with results shown in Figure 2.2, Map4k4 depletion significantly increased ^{14}C-acetate incorporation into TG (Figure 2.3, A-B). Surprisingly, depletion of the two major isoforms of Jnk, Jnk1 and Jnk2, significantly reduced TG synthesis by 56%, opposite to the effects observed upon Map4k4 silencing (Figure 2.3, A-B). Furthermore, ^{14}C-acetate incorporation into FA, a measure of *de novo* lipogenesis, was significantly increased upon Map4k4 silencing (~47%) and decreased upon Jnk depletion (~20%) (Figure 2.3, A, C). Efficient Map4k4 and Jnk protein depletion was confirmed by protein immunoblots (Figure 2.3, D). Therefore, these data demonstrate that while Map4k4 downregulates lipogenesis, Jnk1 and Jnk2 are required for this process. We next examined whether Jnk and Map4k4 depletion affected lipogenic gene expression in a dissimilar fashion using RT-qPCR (Figure 2.3, E). Consistent with the effects observed using ^{14}C-acetate, Map4k4 depletion significantly enhanced the mRNA expression of Srebp-1, Chrebp, Fasn, Scd-1, Pepck, and Glut4, while Jnk depletion decreased the mRNA expression of these genes (Figure 2.3, E). These results indicate that Map4k4 is a repressor of adipose lipogenesis while Jnk is an unexpected positive regulator of this metabolic process. Furthermore, Map4k4 does not repress lipogenesis in a Jnk-dependent manner.

Figure 2.3 Map4k4 does not regulate lipid synthesis via Jnk.

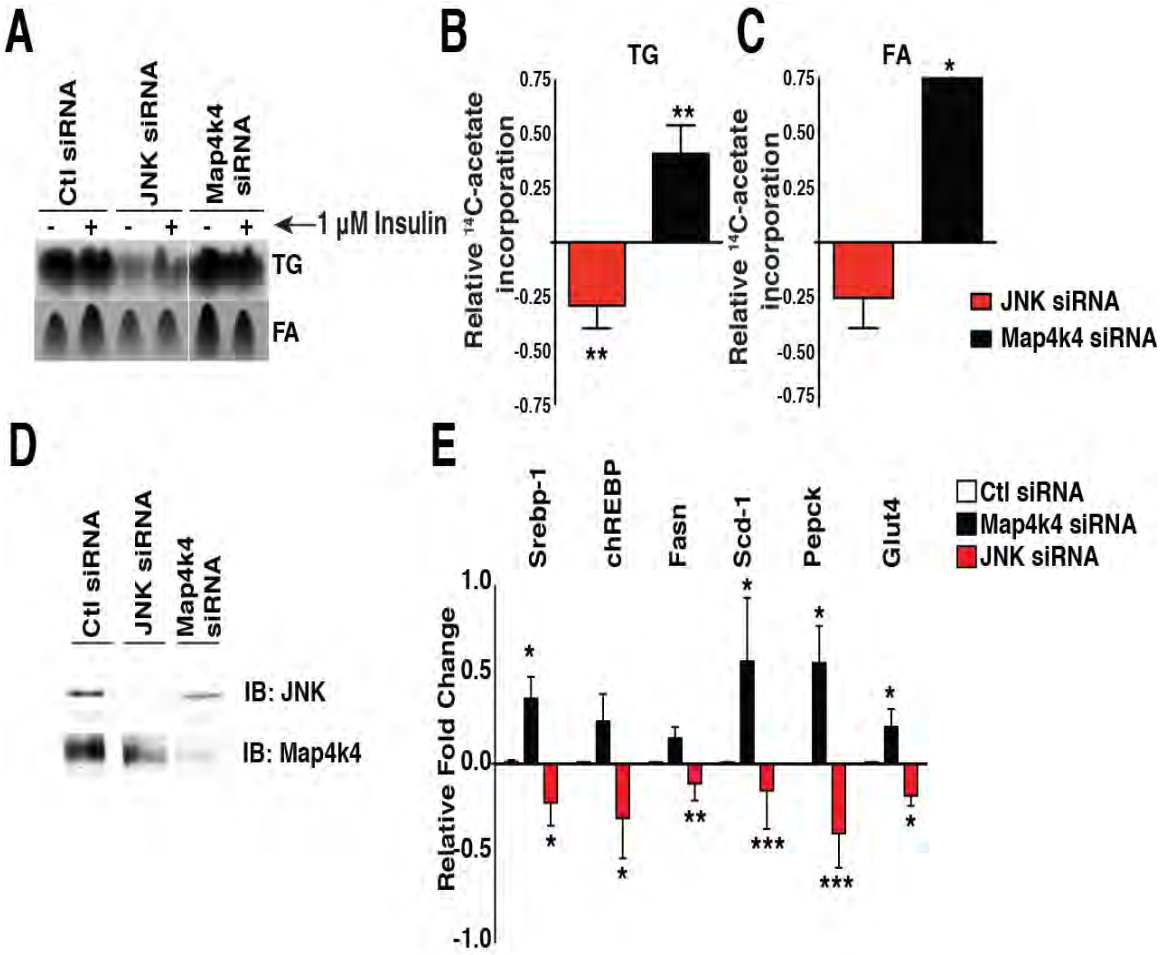

Figure 2.3 Map4k4 does not regulate lipid synthesis via Jnk. (A) Autoradiogram of TLC analysis of TG and FA extracted from adipocytes that were transfected with scrambled siRNA, Jnk1 and Jnk2 siRNA, or Map4k4 siRNA. 72 hrs. post transfection, adipocytes were incubated with ^{14}C-acetate and incorporation into TG and FA was determined. Samples were noncontiguous on the same TLC plate. **(B-C)** Changes in ^{14}C-acetate incorporation into TG **(B)** and FA **(C)** in Jnk- and Map4k4-depleted mature adipocytes relative to Scrambled control. **(D)** Representative immunoblots for Map4k4 and Jnk protein expression in control, Map4k4- and Jnk-depleted cells. **(E)** RT-qPCR analysis of lipogenic gene expression in control, Map4k4- and Jnk-depleted adipocytes relative to scrambled control siRNA-treated cells (N=5). Data are presented as average +/- SE and were compared between groups by Student's T-test. * P<. 01, ** P<. 001, *** P<. 0001.

Map4k4 does not activate the Jnk signaling pathway in adipocytes

These divergent effects of Map4k4 and Jnk were unexpected in light of previous reports that suggest Map4k4 functions as an upstream activator of Jnk in various cell models (267-269). To further investigate whether increased Map4k4 expression and activity would be sufficient to increase endogenous Jnk signaling in adipocytes, we used adenoviral-mediated Map4k4 overexpression followed by stimulation with tumor necrosis factor alpha (Tnf-α), a potent Jnk activator (Figure 2.4). Despite increased expression and activity of Map4k4 (Figure 2.4, A), phosphorylation of Jnk and its downstream substrate cJun did not differ between empty virus (Ad: HA-control) and Map4k4 adenoviral (Ad: HA-Map4k4)-treated adipocytes in both basal and Tnf-α-treated conditions (Figure 2.4, B). Thus, while increased Map4k4 expression and activity inhibited TG synthesis (Figure 2.2), it was not sufficient to alter endogenous Jnk signaling in adipocytes. Furthermore, if Map4k4 is a required upstream activator of Jnk, Map4k4 depletion should attenuate Jnk activation in response to Tnf-α treatment. Map4k4 depletion, however, did not attenuate Jnk activation (Figure 2.4, C) or affect the expression of activator protein-1 (AP-1) transcriptional factors – cJun, C-fos, and JunD – in response to Tnf-α (Figure 2.4, D). As expected and consistent with previous results (279), Jnk depletion attenuated the maximal response of these AP-1 transcriptional factors in response to Tnf-α (Figure 2.4, D). These results indicate that Map4k4 is neither sufficient nor required to induce Jnk activation in adipocytes. Furthermore, using gain-of-function approaches in HEK 293T cells, we show that co-transfection of both Map4k4 and Jnk increases Jnk activity, consistent with published results (Figure 2.5, A-B);

however, depletion of endogenous Map4k4 does not diminish Jnk activity (Figure 2.5, C), suggesting that Map4k4 is not an endogenous modulator of Jnk signaling. These results support the notion that endogenous Map4k4 is not required for optimal endogenous Jnk activation in adipocytes or HEK 293T cells, but that artificially high levels of exogenously expressed Map4k4 and Jnk can enhance Jnk signaling.

Figure 2.4 Map4k4 is neither necessary nor sufficient for canonical Jnk signaling.

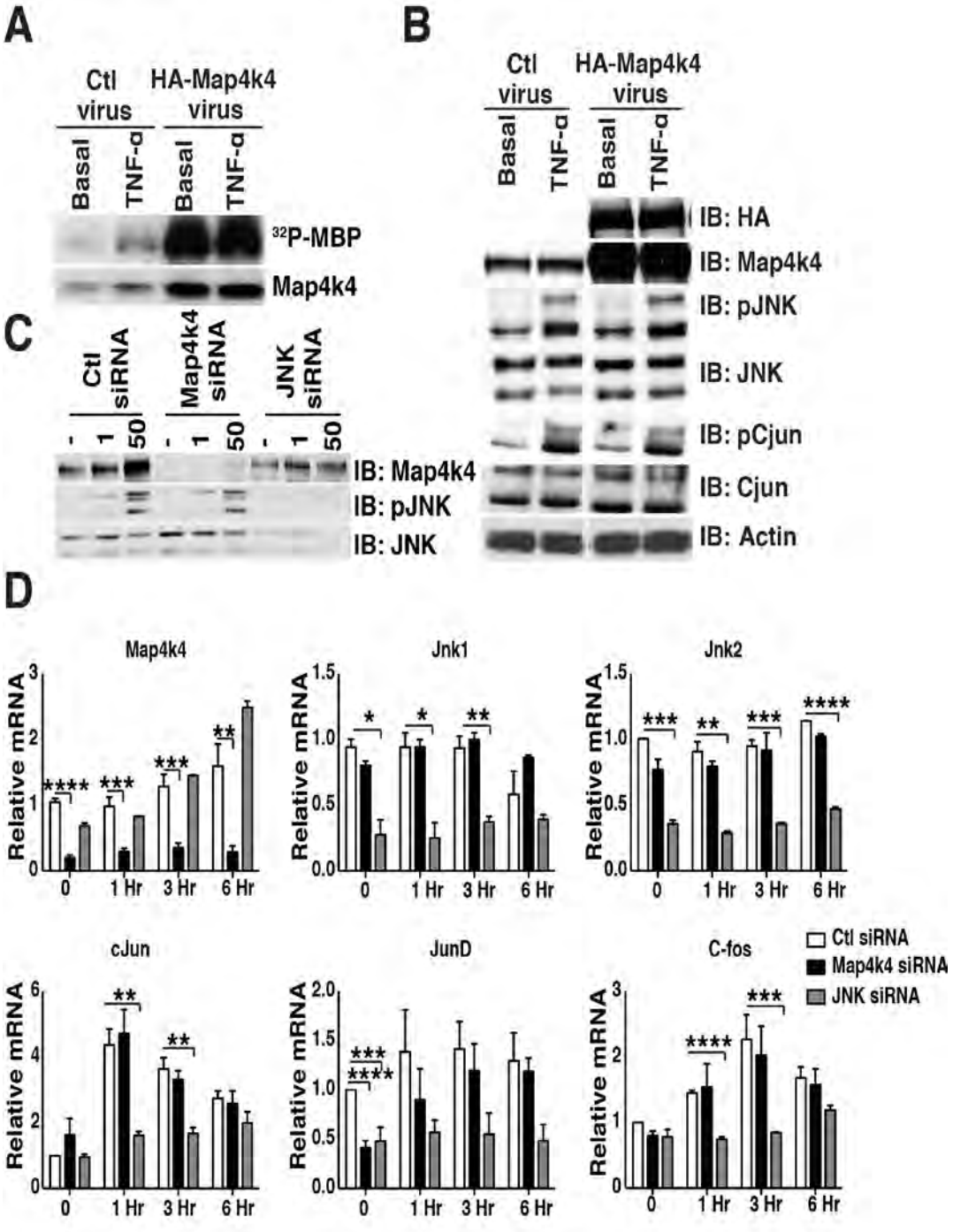

Figure 2.4 Map4k4 is neither necessary nor sufficient for canonical Jnk signaling. **(A)** Map4k4 kinase activity in control and Map4k4-overexpressing adipocytes stimulated with Tnf-α for 30 min. **(B)** Protein immunoblots of control and Map4k4-overexpressing adipocytes treated with 50 ng/mL Tnf-α for 15 min (N=4). Samples were noncontiguous on the same gel. **(C)** Protein immunoblot of electroporated adipocytes treated with control, Map4k4 or Jnk1 and Jnk2 siRNA and stimulated with 50 ng/mL Tnf-α for 15 min (N=4). **(D)** RT-qPCR analysis of AP-1 transcription factors in response to 50 ng/mL Tnf-α treatment in control, Map4k4-depleted or Jnk-depleted adipocytes (N=3).

Figure 2.5 Ectopic Jnk and Map4k4 expression enhances Jnk signaling.

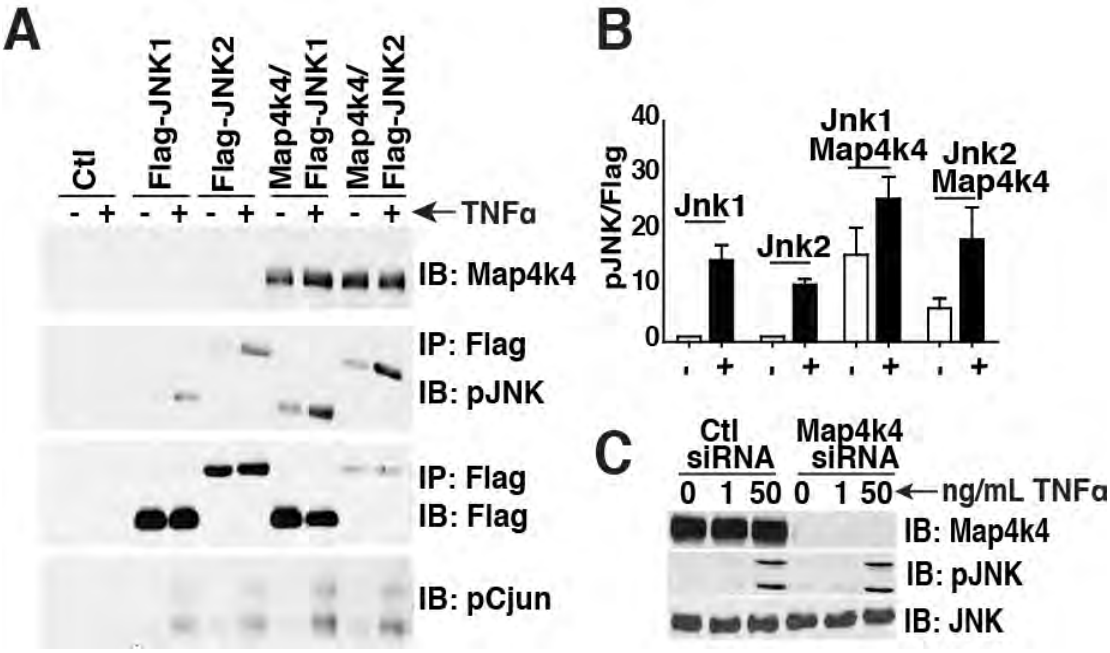

Figure 2.5 Ectopic Jnk and Map4k4 expression enhances Jnk signaling. (A) Protein immunoblots depicting Jnk activation in response to 50ng/mL Tnf-α in HEK 293T cells transfected with equal amounts of empty vector, HA-Map4k4, Flag- Jnk1 or Flag- Jnk2 constructs (N=3). **(B)** Quantification of **(A). (C)** Map4k4 was depleted in HEK 293T cells using siRNA and cells were stimulated with 1 ng/mL and 50 ng/mL Tnf-α for 15 min. Protein immunoblots depicting Jnk activation are shown (N=3).

Map4k4 inhibits lipid synthesis in an mTORC1-dependent manner

We have previously demonstrated that Map4k4 impairs mTORC1 signaling (261) and since mTORC1 signaling enhances lipid synthesis (254, 256, 266, 280), we tested whether Map4k4 required mTORC1 to inhibit lipid synthesis. We depleted Map4k4 using siRNA and treated cells with rapamycin, an mTOR inhibitor, to repress mTORC1 signaling. Consistent with previous reports, Map4k4 depletion enhanced mTORC1 signaling as demonstrated by increased ribosomal protein S6 (S6) and eukaryotic translation initiation factor 4E binding protein 1 (4E-bp1/Eif4ebp1) protein phosphorylation (261) (Figure 2.6, A). Interestingly, Map4k4 depletion also increased Srebp-1 protein levels, an important lipogenic transcription factor (Figure 2.6, A). Rapamycin treatment inhibited mTORC1 signaling, as evidenced by a lack of S6 and 4E-bp1 protein phosphorylation, and abolished the increase in Srebp-1 protein expression that resulted from Map4k4 silencing (Figure 2.6, A). Rapamycin treatment also diminished the Map4k4 silencing-induced increase in ^{14}C-glucose incorporation into TG (Figure 2.6, B) and FA (Figure 2.6, C). These results indicate that proper mTORC1 function is necessary for Srebp-1 expression and optimal lipid synthesis in cultured adipocytes and support the notion that Map4k4 represses the mTORC1/Srebp pathway to inhibit adipose lipogenesis.

Figure 2.6. Map4k4 regulates mTORC1 to inhibit Srebp-1 expression and triglyceride synthesis.

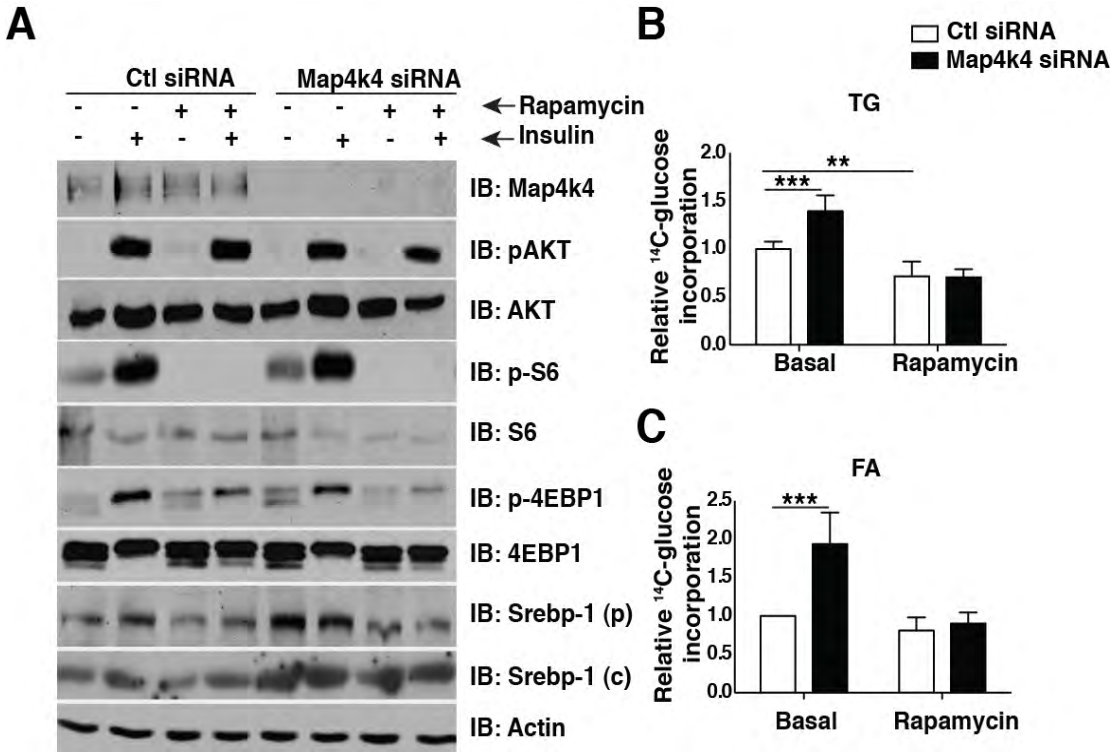

Figure 2.6 Map4k4 regulates mTORC1 to inhibit Srebp-1 expression and triglyceride synthesis. (A) 3T3-L1 adipocytes were electroporated with control siRNA or Map4k4 siRNA and treated with 100 nM rapamycin for 48 hrs. and/or insulin for 1.5 hrs. Protein immunoblots depicting insulin-induced Akt and mTORC1 activation and rapamycin-induced inhibition in control and Map4k4-depleted adipocytes. **(B-C)** Incorporation of ^{14}C-glucose into TG **(B)** and saponifiable FA **(C)** in control siRNA treated or Map4k4-depleted adipocytes treated with rapamycin. The data are represented as the average +/- SE and were compared between groups by Student's T-test (N=4, *** P<. 0001).

Map4k4 depletion requires Srebp expression to enhance lipid synthesis

We demonstrated that Map4k4 depletion enhances mTORC1 signaling and increases Srebp-1 protein expression (Figure 2.6, A). As an alternative approach to assess the effect of impaired Map4k4 function, we used a kinase-inactive mutant of Map4k4 (AdMap4k4 D152N) (281), previously shown to function as a dominant-negative inhibitor (234). Consistent with silencing experiments using siRNA (Figure 2.6, A), Map4k4 D152N overexpression resulted in increased cleaved Srebp-1 protein levels (Figure 2.7, A-B). Similarly, adenovirus-mediated overexpression of wild-type Map4k4 results in decreased Srebp-1 protein levels (Figure 2.8, A) and decreased lipogenic gene expression (Figure 2.8, B), consistent with reduced lipid synthesis (Figure 2.2, A-C). To determine whether Map4k4 depletion requires the increase in Srebp-1 protein to enhance lipid synthesis, we performed gene silencing experiments using siRNA to suppress either Map4k4, Srebp-1 and Srebp-2, or Map4k4/Srebp-1/Srebp-2 expression in mature cultured adipocytes and examined conversion of ^{14}C-glucose into TG and FA. Depletion of both Srebp-1 and Srebp-2 was required in these experiments because depletion of either transcription factor alone resulted in a compensatory increase by the other transcription factor (data not shown). Protein immunoblots demonstrated that Map4k4 knockdown resulted in a significant increase in precursor and cleaved Srebp-1 protein levels as well as an increase in total Srebp-2 protein levels (Figure 2.9, A). Consistent with Figure 2.1 (B) and Figure 2.3. (E), Map4k4 silencing significantly increased the mRNA expression of known Srebp-1 lipogenic target genes including Acaca (~73%), Scd-1 (~78%), and Fasn (~23%) (247, 249, 250) (Figure 2.9, B). Interestingly, Map4k4 depletion requires Srebp

expression to increase lipogenic gene expression as depletion of Srebp-1 and Srebp-2 in the context of Map4k4 depletion severely blunted the enhanced expression of these lipogenic genes (Figure 2.9, B). Map4k4 depletion also significantly increased ^{14}C-glucose conversion into both TG (Figure 2.9, C) and FA (Figure 2.9, D), as demonstrated in previous figures, and depletion of both Srebp transcription factors significantly blunted the increase in radiolabel incorporation into TG and FA in response to Map4k4 silencing (Figure 2.9, C-D). Consistent with Srebp transcription factors regulating lipid synthesis, depletion of both Srebp-1 and Srebp-2 significantly reduced adipose lipogenesis as assessed by reduced radiolabel incorporation into TG and FA (Figure 2.9, C-D). These results indicate that Srebp proteins are necessary for optimal adipose lipogenesis and are also required to mediate the effects of Map4k4 on lipid synthesis.

Figure 2.7 Map4k4 kinase inactivity results in increased Srebp-1 protein levels.

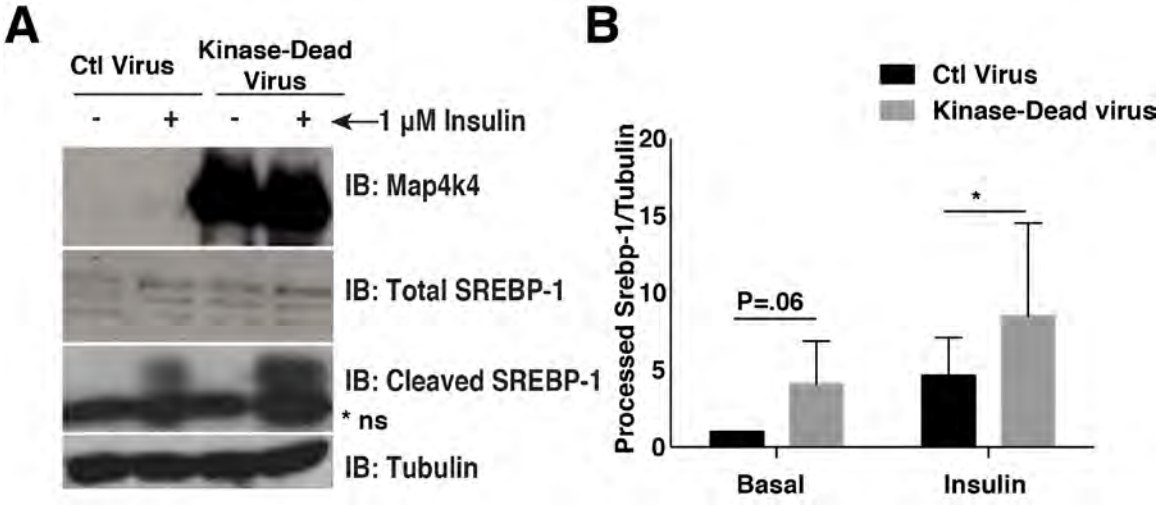

Figure 2.7 Map4k4 kinase inactivity results in increased Srebp-1 protein levels. (A) Representative Srebp-1 protein immunoblot of mature adipocytes infected with control or Map4k4 dead-kinase virus. 72 hrs. post-infection, cells were serum-starved for 2 hrs. and treated with 1 μM insulin for 3.5 hrs. **(B)** Quantification of **A** (N=3). Data are presented as average +/- SEM and compared between groups by Student's T-test (*P<.05).

Figure 2.8 Increased Map4k4 expression and activity decreases lipid synthesis.

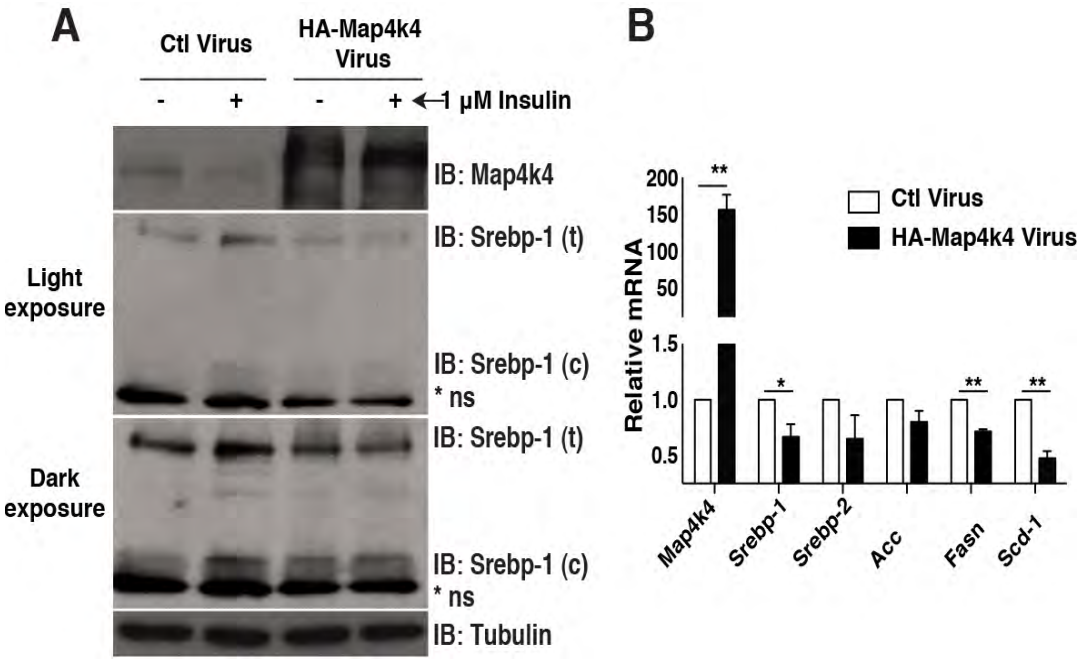

Figure 2.8 Increased Map4k4 expression and activity decreases lipid synthesis. **(A)** Representative Srebp-1 protein immunoblot of control and Map4k4-overexpressing adipocytes treated with 1 uM insulin for 3.5 hrs. (N=4). **(B)** RT-qPCR analysis of lipogenic gene expression in control and Map4k4-overexpressing adipocytes (N=4). Data are presented as average +/- SE and were compared between groups by Student's T-test. * P<.01, ** P<.001.

Figure 2.9 Map4k4 regulates lipogenesis via Srebp.

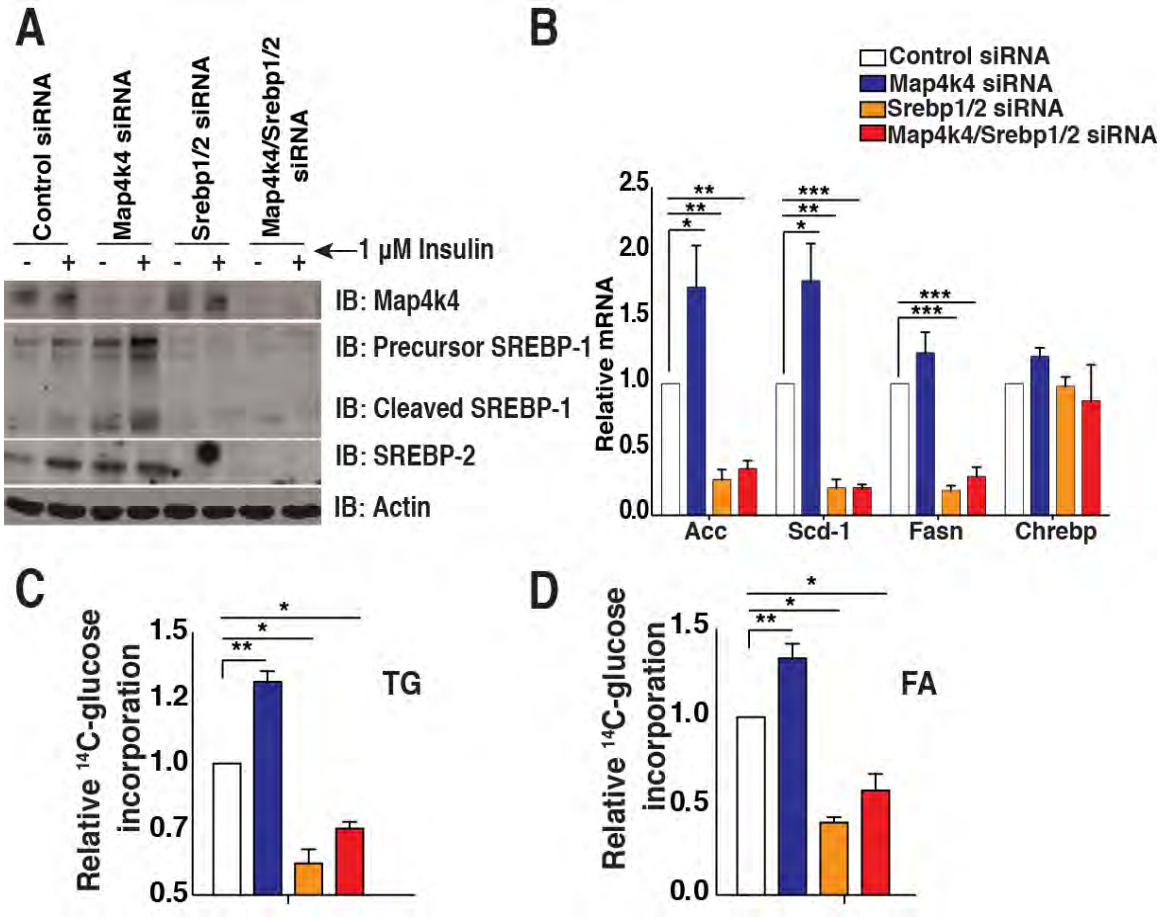

Figure 2.9 Map4k4 regulates lipogenesis via Srebp. (A) Mature 3T3-L1 adipocytes were transfected with control siRNA, Map4k4 siRNA, Srebp-1 and Srebp-2 siRNA, or Map4k4/Srebp-1/Srebp-2 siRNA and treated with 1 μM insulin for 1.5 hrs. Cells were harvested and Map4k4, Srebp-1, and Srebp-2 protein expression was analyzed by protein immunoblots. **(B)** RT-qPCR analysis of lipogenic gene expression in control, Map4k4, Srebp1 and Srebp2, and Srebp1, Srebp2 and Map4k4-depleted adipocytes. **(C-D)** Incorporation of ^{14}C-glucose into TG **(C)** and FA **(D)** in control, Map4k4-depleted, Srebp-1 and Srebp-2 depleted or Map4k4/Srebp-1/Srebp-2 depleted adipocytes was measured. The data are represented as the average +/- SE and were compared between groups by Student's T-test. (N=4, * P<. 01, ** P<. 001, *** P<. 0001).

Map4k4 is a positive regulator of Ampk.

Map4k4 has been implicated as a positive regulator of Ampk activity (282), and Ampk is a negative regulator of mTORC1, suggesting a plausible mechanism by which Map4k4 may negatively regulate mTORC1 and inhibit lipogenesis. We verified that Map4k4 regulates Ampk signaling in cultured adipocytes by treating Map4k4-depleted adipocytes with oligomycin, an inhibitor of ATP synthase and potent activator of Ampk. As expected, treatment of adipocytes with oligomycin (500 nM for 30 minutes) increased Ampk phosphorylation. This response was significantly blunted in Map4k4-depleted adipocytes (Figure 2.10, A-B). Furthermore, decreased Ampk activation results in increased mTOR signaling (as assessed by decreased Raptor phosphorylation (Ser792)) and increased lipogenesis (as assessed by ACC phosphorylation (Ser79)) (Figure 2.10, A). Attenuation of Ampk signaling in response to Map4k4 depletion also occurs with other Ampk activators including glucose withdrawal and phenformin (data not shown). On the other hand, increased Map4k4 expression and activity results in increased Ampk signaling as assessed by increased pAmpk and pACC in response to oligomycin treatment (Figure 2.10, C). These results suggest Map4k4 is necessary for optimal Ampk activation and provide insights into the mechanism by which Map4k4 inhibits mTORC1 and lipid synthesis in mature adipocytes.

Figure 2.10 Map4k4 regulates Ampk signaling.

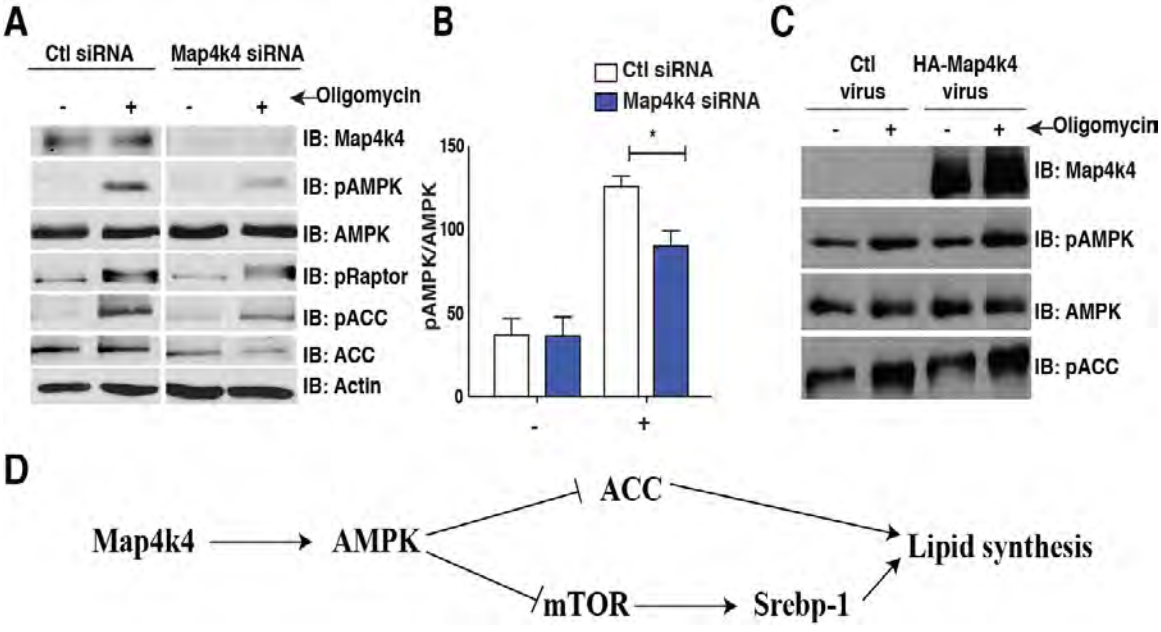

Figure 2.10 Map4k4 regulates Ampk signaling. (A) Protein immunoblot of 3T3-L1 adipocytes transfected with control siRNA or Map4k4 siRNA and treated with 500 nM oligomycin for 30 minutes (N=5). **(B)** Quantification of **(A). (C)** Protein immunoblot of 3T3-L1 adipocytes infected with control virus (empty adenovirus) or HA-Map4k4 adenovirus and treated with 500 nM oligomycin for 30 minutes (N=4). **(D)** Schematic model coupling Map4k4 to Ampk and mTOR to inhibit lipid synthesis.

Discussion

Here we show that adipose Map4k4 represses glucose incorporation into FA and TG, at least in part via Ampk regulation, which results in downregulation of mTORC1 function and Srebp-1 expression. We found that Map4k4 depletion enhances the conversion of both ^{14}C-glucose and ^{14}C-acetate into TG and FA (Figure 2.2, Figure 2.3), suggesting Map4k4 inhibits both *de novo* FA synthesis and FA esterification. Conversely, increased Map4k4 expression decreases the conversion of ^{14}C-glucose into TG (Figure 2.2, A-C). We provide strong evidence to suggest that the ability of Map4k4 to repress adipose lipogenesis is independent of the Jnk signaling pathway, which we unexpectedly found to be required for optimal TG synthesis in cultured adipocytes (Figure 2.3). These findings have direct relevance to the adipose dysfunction, including chronic inflammation and impaired lipid storage capacity, that occurs with obesity, because Map4k4 expression is elevated with increasing body mass index (BMI) (271). This increased Map4k4 expression could contribute to impaired lipid buffering (TG synthesis and storage) in obese adipose tissue. Upon evaluating underlying mechanisms of Map4k4 action, we show that Map4k4 is required for activation of Ampk signaling, which in turn is expected to modulate mTORC1 and Srebp-1 activity, and adipose lipogenesis. Thus, our results provide evidence for a model in which Map4k4 modulates Ampk, suppressing mTORC1 function and Srebp-1 expression to depress lipogenesis (Figure 2.10, D).

Our results are consistent with previous studies that describe a positive role of Jnk in adipose lipogenesis (283-285). Jnk1 depletion using anti-sense oligonucleotides in

adipose tissue attenuates the expression of lipogenic enzymes Acly, Acaca, Fasn, and Scd-1 (283) and Jnk2 suppression in human adipocytes attenuates Srebp-1 expression and activity resulting in decreased target lipid enzymes (285). Mice expressing a mature, transcriptionally active Srebp-1 variant lacking all of the Jnk phosphorylation sites are protected from hepatic steatosis and weight gain, thus demonstrating that Jnk positively regulates Srebp-1 function (286). Furthermore, Jnk is required for optimal Srebp-1 activation and the subsequent increase in Scd-1 and Fasn in response to keratinocyte growth factor treatment (284). We have therefore confirmed the positive role of Jnk in adipose lipogenesis and have further established that Map4k4 does not require Jnk to inhibit TG synthesis. We also provide evidence that Map4k4 is neither required nor sufficient to activate endogenous Jnk signaling. Consistent with previous reports, we find that co-transfection of Jnk and Map4k4 enhanced Jnk signaling (267-269); however, increased Map4k4 activity and expression alone were not sufficient to activate endogenous Jnk, and Map4k4 depletion did not attenuate Tnf-α-induced Jnk activation (Figure 2.4). Therefore, our results suggest that Map4k4 is not an upstream activator of Jnk in cultured adipose cells or HEK 293T cells (Figure 2.5), and that previous results placing Map4k4 in the Jnk signaling pathway may be due to artificially high ectopic expression of both of these protein kinases.

These results extend our previous findings that Map4k4 represses mTORC1 signaling in adipocytes (261) and shed insight into the mechanism by which Map4k4 represses lipid synthesis. The role of Srebp-1 in adipose lipogenesis has been largely dismissed because

Srebp-1 null animals form functional fat depots (287, 288). However, the loss of Srebp-1 increases Srebp-2 expression and activity, compensating for the loss of Srebp-1 (287, 288). Furthermore, while overexpression of the nuclear fragment of Srebp-1c causes lipodystrophy (289), overexpression of a different isoform, Srebp-1a, increases the expression of downstream lipogenic target genes such as Fasn and Scd-1 (290). Because we observed compensation of Srebp isoforms in cultured adipocytes (data not shown), we targeted both Srebp-1 and Srebp-2 to deplete lipogenesis (Figure 2.9). Interestingly, liver specific depletion of SCAP, a regulatory protein that is required for Srebp protein proteolytic cleavage, decreased Srebp-1 and Srebp-2 expression with a concomitant reduction in obesity-induced hepatic steatosis, consistent with the notion that depletion of both Srebp proteins is required to diminish lipogenesis (195, 291). Our results support an active role for Srebp-1 and Srebp-2 in adipose lipogenesis and demonstrate that Map4k4 inhibits lipid synthesis via suppression of Srebp proteins (Figure 2.9).

Mechanistically, it is unclear how mTORC1 regulates Srebp-1 function (254-257). Rapamycin, a general mTOR inhibitor, disrupts Srebp-1 expression and maturation, thus decreasing lipogenesis (254, 256, 263-265). We have previously shown that Map4k4 inhibits mTORC1 function and we further show that this inhibition decreases Srebp-1 expression (Figure 2.8) and adipose lipogenesis. Map4k4 depletion enhances protein translation in an mTORC1-dependent manner (261) and this may explain the increased Srebp-1 protein expression (both precursor and cleaved product) upon Map4k4 depletion. Interestingly, Map4k4 depletion does not affect Srebp-1 protein stability (data not shown)

as previously reported for Pparγ (261) and Myf5 (234). Furthermore, we provide data that suggests Map4k4 inhibits mTORC1 function via Ampk modulation. Map4k4 depletion attenuates Ampk signaling (Figure 2.10, A-B), resulting in decreased ACC and Raptor phosphorylation, translating into increased lipid synthesis. Thus, Map4k4 represses lipid synthesis in an mTORC1- and Srebp-1-dependent manner and this is independent of Jnk-signaling. Because adipose tissue Map4k4 expression is increased during obesity (271), Map4k4 may be an important negative regulator of adipose lipogenesis in metabolic disease.

ACKNOWLEDGEMENTS

This work was supported by the National Institutes of Health Grant DK030898 (to M.P.C.) and core facility support from the University of Massachusetts Medical School Diabetes and Endocrinology Research Center (DERC) Grant DK032520.

CHAPTER III:

Inducible deletion of protein kinase Map4k4 in obese mice improves insulin sensitivity in liver and adipose tissues.

This chapter is derived from the article of the same name that appeared in publication in Molecular and Cellular Biology:

Laura V. Danai, Rachel J. Roth Flach, Joseph V. Virbasius, Lorena Garcia Menendez, , Dae Young Jung, Jong Hun Kim, Jason K. Kim, Michael P. Czech.Mol Cell Biol. 2015.

Author Contributions

- **Figure 3.1 A-E, H. Tamoxifen-inducible mice generation and characterization.**This work was performed in conjunction with Rachel J. Roth Flach, Czech Lab. These experiments include backcrossing Map4k4 Floxed mice into pure C57BL/6J mice, isolation of various tissues for RNA and protein extraction, body weight measurements, and tissue histology.
- **Figure 3.1 F-G. Metabolic cage analysis of inducible Map4k4-KO mice.** These experiments were performed byDae Young Jung, Kim Lab.
- **Figure 3.2 B-E. Fluorescence-activated cell sorting (FACs).** These experiments were performed by Rachel J. Roth Flach, Czech Lab.
- **Figure 3.3. Metabolic characterization of inducible Map4k4-KO mice.** These experiments were performed in conjunction with Rachel J. Roth Flach, Czech Lab.
- **Figure 3.6 D, G, H-K. Metabolic cage analysis of Myf5-Map4k4-KO mice.** These experiments were performed byDae Young Jung, Kim Lab.
- The rest the experiments presented in this chapter were performed by Laura V. Danai.
- This manuscript was written by Laura V. Danai with helpful suggestions from Rachel J. Roth Flach, Joseph V. Virbasius, and Michael P. Czech.

.

Summary

Studies *in vitro* suggest that the protein kinase Map4k4 attenuates insulin signaling, but confirmation *in vivo* is lacking since global Map4k4 deletion is lethal during embryogenesis. We thus generated mice with floxed Map4k4 alleles and a tamoxifen-inducible Cre/ERT^2 recombinase under the control of the Ubiquitin C promoter to induce whole-body Map4k4 deletion after animals reach maturity. Tamoxifen administration induced Map4k4 deletion in all tissues examined, causing decreased fasting blood glucose concentrations and enhanced insulin signaling to Akt in adipose tissue and liver, but not skeletal muscle. Surprisingly, however, mice generated with conditional Map4k4 deletion in adiponectin-positive adipocytes or in albumin-positive hepatocytes displayed no detectable metabolic phenotypes. Instead, mice with Map4k4 deleted in Myf5-positive tissues, including all skeletal muscles tested, were protected from obesity-induced glucose intolerance and insulin resistance. Remarkably, these mice also showed increased insulin sensitivity in adipose tissue but not skeletal muscle, similar to the metabolic phenotypes observed in inducible whole-body knockout mice. Taken together, these results indicate that, 1.) Map4k4 controls a pathway in Myf5-positive cells that suppresses whole-body insulin sensitivity and 2.) Map4k4 is a potential therapeutic target for improving glucose tolerance and insulin sensitivity in type-2 diabetes.

Introduction

Whole-body glucose homeostasis in humans is maintained by an elaborate physiological system that involves multi-organ regulation. In the post-prandial state, glucose and amino acids induce β-cells in the pancreas to secrete insulin, promoting glucose uptake in skeletal muscle and adipose tissue while suppressing glucose production from the liver. These effects of insulin to maintain glucose homeostasis can be disrupted in obesity, causing an insulin-resistant state that contributes to elevated blood glucose levels and an increased incidence of type-2 diabetes (T2D) (292). While metformin (thought to mainly affect liver glucose metabolism) and insulin secretagogues are clinical mainstays for the treatment of T2D, further intervention is often required (15). Treatments that address the underlying peripheral insulin resistance in T2D are now limited due to contra-indications to the use of thiazolidinediones (TZDs), a major drug class that alleviates insulin resistance by targeting Peroxisome Proliferator-Activated Receptor (Pparγ) (16, 17). Thus, novel proteins that could be targeted with drugs to enhance peripheral insulin sensitivity would prove useful in developing therapies for T2D.

In screening the adipocyte kinome for such negative regulators of insulin signaling to glucose transport *in vitro*, we identified Map4k4, a serine/threonine protein kinase with homology to yeast Ste20 protein kinases (212). Interestingly, single nucleotide polymorphisms (SNPs) in the Map4k4 locus appear to be associated with insulin resistance (293) and T2D (294). We therefore hypothesized that Map4k4 may be a novel therapeutic target for improving obesity-induced peripheral insulin resistance. The

functions of Map4k4 in insulin signaling and energy metabolism were subsequently studied in various cell culture models. In adipocytes, Map4k4 repressed glucose transport and lipid synthesis (212, 236) while in human myotubes, Map4k4 depletion protected cells from Tnf-α-induced insulin resistance (232). These studies suggested that systemic Map4k4 depletion might improve whole-body glucose metabolism in obesity. However, the effects of systemic Map4k4 deficiency on metabolic disease *in vivo* have not yet been studied due to the embryonic lethality of Map4k4-*null* mice (214). To circumvent this problem, we generated an inducible gene deletion mouse model to investigate the physiological effects of Map4k4 depletion once mice reach maturity. We sought to address several questions employing this model. First, is Map4k4 required for viability of adult mice? Second, is Map4k4 a negative regulator of systemic insulin sensitivity and metabolic function in obese animals? Lastly, in what tissue or tissues may Map4k4 operate to modulate whole-body glucose homeostasis and insulin responsiveness?

Here we report that mature mice with induced systemic Map4k4 ablation (iMap4k4-KO mice) are viable, and when challenged with high-fat feeding display lower fasting glucose levels and improved peripheral insulin sensitivity. By generating multiple tissue-specific Map4k4 knockout mice, we found that Map4k4 deficiency in cells with a Myf5-lineage, which include skeletal muscles, but not selective Map4k4 deficiency in adipose cells or hepatocytes, recapitulates the improved systemic insulin sensitivity observed in whole-body iMap4k4-KO mice.

Materials and methods

Animal Studies

All of the studies performed were approved by the Institutional Animal Care and Use Committee (IACUC) of the University of Massachusetts Medical School. Animals were maintained in 12hr light/dark cycle and fed standard chow (Lab diet 5P76) unless otherwise stated. Mice with conditional Map4k4 floxed alleles were generated as described elsewhere (295) and were backcrossed to C57BL/6J for at least 7 generations. To inactivate Map4k4 in adult mice, homozygous Map4k4$^{flox/flox}$ animals were crossed to B6.Cg-Tg(UBC-cre/ERT2)1Ejb/J (Jackson Laboratories). 8wk-old mice (both Map4k4$^{flox/flox}$ and Map4k4-$^{flox/flox}$-UBC-cre ERT2) were treated via intraperitoneal injection (IP) with 30 μ g tamoxifen/40g body weight dissolved in corn oil for 5 consecutive days. 2wks after first tamoxifen injection, animals were fed normal chow (ND) or high-fat diet (HFD) (12492i Harlan) for 16wks.

Adiponectin-cre mice (B6;FVB-Tg(Adipoq-cre)1Evdr/J), Albumin-cre mice (C57BL/6-Tg(Alb-cre)21Mgn/J) and Myf-5 cre mice (B6.129S4-Myf5$^{tm3(cre)Sor}$/J) were obtained from Jackson Laboratories.

Mice were fasted for 16hrs for GTT and PTT or 4hrs for ITT. Fasted mice were IP injected with glucose (1g/kg), pyruvate (1g/kg), or insulin (1 IU/kg). Blood samples were withdrawn by tail vein and blood glucose levels were determined using the Breeze-2-glucose meter (Bayer).

Metabolic cage and body composition analyses were performed by the UMass Mouse Metabolic Phenotyping Center. The metabolic cages were used to measure food and

water intake over a 3-day period and average food intake/day calculated (TSE Systems). Whole-body fat and lean mass was measured using ^{1}H-MRS (Echo Medical System).

RNA Isolation and RT-qPCR

Total RNA was isolated from tissues using TriPure isolation reagent (Roche) following the manufacturer's protocol. Isolated RNA was DNAse treated (DNA-free, Life Technologies), and cDNA was synthesized using iScript cDNA synthesis kit (BioRad). RT-qPCR was performed using iQ SybrGreen supermix and 36B4 (Rplp0) served as reference gene. Primer sequences are as follows:

Rplp0 (5'–TCCAGGCTTTGGGCATCA–3', 3'–CTTTATCAGCTGCACATCACTCAGA–5'); Map4k4 (5'–CATCTCCAGGGAAATCCTCAGG–3', 3'–TTCTGTAGTCGTAAGTGGCGTCTG–5'); Emr-1 (5'–CCCCAGTGTCCTTACAGAGTG–3', 3'–GTGCCCAGAGTGGATGTCT–5'); CD68 (5'–CCATCCTTCACGATGACACCT–3', 3'– GGCAGGGTTATGAGTGACAGTT–5'); Itgam (5'–ATGGACGCTGATGGCAATACC–3', 3'–TCCCCATTCACGTCTCCCA–5'); Itgax (5'–CTGGATAGCCTTTCTTCTGCTG–3', 3'–GCACACTGTGTCCGAACTCA–5'); Il-1β (5'–GCAACTGTTCCTGAACTCAACT–3', 3'–ATCTTTTGGGGTCCGTCAACT–5'); CCL2 (5'–TTAAAAACCTGGATCGGAACCAA–3', 3'–GCATTAGCTTCAGATTTACGGGT–5'); Tnf-α (5'–CAGGCGGTGCCTATGTCTC–3', 3'–CGATCACCCCGAAGTTCAGTAG–5'); Pepck (5'–CTGCATAACGGTCTGGACTTC–3', 3'–CAGCAACTGCCCGTACTCC–5'); G6pc

(5'–CGACTCGCTATCTCCAAGTGA–'3, 3'–GTTGAACCAGTCTCCGACCA–5'); Gck (5'–TGAGCCGGATGCAGAAGGA–3', 3'–GCAACATCTTTACACTGGCCT–5'); Fasn (5'–GGAGGTGGTGATAGCCGGTAT–3', 3'–TGGGTAATCCATAGAGCCCAG–5'); Scd-1 (5'–TTCTTGCGATACACTCTGGTGC–3', 3'– CGGGATTGAATGTTCTTGTCGT–5').

Plasma analysis

Mice were fasted overnight and plasma collected via cardiac puncture. Serum NEFA levels were measured using a colorimetric assay (Wako Diagnostics) according to manufacturer's instructions. Alternatively, animals were injected with .5mg/kg CL 316,243 (Santa Cruz) dissolved in PBS and blood was collected via the tail vein after 1hr. Insulin measurements were performed using an Insulin ELISA kit (Millipore) according to the manufacturer's instructions.

Histology

Tissues were isolated and fixed in 10% formalin, paraffin embedded, sectioned, and stained with hematoxylin and eosin (H&E). The UMass Morphology Core performed the embedding and sectioning.

Adipocyte isolation

Adipose tissue was minced in digestion buffer (5% BSA, 1mg/mL collagenase (Sigma, #C6885) in HBSS) and digested in a 37° C water-bath for 30-45 minutes. Digested tissue was filtered through a 200 μ m nylon mesh and centrifuged at a low speed for 5 minutes. Floating adipocytes were washed several times in HBSS followed by centrifugation.

Hepatocyte isolation

Hepatocytes were isolated as previously described (296). Briefly, chow-fed animals were anesthetized via IP ketamine/xylazine injection. Livers were perfused then digested with 50mg/mL collagenase (Sigma #C2139) in HBSS that had been supplemented with .5M EGTA and 1mM $CaCl_2$. Digested livers were collected, filtered through a 100μm cell strainer, and centrifuged and washed several times at a low speed.

Immunoblotting

For *in vivo* insulin signaling studies, mice were fasted for 4hrs and injected with PBS or insulin (1IU/kg). 15 minutes after the injection, tissues were rapidly harvested. Tissues were homogenized in lysis buffer (20mM Hepes pH 7.4, 150mM NaCl, 2mM EDTA, 1% Triton X-100, .1% SDS, 10% Glycerol, .5% sodium deoxycholate) that had been supplemented with HALT protease and phosphatase inhibitors (Thermo Pierce). For Map4k4 expression analysis, tissues were homogenized in lysis buffer containing 150mM NaCl, 2mM EDTA, and 2% SDS supplemented with protease and phosphatase inhibitors. Immunoblotting was performed using standard protocols. Membranes were blotted with the following antibodies: Akt (T308 #2965, S473 #3787, total #2920; Cell Signaling Technology) and Map4k4 (#A301-503A; Bethyl laboratories).

Triglyceride (TG) extraction

Livers were isolated from HFD-fed animals and frozen in liquid nitrogen. Hepatic TGs were extracted using the Folch method (297). Evaporated lipids were re-suspended in 1% Triton-X100 dissolved in isopropanol. TG content was determined using manufacturer's protocol (Triglyceride Determination Kit, Sigma).

Flow cytometry

The stromal vascular fraction (SVF) of the visceral adipose tissue (VAT) was isolated and weighed, and subsequent flow cytometry was performed as previously described (298). Briefly, VAT was minced in digestion buffer (5% BSA and 2mg/mL collagenase in HBSS) and incubated in a 37°C water-bath for 30-45 minutes. The digested tissue was passed through a 100μm cell strainer and centrifuged. The pelleted cells were collected as SVF and red-blood cells were lysed by incubation with red-blood cell lysis buffer. SVF cells were blocked in mouse IgG and counted. Antibodies used included F4/80 (APC, ABd serotec), CD11b (Percp 5.5, BD), and CD11c (V450, BD).

Statistics

Results are described as the mean ± SEM. Significance was assessed using a two-tailed Student's t-test.

Results

iMap4k4-KO mice display low fasting blood glucose levels and improved insulin responsiveness.

To investigate the functional role of Map4k4 in whole-body glucose homeostasis, we deleted Map4k4 systemically. Since whole-body Map4k4-KO animals die at E9.5 due to failure of mesodermal cells to migrate away from the primitive streak (214), we generated Map4k4 floxed mice (bearing loxP sites around exon 7) with tamoxifen-inducible UBC-cre ERT^2 recombinase to inducibly delete Map4k4 in adult mice (Figure 3.1, A). Tamoxifen was administered via intraperitoneal (IP) injection to both $Map4k4^{flox/flox}$ (control) and Map4k4-$^{flox/flox}$-UBC-cre ERT^2 (iMap4k4) mice (Figure 3.1, B). Tamoxifen induced cre recombinase activity and Map4k4 deletion in iMap4k4 mice, resulting in animals we denote as iMap4k4-KO mice. As expected, Map4k4 mRNA and protein expression was significantly reduced in iMap4k4-KO mice 18wks post-tamoxifen treatment in all of the tissues collected (Figure 3.1, C, D). Furthermore, both control and iMap4k4-KO mice continued to develop normally after tamoxifen treatment and did not display any obvious motor or behavioral defects (data not shown). These results indicate that Map4k4 is not required for adult mouse viability, and this inducible Map4k4 deletion mouse model can be used to address the metabolic functions of Map4k4 in obese animals.

Figure 3.1 Characterization of tamoxifen-inducible whole-body iMap4k4-KO mice.

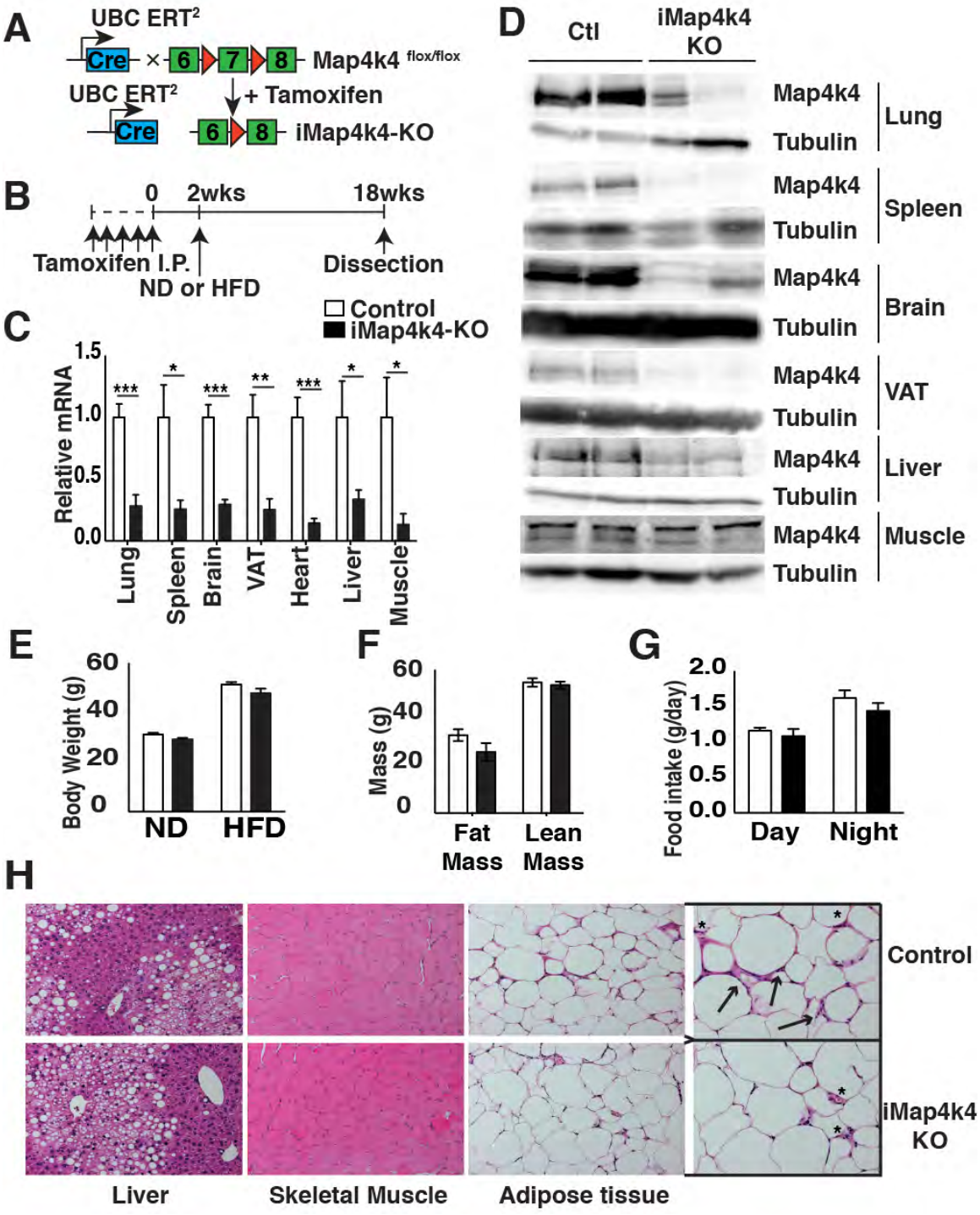

Figure 3.1. **Characterization of tamoxifen-inducible whole-body iMap4k4-KO mice. A.** Schematic of alleles and transgenes used to inactivate Map4k4 systemically in adult tissues using tamoxifen. **B.** Schematic of experimental design. Both control (Map4k4$^{flox/flox}$) and iMap4k4 (Map4k4-$^{flox/flox}$-UBC-cre ERT^{2}) mice were injected with tamoxifen as detailed in Materials and Methods to produce iMap4k4-KO mice. **(C-D)** Analysis was performed 18wks after first tamoxifen injection. **C.** Map4k4 mRNA expression (N=6-10). **D.** Representative Map4k4 protein immunoblot with tubulin as loading control (N=6). **(E)** Body weight (g) of control and iMap4k4-KO mice were fed normal chow (ND) or high-fat diet (HFD) for 16wks starting 2wks after 1st tamoxifen injection (N= 16). **(F-H)** Both control and iMap4k4-KO mice were fed HFD for 16wks. **F.** Fat and lean mass analysis (N=4-6). **G.** Food intake (g/day) (N=4-6). **H.** Representative liver, skeletal muscle, and adipose tissue histology of HFD-fed mice stained for H&E. Arrows represent crown-like-structures and asterisk represents immune cells (N=6). Data represent the mean ± SEM (* $P < 0.01$, ** $P < 0.001$, *** $P < 0.0001$).

To assess the role of Map4k4 in metabolic disease, animals were challenged with a lard-based 60% high-fat diet (HFD). Animals with systemic Map4k4 deletion did not display body weight or adiposity differences compared to littermate controls (Map4k4$^{flox/flox}$ mice treated with tamoxifen) (Figure 3.1E, F). Consistent with this observation, both control and iMap4k4-KO mice consumed similar quantities of food (Figure 3.1, G). Furthermore, although no gross histological changes were observed in metabolic tissues (Figure 3.1, H), the visceral adipose tissue (VAT) displayed a slight reduction in macrophage content as assessed by histology (Figure 3.1, H), RT-qPCR (Figure 3.2, A), and flow cytometry (Figure 3.2, B-E). Interestingly, despite similar adiposity, HFD-fed iMap4k4-KO animals showed enhanced whole-body insulin responsiveness as assessed by an insulin tolerance test (ITT) (Figure 3.3, A). Strikingly, the ITT curves of HFD-fed iMap4k4-KO mice overlapped with age-matched lean animals (Figure 3.3, A), suggesting that whole-body Map4k4 deficiency in obese animals improves peripheral insulin sensitivity to levels similar to those observed in lean controls. We also found that iMap4k4-KO mice had a significant 20% reduction in fasting glucose levels (Figure 3.3, B), as well as lower circulating insulin levels (Figure 3.3, C), consistent with increased insulin responsiveness *in vivo*. However, no detectable changes in glucose tolerance (GTT) were detected (Figure 3.3, B).

Figure 3.2. Systemic Map4k4 deletion reduces adipose tissue inflammation without changing adiposity.

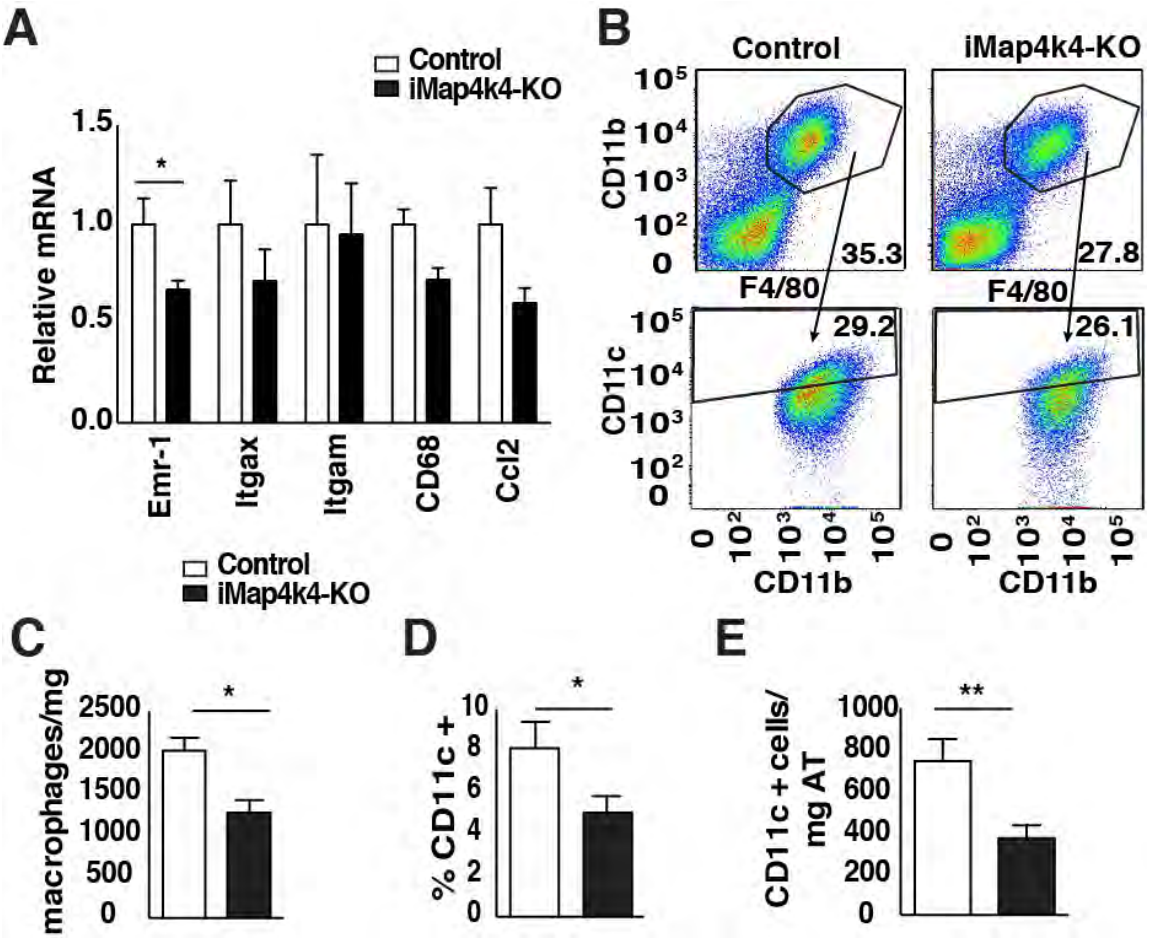

Figure 3.2. Systemic Map4k4 deletion reduces adipose tissue inflammation without changing adiposity. (A-E) Animals were fed HFD for 16wks and visceral adipose tissue was isolated. **A.** Relative mRNA expression of various inflammatory genes as indicated (N=7). **B.** VAT stromal vascular fraction was isolated and FACs analysis performed. Representative FACs scatter plot is shown. Left panel shows control mice and right panel iMap4k4-KO mice. Upper panel shows F4/80 and CD11b positive cells while lower panel shows CD11b and CD11c positive cells (N=10-13). **C.** Number of macrophages (F4/80-positive cells) per mg of VAT (N=10-13). **D.** Percentage of CD11c-positive cells (N=10-13). **E.** CD11c-positive cells per mg of VAT. (N=10-13). Data represent average mean ± SEM (* $P < 0.05$, ** $P < 0.005$).

As an additional assessment of insulin sensitivity on a cellular level, we measured insulin signaling in adipose tissue, liver, and muscle following a bolus insulin injection into HFD-fed animals. Consistent with enhanced whole-body insulin responsiveness, iMap4k4-KO mice showed significant improvements in insulin-induced Akt phosphorylation (at Ser473 and Thr308) in the liver and in the VAT (Figure 3.3 D, E). These data indicate that iMap4k4-KO mice are protected from obesity-induced insulin resistance at least in part by enhancing insulin signaling to Akt in adipose tissue and liver. Because obesity leads to glucose intolerance and insulin resistance in various organs including adipose tissue, liver, and skeletal muscle, we aimed to identify the contribution of Map4k4 in each of these tissues to affect whole-body glucose homeostasis and insulin sensitivity.

Figure 3.3 Systemic Map4k4 deletion ameliorates obesity-induced metabolic dysfunction and enhances insulin signaling in adipose and liver.

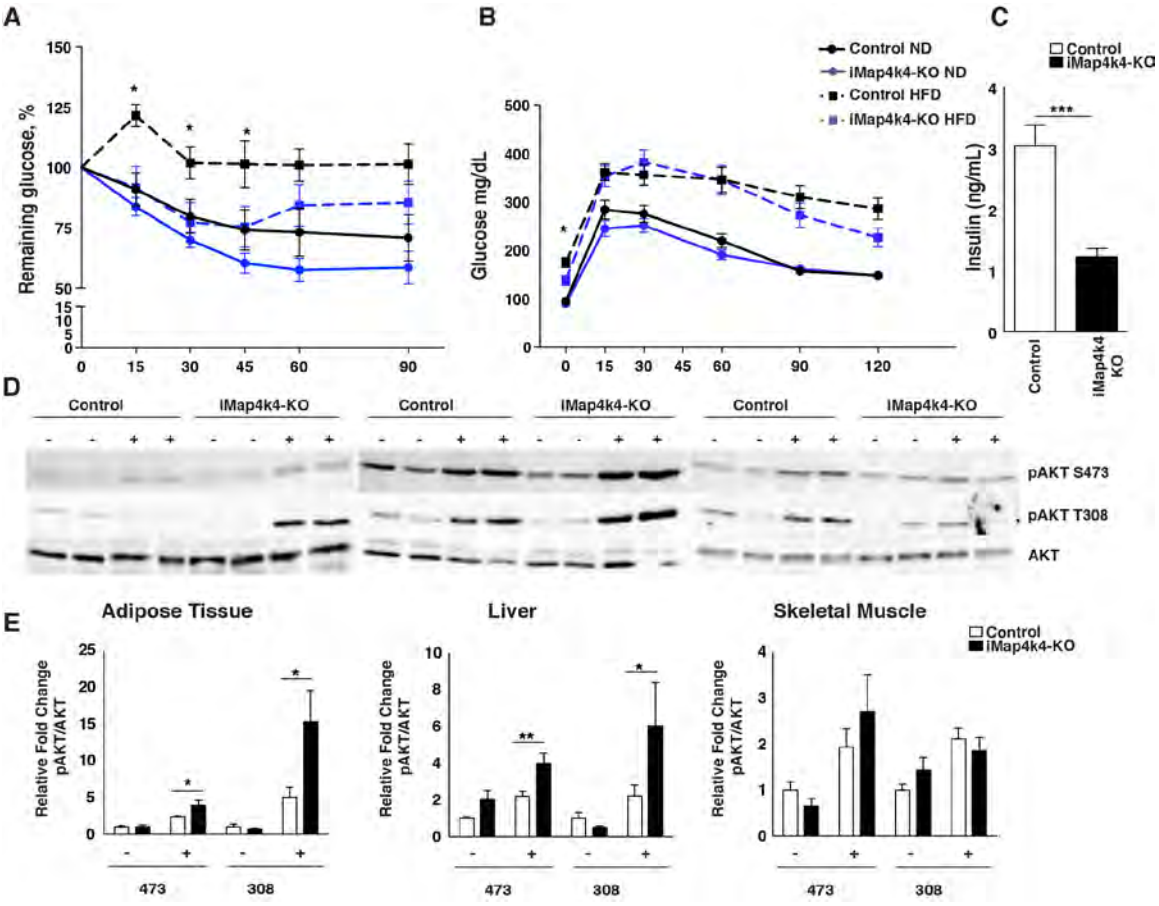

Figure 3.3 Systemic Map4k4 deletion ameliorates obesity-induced metabolic dysfunction and enhances insulin signaling in adipose and liver. (A-B). Control and iMap4k4-KO mice were fed ND or HFD for 16wks. **A.** Percentage of basal glucose remaining during insulin tolerance test (ITT) (N=7-17). **B.** Blood glucose levels during glucose tolerance test (GTT) (N=10-17). **C.** Fasting insulin levels in HFD-fed mice (N=13). **D.** Representative protein immunoblots of Akt signaling (total, thr308, ser473) in liver, adipose tissue and skeletal muscle 15 minutes after PBS or insulin injection in HFD-fed animals as described in Materials and Methods. **E.** Densitometry analyses of **D** (N=6-10). Results are the mean ± SEM (* $P < 0.05$, ** $P < 0.005$, *** $P < 0.0005$).

Adipose Map4k4 does not influence whole-body glucose homeostasis.

Obesity-induced adipose tissue dysfunction – including adipose tissue inflammation, altered adipokine secretion and reduced lipid-buffering capacity – contribute to the development of whole-body insulin resistance (55, 56, 100-102). Since Map4k4 expression is elevated in obese human adipose tissue (271) and studies performed *in vitro* suggest Map4k4 is a negative regulator of insulin action (212, 236), we aimed to specifically ablate Map4k4 expression in adipocytes by crossing $Map4k4^{flox/flox}$ mice to Adiponectin-cre transgenic mice (Figure 3.4, A). As controls, $Map4k4^{flox/flox}$ littermates that do not express cre recombinase were used. The resulting adipose-specific knockout (Ad-Map4k4-KO) mice displayed disrupted Map4k4 expression in adipocyte fractions of all the adipose tissue depots examined (visceral, subcutaneous, and brown adipose) but not in the spleen or the heart (Figure 3.4, B-C). Isolated adipocytes were used to confirm Map4k4 depletion as the adipose tissue is composed of various cell types including immune cells, pre-adipocytes, and the vasculature that could contribute to Map4k4 expression in whole tissue. To test whether the enhanced insulin sensitivity previously observed in obese iMap4k4-KO mice was mediated by the actions of Map4k4 in adipose tissue, animals were challenged with a HFD for 16wks. Ad-Map4k4-KO animals developed normally and gained similar weight and fat mass as control littermates fed ND or HFD (Figure 3.4 D-F). To assess whether Ad-Map4k4-KO mice displayed altered FA release, which might impact glucose metabolism, non-esterified fatty-acid (NEFA) levels were measured under basal conditions and post-β_3-adrenergic stimuli (IP injection of CL 316,243). As expected, NEFA levels were increased following CL 316,243 injection;

however, both control and Ad-Map4k4-KO mice displayed comparable plasma NEFA levels (Figure 3.4, G). Metabolic function as assessed by glucose tolerance (GTT) and insulin sensitivity (ITT) was also similar between control and Ad-Map4k4-KO mice fed ND or HFD (Figure 3.4, H-I). Consistent with the lack of metabolic changes, control and Ad-Map4k4-KO mice displayed similar fasting insulin levels (Figure 3.4, J). Furthermore, inflammation in both subcutaneous and visceral adipose tissue as assessed by histology (Figure 3.4, K) and RT-qPCR (Figure 3.4 L-M) was also similar between groups. Overall, these results indicate that loss of Map4k4 in adipocytes does not alter the adipose functions tested or whole-body glucose metabolism and suggest that the improved adipose insulin sensitivity observed in iMap4k4-KO mice is not mediated by the actions of Map4k4 in the adipose tissues.

Figure 3.4. Adipose-specific Map4k4 deletion in mice does not alter systemic glucose tolerance or insulin responsiveness.

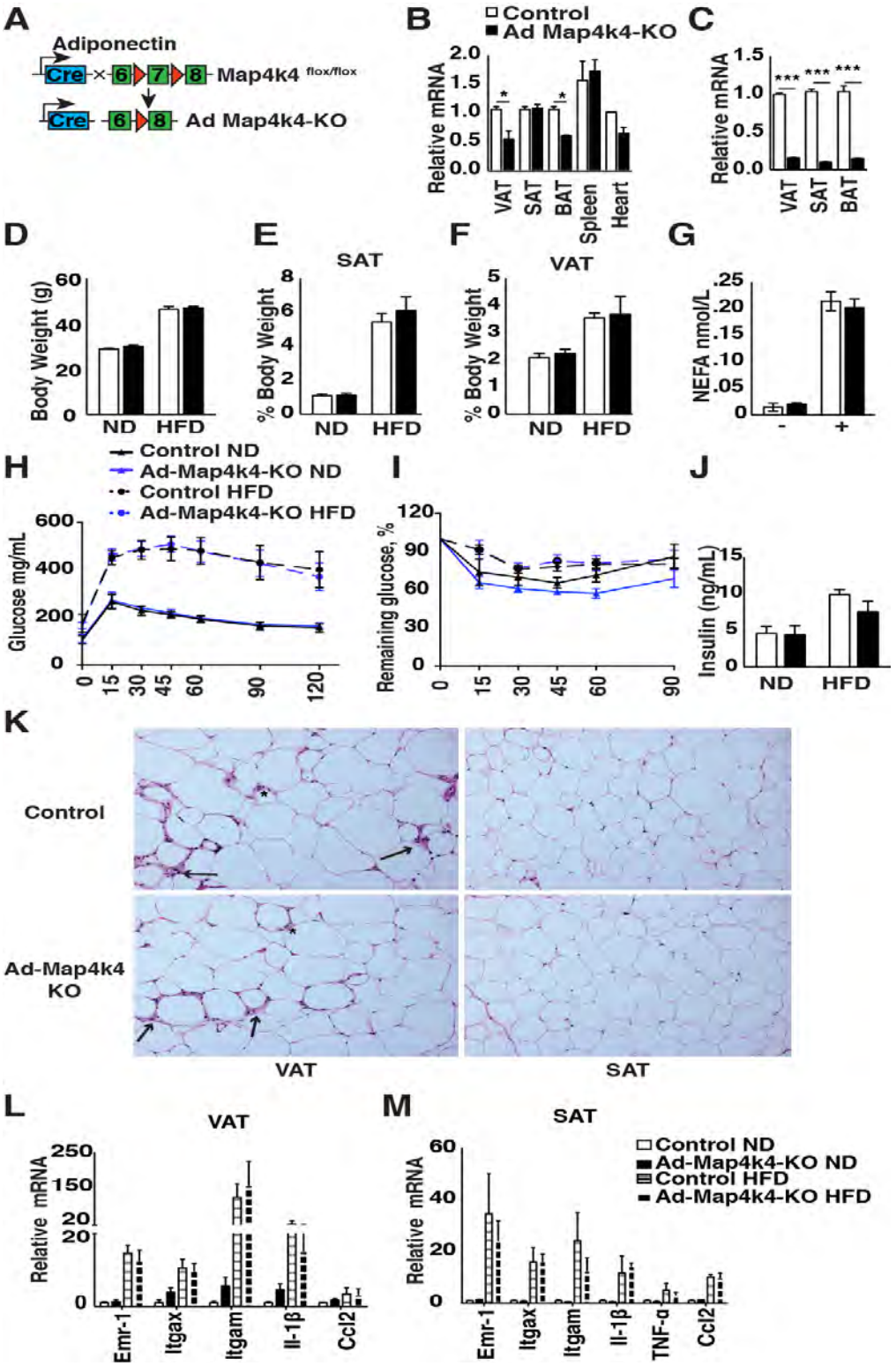

Figure 3.4. Adipose-specific Map4k4 deletion in mice does not alter systemic glucose tolerance or insulin responsiveness. A. Schematic of alleles and transgenes used to inactivate Map4k4 in the adipose using adiponectin-cre transgene. **B.** Relative Map4k4 mRNA expression in adipose tissues, spleen, and heart (N=4). **C.** Relative Map4k4 mRNA expression in isolated adipocytes from visceral adipose tissue (VAT), subcutaneous adipose tissue (SAT), and brown adipose tissue (BAT) (N=3). **(D-M)** Control and Ad-Map4k4-KO mice were fed ND or HFD for 16wks. **D.** Body weight (g) (N=8-14). **E.** SAT mass relative to body weight (N=5). **F.** VAT mass relative to body weight (N=5). **G.** NEFA levels in HFD-fed mice before and after 1hr CL 316,243 IP injection (N=5). **H.** GTT (N=10-15). **I.** ITT (N=10-15). **J.** Fasting insulin levels (N=5-6). **K.** Representative histology of VAT and SAT in HFD-fed mice. Slides were stained with H&E (N=10). Arrows represent crown-like-structures and asterisks represent immune cell infiltration **(L-M)** Relative mRNA of various inflammatory genes assessed in VAT **(L)** (N=6-8) and SAT **(M)** (N=6-8). Results are the mean ± SEM (* $P < 0.05$, *** $P < 0.0001$).

Hepatocyte-specific Map4k4 deletion does not improve metabolic parameters in lean or obese mice.

In the fed state, insulin suppresses glycogenolysis and gluconeogenesis while stimulating lipid synthesis in the liver; while in obesity-induced insulin resistance, insulin fails to suppress hepatic glucose production, thereby contributing to elevated blood glucose levels (299). To assess whether hepatic Map4k4 could account for the improved insulin sensitivity observed in the HFD-fed iMap4k4-KO mice, Map4k4$^{flox/flox}$ animals were crossed to mice expressing a cre transgene driven by the hepatocyte-specific albumin promoter (Figure 3.5, A). Map4k4$^{flox/flox}$ littermates that do not express cre recombinase were used as controls. Since the liver consists of several cell types including Kupffer cells, we isolated hepatocytes to confirm hepatocyte-specific deletion of Map4k4 in Map4k4$^{flox/flox}$-Alb-cre (Alb-Map4k4-KO) mice (Figure 3.5, B-C). To assess whether hepatic Map4k4 contributed to whole-body glucose metabolism, control and Alb-Map4k4-KO mice were challenged with a HFD for 16wks. Both control littermates and Alb-Map4k4-KO animals gained similar weight upon high-fat feeding (Figure 3.5, D-E), and fasting insulin and NEFA levels were unchanged between groups (Figure 3.5. F-G). Furthermore, no alterations in fasting glucose levels, pyruvate tolerance test (PTT), GTT, or ITT were observed among control and Alb-Map4k4-KO animals on ND or HFD (Figure 3.5, H-K). Although liver histology of Alb-Map4k4-KO mice revealed a slight increase in hepatic lipid accumulation compared to controls (Figure 3.5, L), this modest increase was not statistically significant as assessed by hepatic triglyceride content (Figure 3.5, M). These results indicate that hepatic Map4k4 depletion does not contribute

to the reduced basal glucose levels or improved insulin sensitivity observed upon inducible whole-body Map4k4 deficiency.

Figure 3.5. Hepatic Map4k4 does not contribute to systemic glucose tolerance or insulin responsiveness.

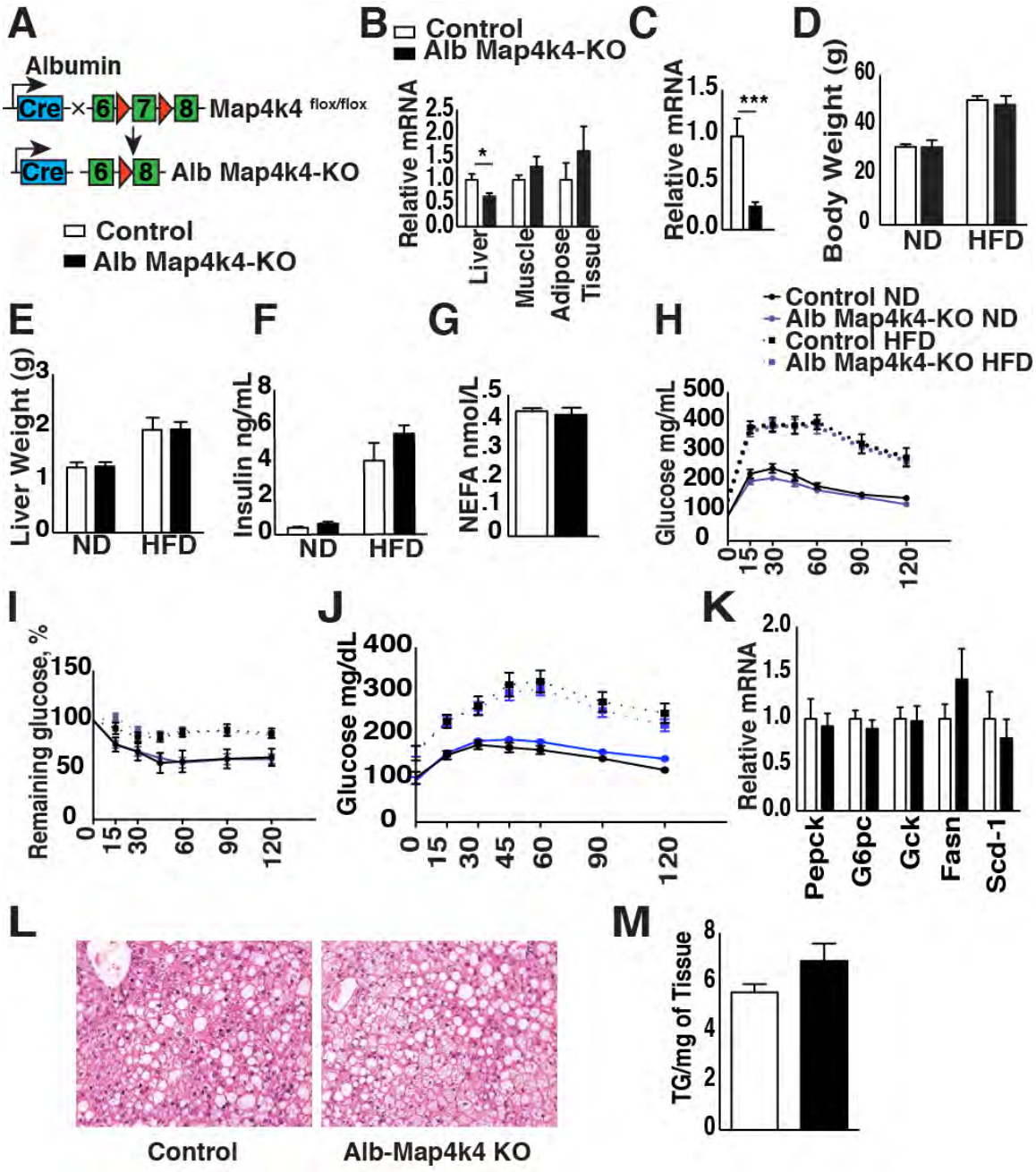

Figure 3.5. Hepatic Map4k4 does not contribute to systemic glucose tolerance or insulin responsiveness. A. Schematic of alleles and transgenes used to inactivate Map4k4 using albumin-cre transgene. **B.** Relative Map4k4 mRNA expression in liver, skeletal muscle, and adipose tissue (N=7-14). **C.** Relative Map4k4 mRNA expression in isolated hepatocytes (N=3). **(D-M)** Mice were fed ND or HFD for 16wks. **D.** Body weight (g) (N=6-13). **E.** Liver weight (g) (N=6-17). **F.** Fasting insulin levels (N=4-15). **G.** NEFA levels of HFD-fed mice (N=4-15). **H.** GTT (N=8-16). **I.** ITT (N=8-16). **J.** Blood glucose levels during pyruvate tolerance test (PTT) (N=7-16). **K.** Livers were isolated and RT-qPCR performed on the indicated genes of HFD-fed animals (N=5-7). **L.** Representative liver histology of HFD-fed mice. Slides were stained with H&E (N=10). **M.** Liver triglyceride extraction (TG/mg of liver) of HFD-fed mice (N=5-11). Results are the mean ± SEM (* $P < 0.01$, *** $P < 0.0001$).

Map4k4 deletion in Myf5-positive cells results in improved metabolic parameters.

Skeletal muscle plays a major role in regulating whole-body glucose metabolism and is responsible for the largest fraction of insulin-mediated glucose uptake from the blood. To determine whether Map4k4 in skeletal muscle affects whole-body metabolism, we crossed Map4k4$^{flox/flox}$ animals to mice that express cre recombinase under the control of the Myf5 promoter (Figure 3.6, A). Myf5-cre was used to delete Map4k4 in muscle precursors because previous reports from our laboratory have demonstrated that Map4k4 plays a key role during early stages of muscle differentiation in C2C12 cells (234). As controls, we used Map4k4$^{flox/flox}$ littermates, which do not express cre recombinase. As expected, Map4k4 expression was diminished in several of the skeletal muscles collected (*i.e.,* trapezius, triceps, and soleus) as well as brown adipose tissue (BAT), as Myf5 is expressed in muscle and BAT precursors (Figure 3.6, B) (300-302). Consistent with previous reports on Myf5 expression pattern, Map4k4 expression was not altered in the visceral adipose tissue (VAT) (Figure 3.6, B) (300-302). When challenged with a HFD, both control and Map4k4$^{flox/flox}$-Myf5-cre (Myf5-Map4k4-KO) mice gained weight, although the Myf5-Map4k4-KO animals trended to be smaller (Figure 3.6, C). Whole-body lean and fat mass analysis, however, did not reveal any statistical differences between control and Myf5-Map4k4-KO mice as measured by ^{1}H-MRS (Figure 3.6, D) or individual tissue weights (Figure 3.6, E-F). Furthermore, energy metabolism as assessed by food intake (Figure 3.6, G), oxygen consumption (Figure 3.6, H), carbon dioxide production (Figure 3.6, I), energy expenditure (Figure 3.6, J), and physical activity levels (Figure 3.6, K) were not statistically different between groups. Fasting insulin and NEFA

levels were also unchanged in Myf5-Map4k4-KO mice compared to control mice (Figure 3.6, L-M). Strikingly, however, despite similar adiposity, HFD-fed Myf5-Map4k4-KO animals displayed decreased fasting glucose levels and improved glucose clearance during a GTT, suggesting Myf5-Map4k4-KO mice were more glucose tolerant than controls (Figure 3.6, N). We then performed an ITT, and consistent with enhanced glucose tolerance, Myf5-Map4k4-KO mice were significantly more insulin sensitive compared to controls (Figure 3.6, O-P). These results suggest that Map4k4 deletion in Myf5-positive cells recapitulates in large part the metabolic benefits observed in HFD-fed iMap4k4-KO mice, and demonstrate that Map4k4 in Myf5-positive cells promotes obesity-induced metabolic dysfunction.

Figure 3.6. Map4k4 deletion in Myf5-positive tissues improves glucose tolerance and insulin responsiveness.

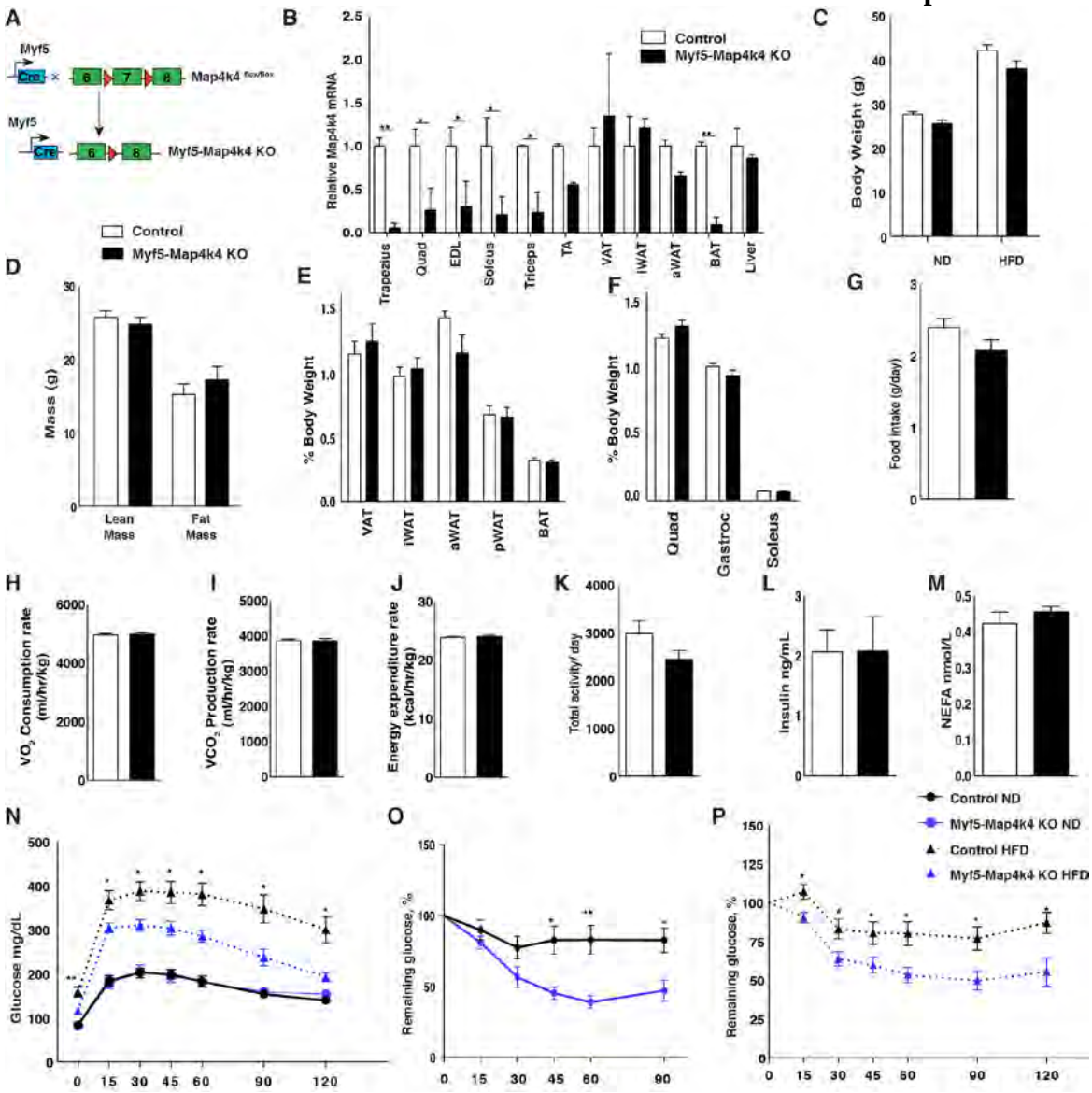

Figure 3.6. Map4k4 deletion in Myf5-positive tissues improves glucose tolerance and insulin responsiveness. A. Schematic of alleles and transgenes used to inactivate Map4k4 using Myf5-cre knockin allele. **B.** Relative Map4k4 mRNA expression in various muscles, adipose tissues, and liver (N=5). **C.** Body weight (g) of ND and HFD-fed mice (N=7-18). **D.** Fat and lean mass (g) analysis using ^{1}H-MRS of HFD-fed mice (N= 5). **E.** Adipose tissues relative to body weight in ND-fed mice. Visceral adipose tissue (VAT), inguinal subcutaneous adipose tissue (iWAT), axial subcutaneous adipose tissue (aWAT), perirenal adipose tissue (pWAT) and brown adipose tissue (BAT) (N=8). **F.** Muscle weight relative to body weight in ND-fed mice (N=8). **(G-M)** Mice were fed HFD for 8wks. **G.** Food intake (g/day) (N=5). **H.** Oxygen consumption rate (VO_2) (N=5). **I.** Carbon dioxide production rate (VCO_2) (N=5). **J.** Energy expenditure (N=5). **K.** Total activity levels (N=5). **L.** Fasting insulin levels of (N=6-8). **M.** Fasting NEFA levels (N=5). **N.** GTT (N=7-17). **O.** ITT of ND-fed animals (N=11-19). **P.** ITT of HFD-fed animals (N=7-13). Results are the mean ± SEM (* $P < 0.05$, ** $P < 0.005$).

To further assess peripheral insulin sensitivity in the Myf5-Map4k4-KO mice, HFD-fed control and Myf5-Map4k4-KO animals were injected with PBS or insulin, followed by collection of liver, adipose tissue, and skeletal muscle samples. Myf5-Map4k4-KO mice displayed a modest increase in Akt phosphorylation in response to insulin in the soleus muscle, a tissue with near-complete Map4k4 ablation, and no changes in Akt phosphorylation in the liver (Figure 3.7, A-B). Surprisingly, Myf5-Map4k4-KO mice displayed a striking enhancement of Akt phosphorylation in the VAT (Figure 3.7, A-B), a tissue that expressed normal Map4k4 levels in these mice (Figure 3.6, B). No gross morphological changes were observed in either skeletal muscle or VAT that could explain improved whole-body insulin action (Figure 3.7, C), and both groups of mice displayed similar adipose tissue inflammation profiles as assessed by histology and inflammatory marker gene expression (Figure 3.7, C-D). We also measured the gene expression and total circulating levels of muscle-secreted factors (myokines) including Fgf-21, IL-6, and Irisin and found no differences between control and Myf5-Map4k4-KO mice (Figure 3.7, E-H). These results demonstrate that Map4k4 deletion in Myf5-positive tissues protects mice from obesity-induced glucose intolerance and insulin resistance and this protection may be mediated in part via an indirect effect on the visceral adipose tissue.

Figure 3.7. Map4k4 deletion in Myf-5-positive tissues improves insulin signaling in visceral adipose tissue.

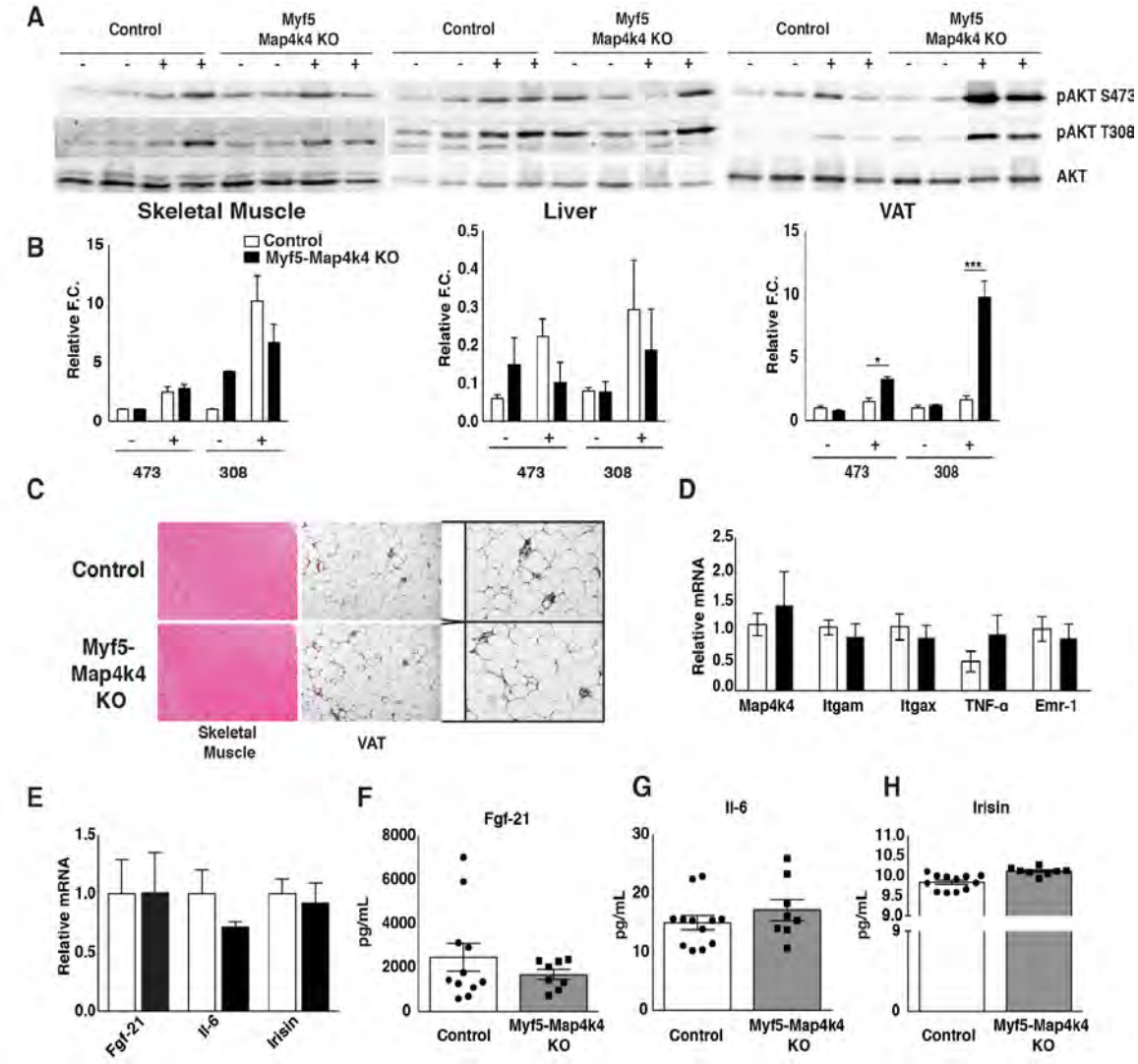

Figure 3.7. Map4k4 deletion in Myf-5-positive tissues improves insulin signaling in visceral adipose tissue. (A-H) Animals were fed ND or HFD for 8wks. **A.** Representative protein immunoblot of Akt signaling in liver, skeletal muscle and VAT in response to a bolus insulin injection (1U/kg) as described in Materials and Methods. **B.** Densitometry analysis of **A** (N=6-7). **C.** Representative skeletal muscle (soleus) and VAT histology of HFD-fed control and Myf5-Map4k4-KO mice. Slides were stained with H&E (N=10). **D.** VAT was isolated and RT-qPCR performed on the indicated genes of HFD-fed animals (N=6-12). **E.** Gene expression of various myokines in skeletal muscle (soleus) (N=7-14). **(F-H)** Circulating levels of Fgf-21 **(F)**, IL-6 **(G)**, and Irisin **(H).** Results are the mean ± SEM (* $P < 0.05$, ** $P < 0.005$, *** $P < 0.0001$).

Taken together, the data obtained from our four Map4k4 knockout mouse models presented here suggest that the metabolic improvements observed in iMap4k4-KO mice may be due primarily to the actions of Map4k4 in cells derived from Myf5-positive skeletal muscle cells and not to the actions of Map4k4 expressed in adipose cells or hepatocytes. Since Ad-Map4k4-KO animals (which also induce Map4k4 deletion in BAT) do not display any metabolic changes, skeletal muscle rather than BAT is more likely responsible for the metabolic improvements observed in Myf5-Map4k4-KO mice. Furthermore, these data suggest there is physiological cross-talk between Myf5-positive cells and the visceral adipose tissue that contributes to obesity-induced insulin resistance, and Map4k4 may be an important key regulator of this cross-talk.

Discussion

The results presented here demonstrate a role for Map4k4 in promoting obesity-induced insulin resistance, suggesting Map4k4 as a novel potential therapeutic target for the treatment of T2D. Induced systemic Map4k4 deficiency improves metabolic health in obese mice by lowering fasting glucose levels and improving insulin sensitivity (Figure 3.3). While this beneficial effect of systemic Map4k4 deletion in mature mice is associated with enhanced insulin signaling to Akt in adipose tissue and liver (Figure 3.3), conditional KO mice with selective Map4k4 deletion either in adipose tissue depots (Figure 3.4) or in liver (Figure 3.5) display no overt metabolic phenotypes. Rather, Map4k4 deficiency in Myf5-positive cells, including all skeletal muscles, largely recapitulates the effects observed in inducible whole-body Map4k4-ablated mice, improving metabolic functions in the obese state (Figure 3.6). Surprisingly, Map4k4

deletion in Myf5-positive cells causes enhancement of insulin signaling to Akt in VAT (Figure 3.7), a tissue that is nearly devoid of Myf5 expression (303), indicating interesting inter-tissue signaling between Map4k4 deficient Myf5-positive cells and white adipocytes.

Employing iMap4k4-KO mice, we bypassed the embryonic lethality observed in constitutive Map4k4-*null* mice (214) and found that Map4k4 is not essential for adult viability. Indeed, the iMap4k4-KO mice presented here did not display obvious behavioral defects and continued to gain weight throughout the study (Figure 3.1, E-F). Furthermore, despite similar adiposity, inducible systemic Map4k4 deletion enhances whole-body insulin action via improved adipose and liver insulin sensitivity (Figure 3.3, A, D-E). Interestingly, iMap4k4-KO mice displayed slightly reduced adipose tissue inflammation (Figure 3.2); consistent with previous data showing Map4k4 silencing in macrophages *in vivo* dampens inflammation in lean mice (231). Future studies using conditional Map4k4 deletion in macrophages will be required to assess the role of Map4k4 in immune cells in metabolic disease.

Previous reports have shown that enhanced peripheral insulin sensitivity can be associated with lowered insulin levels, as less insulin is needed to clear glucose from the circulation (304-306). Consistent with these reports, iMap4k4-KO mice displayed reduced insulin levels compared to controls (Figure 3.3, C). However, although obese iMap4k4-KO mice were more insulin sensitive and displayed lower fasting glucose levels

compared to controls (Figure 3.3, A-B), no changes in glucose clearance were detected (Figure 3.3, B). We hypothesize that the reduced insulin levels in the iMap4k4-KO mice are at least in part secondary to enhanced peripheral insulin sensitivity. However, lower insulin levels could also explain improvements in whole-body insulin action with minimal changes in glucose tolerance. Thus, these results are not inconsistent with the notion that Map4k4 plays a role in pancreatic β-cell function, potentially promoting insulin secretion in the obese state. Additional studies will be required to address a possible role for Map4k4 in pancreatic β-cell function *in vivo*.

Using Myf5-cre mice to deplete Map4k4 in skeletal muscle, we found that despite equal adiposity (Figure 3.6, C-E), Myf5-Map4k4-KO mice were resistant to obesity-induced metabolic dysfunction (Figure 3.6, N, P). Because previous work from our laboratory suggested Map4k4 is highly expressed in satellite cells and may play a role during early stages of muscle differentiation (234), we selected a cre recombinase driven by a promoter that is expressed during this time frame (307-309). However, skeletal muscle weights (Figure 3.6, F) and histology results (Figure 3.7. C) appear normal in Myf5-Map4k4-KO mice, suggesting no changes in muscle development. Although recent studies indicate that Myf5 is also expressed in certain adipose tissue depots (300-302), we hypothesize that Myf5-expressing myocytes and not brown adipose cells mediate the metabolic effects observed in Myf5-Map4k4-KO mice, as Ad-Map4k4-KO animals, which also delete in the BAT, do not display any improvements in metabolic function (Figure 3.4).

Map4k4 deletion in the Myf5-positive tissues largely recapitulates the improved metabolic effects observed upon systemic Map4k4 ablation, protecting mice from obesity-induced metabolic dysfunction. Although both iMap4k4-KO and Myf5-Map4k4-KO mice display enhanced whole-body insulin action and reduced fasting glucose levels (Figure 3.3, 3.6), glucose clearance was not altered in iMap4k4-KO mice (Figure 3.3, B). Since iMap4k4-KO mice deplete Map4k4 systemically, this discrepancy between models may be due to a potential role of Map4k4 in the pancreas, which is only observed in iMap4k4-KO mice. Consistent with this hypothesis, iMap4k4-KO mice display reduced fasting insulin levels (Figure 3.3, C), whereas Myf5-Map4k4-KO mice do not. Both models, however, display improved peripheral insulin sensitivity in association with enhanced insulin signaling to Akt in VAT (Figure 3.3, D-E, and Figure 3.7, A-B) and these data are consistent with previous studies that show silencing Map4k4 expression prevents cytokine-induced insulin resistance (232).

Because Myf5-Map4k4-KO mice display improved insulin sensitivity in the VAT (Figure 3.7, A-B), a tissue that does not show Map4k4 deletion (Figure 3.6, B), Map4k4 ablation in Myf5-positive cells apparently impacts Myf5-negative tissues. This observation suggests that Map4k4 could regulate production or activity of an as yet unidentified factor (or factors) that in turn influences adipose tissue insulin sensitivity. Several muscle-derived mediators have been identified including Fgf-21, IL-6, and Irisin (207). Fgf-21 and IL-6 are mostly secreted from other tissues including the liver during fasting

conditions (Fgf-21) and immune cells during an inflammatory response (IL-6) (207). We measured relative gene expression and circulating levels of these two secreted factors and found no statistical differences between control and Myf5-Map4k4 KO mice (Figure 3.7, E-G). Furthermore, although highly controversial, Irisin circulating levels have been reported to increase after exercise and induce a white-to-brown shift in adipocytes (209). We do not observe any gene expression changes or circulating levels of Irisin in our mice (Figure 3.7, E, H). Thus, future studies will aim to identify the circulating factor(s) that improve insulin sensitivity in Myf5-Map4k4 KO mice.

ACKNOWLEDGEMENTS

This work was supported by NIH Merit Award grant R37-DK030898 and a grant from the International Research Alliance at Novo Nordisk Foundation Center for Metabolic Research. Part of this study was performed at the National Mouse Metabolic Phenotyping Center (MMPC) at UMass funded by NIH grant U24-DK093000.

Chapter IV: Concluding remarks and future directions

Adipose dysfunction links obesity to insulin resistance (56). Therefore, our laboratory is interested in identifying novel regulators of adipocyte function, as these signaling pathways can contribute to the maintenance of healthy systemic glucose metabolism. One of these potential regulators of adipocyte function is Map4k4, a protein kinase identified by previous colleagues in the Czech laboratory as a negative regulator of insulin action and glucose transport (212). The work presented here asked the following questions: **Does Map4k4 regulate other adipocyte functions besides glucose transport? If so, what are the mechanisms?** Given than Map4k4 is a pro-inflammatory protein kinase (231) and its expression increases during obesity (data not shown), **what is the effect of systemic Map4k4 depletion on metabolic disease?**

To answer the first question, I used ^{14}C-tracing experiments in cultured 3T3-L1 adipocytes to measure lipid synthesis, an important adipocyte function. Specifically, I used ^{14}C-glucose and ^{14}C-acetate separately as tracers to measure overall lipid synthesis (using glucose) and *de novo* lipogenesis (using acetate) by determining the amount of radiolabel incorporation in the neutral lipid fraction (triglycerides). My results indicated that Map4k4 depletion using siRNA results in increased radiolabel (both glucose and acetate) incorporation into triglycerides. Furthermore, Map4k4 overexpression resulted in decreased ^{14}C-glucose incorporation into triglycerides. After establishing a role of Map4k4 as a repressor of lipid synthesis, I assessed the mechanism by which Map4k4 repressed this process. Using gain- and loss-of-function approaches, I determined that

unlike previous published studies, Map4k4 is not necessary or required for Jnk signaling and Map4k4 does not signal via Jnk to repress lipid synthesis. A previous colleague in the Czech laboratory reported that Map4k4 represses mTORC1 (261). Consistent with these findings, depletion of Map4k4 using siRNA enhances mTORC1 signaling as assessed by increases in phospho-S6 and phospho-4E-bp1 proteins. Furthermore, when mTORC1 function was inhibited using rapamycin, the increases in lipid synthesis observed with Map4k4 depletion were abolished, confirming the involvement of mTORC1. I also tested the expression of Srebp-1, a major lipogenic transcription factor that is a downstream target of mTORC1, and found that both protein and mRNA expression of Srebp-1 was elevated upon Map4k4 depletion. Furthermore, depletion of Srebp-1 using siRNA abolishes the effects on lipid synthesis observed upon Map4k4 depletion.

To answer the second question, I used a tamoxifen-inducible cre/ER system to inducibly delete Map4k4 globally in adult mice. Post-tamoxifen treatments, both control and iMap4k4-KO mice were fed a high-fat diet to promote obesity and metabolic disease. Using standard measures of metabolic function (glucose tolerance tests, insulin tolerance tests, plasma insulin and NEFA levels, and *in vivo* peripheral insulin sensitivity), I established that Map4k4 represses insulin sensitivity. To determine the role of Map4k4 in insulin-responsive tissues (skeletal muscle, adipose tissue, and liver), I used conditional knockout mouse models to deplete Map4k4 in each of these tissues and assessed metabolic parameters. I found that only deletion of Map4k4 in Myf5-positive cells, which include skeletal muscle, recapitulates the metabolic effects observed in global inducible

Map4k4 deleted mice. Furthermore, although both hepatic-Map4k4 KO mice and adipose-Map4k4 KO mice display slight enhancements in lipid synthesis, these effects do not alter metabolic disease.

In summary, the data in this thesis furthers our understanding of the functions of the protein kinase Map4k4 in regulating whole-body metabolism and provide support for the notion that Map4k4 targeting could prove beneficial in the treatment of metabolic disease. In trying to understand the role of Map4k4 *in vivo*, we utilized a tamoxifen-inducible system to ubiquitously deplete Map4k4 in mature mice (Figure 3.1, A). Using this model, we found that global Map4k4 depletion (iMap4k4-KO mice) ameliorates obesity-induced metabolic dysfunction by improving whole-body insulin action and reducing fasting hyperglycemia (Chapter III). Interestingly, these effects are associated with enhanced insulin signaling to Akt in adipose tissue and liver (Figure 3.3). Thus, to assess the role of Map4k4 in metabolic tissues responsible for glucose regulation –the adipose tissue, the liver, and the skeletal muscle – we employed tissue-specific knockout models to deplete Map4k4 specifically in these tissues. Based on our findings that Map4k4 suppresses glucose transport and lipid synthesis in cultured adipocytes (Chapter II), we were surprised to find that Map4k4-specific adipose knockout mice did not alter any metabolic parameters tested (Figure 3.4). Similarly, although systemic Map4k4 depletion is also associated with enhanced insulin signaling in the liver, liver-specific Map4k4 knockout mice did not result in improved metabolic phenotypes (Figure 3.5). Interestingly, Map4k4 depletion in Myf5-positive tissues, which include all skeletal

muscles tested, recapitulates the metabolic benefits observed with global Map4k4 depletion, ameliorating obesity-induced metabolic dysfunction and enhancing insulin signaling to Akt in the adipose tissue. Thus, our current view is that Map4k4 in Myf5-positive tissues suppresses systemic insulin sensitivity (Figure 4.1).

Figure 4.1. Schematic representation of Map4k4 action in Myf5-positive cells.

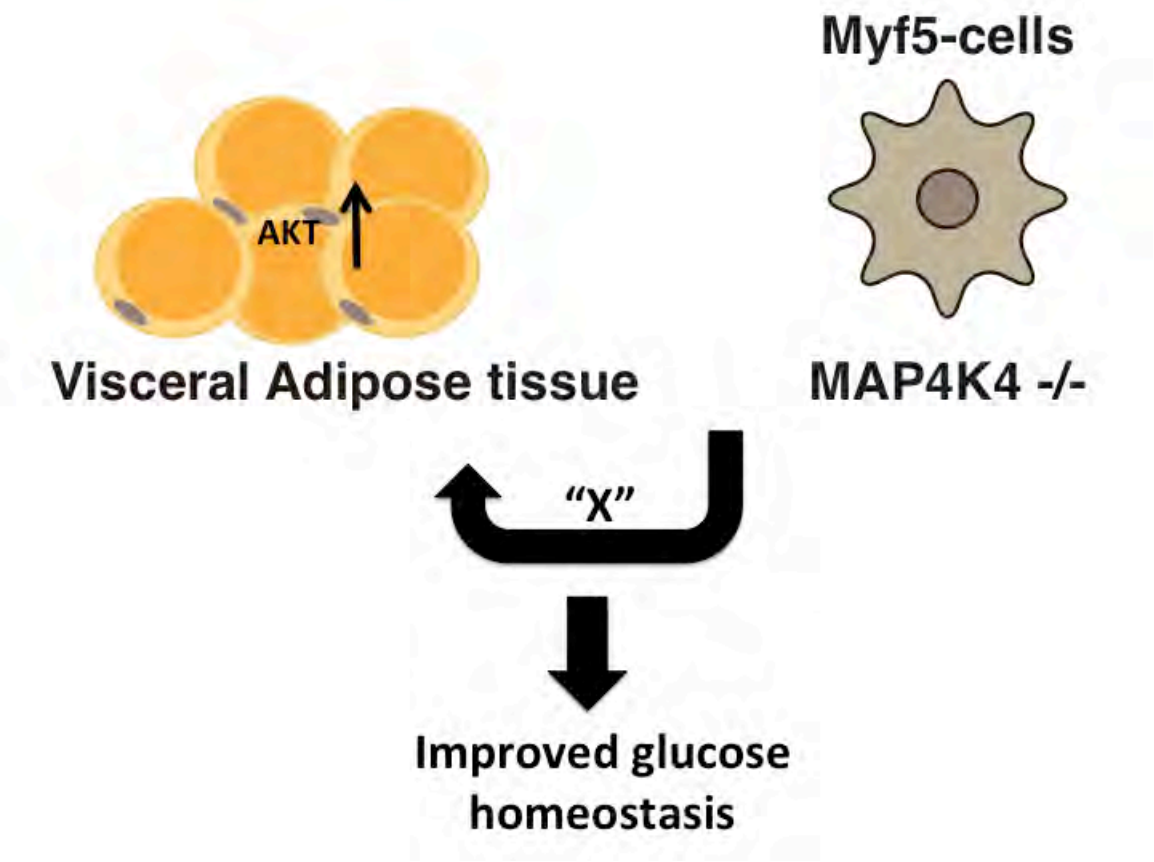

Figure 4.1. Schematic representation of Map4k4 action in Myf5-positive cells. Map4k4 deletion in Myf5-cells, including all skeletal muscles, improves insulin signaling to Akt in the Visceral adipose tissue (VAT) to alter whole-body glucose homeostasis.

Map4k4 as a negative regulator of lipid synthesis

This section will address my interpretations and potential pitfalls of the studies presented in Chapter II. Previous colleagues in the Czech lab discovered Map4k4 in a siRNA-screen as a negative regulator of insulin-stimulated glucose transport in adipocytes (Figure 1.5, A) (212). In Chapter II, I further determined that Map4k4 also represses another important adipocyte function, lipid synthesis, and these effects are independent of glucose transport (Figure 2.2, D-E). I concluded that Map4k4 is a negative regulator of lipid synthesis based on tracing studies using ^{14}C-glucose incorporation into triglycerides in adipocytes that either overexpressed Map4k4 or were depleted of Map4k4. Furthermore, I determined that these effects were independent of glucose transport because tracing studies performed with ^{14}C-acetate (which bypasses glucose transport) also show enhanced radiolabel incorporation in the triglyceride fraction upon Map4k4 depletion. Therefore, I interpreted these results to suggest that Map4k4 is a negative regulator of lipid synthesis in cultured adipocytes and these effects are independent of glucose transport. Although the published studies that identified Map4k4 as a negative regulator of glucose transport using siRNA were not performed by me, a potential caveat of these studies is that Map4k4 does not directly affect glucose transport but rather Map4k4 affects the actin cytoskeleton, which in turn affects glucose transport. This is highly speculative and thus, future experiments addressing the role of Map4k4 in the cytoskeleton needs to be tested.

As a Ste20-like kinase, Map4k4 is predicted to regulate Jnk signaling, and prior publications reported this to be the case (267-269). Since both Map4k4 and Jnk are pro-inflammatory kinases (310), we hypothesized that depletion of Map4k4 would suppress the Jnk signaling cascade and promote lipid synthesis. Surprisingly, however, while Map4k4 depletion enhanced lipid synthesis as assessed by ^{14}C-acetate incorporation into neutral lipids (triglycerides), Jnk depletion using siRNA suppressed this process (Figure 2.3). In other words, mature adipocytes transfected with Map4k4 siRNA displayed an increase in radiolabel incorporation in lipids, while adipocytes transfected with Jnk siRNA displayed a decrease in radiolabel incorporation compared to control siRNA treated cells, suggesting Map4k4 and Jnk regulate lipogenesis in opposite manners (Figure 2.3). These results were surprising because 1) Map4k4 is published to be a positive regulator of the Jnk signaling cascade and 2) as a pro-inflammatory kinase, I predicted Jnk would repress lipid synthesis and thus behave like Map4k4. To test whether I could repeat previously published experiments that suggest Map4k4 is a positive regulator of Jnk, I used gain- and loss-of-function studies to measure endogenous Jnk signaling both at the protein level (Figure 2.4) as well as the mRNA expression of downstream targets (Figure 2.4). Overall, I did not find any evidence to suggest Map4k4 affects Jnk activation in cultured adipocytes (Figure 2.4), fibroblasts, or HEK-293T cells (data not shown). However, when both Map4k4 and Jnk are ectopically overexpressed, as was previously published (267-269), I did observe increased Jnk activity (Figure 2.5). I interpreted these results to suggest that Map4k4 is not an endogenous Jnk activator and that the observed activation of Jnk by Map4k4 is an artifact of overexpression. Thus,

studies in which biological functions of Map4k4 have been attributed to Jnk signaling should be re-evaluated, as these results demonstrate that Map4k4 acts in a Jnk-independent manner. Future studies addressing *bona fide* direct Map4k4 targets will thus be highly informative.

I next assessed the Ampk signaling pathway because Map4k4 has been suggested to promote Ampk signaling and repress mTORC1 activation (261, 282). As a catabolic signaling pathway, Ampk inhibits energy demanding processes, including lipid synthesis, by inhibiting mTORC1 and Acc (311). On the other hand, as a major anabolic-signaling node, mTORC1 promotes energy-demanding processes, including lipid synthesis, in an Srebp-1-dependent manner (42). Using gain- and loss-of-function studies where Map4k4 expression was modulated, I probed the endogenous Ampk signaling pathway with various stimuli (including phenformin, glucose withdrawal, and oligomycin). While Map4k4 depletion significantly attenuated Ampk signaling as assessed by lower phospho-Acc and phospho-Ampk protein levels, Map4k4 overexpression increased phospho-Ampk. I interpreted these results to suggest that Map4k4 is a positive regulator of Ampk signaling (Figure 2.10). I next tested the Map4k4-mediated effects on downstream targets of the Ampk signaling pathway, specifically I tested whether Map4k4 modulated mTORC1 and Srebp-1 activation to affect lipid synthesis. Consistent with previous results, I found that Map4k4 depletion enhanced mTORC1 signaling as assessed by increased phospho-S6 and phospho-4E-bp1 (Figure 2.6) (261). I also found that Map4k4 depletion using siRNA or using a kinase-dead Map4k4 adenovirus results in

increased total and cleaved Srebp-1 protein levels (Figure 2.7). To show Map4k4 depletion requires this increase in mTORC1 signaling and Srebp-1 expression to increase lipid synthesis, I depleted Map4k4 in mature adipocytes using siRNA, blocked mTORC1 signaling using rapamycin and measured the incorporation of ^{14}C-glucose into triglycerides (Figure 2.6). These experiments showed that when mTORC1 signaling is inhibited, Map4k4 depletion no longer enhances lipid synthesis (Figure 2.6). One important caveat of this experiment is that the chronic rapamycin treatment (48hr) could also affect mTORC2. However, phospho-Akt (serine 473) protein immunoblots (a well-known mTORC2 target) are not altered under these conditions (Figure 2.6 A), suggesting mTORC2 signaling is not affected. Furthermore, I depleted Map4k4 and Srebp-1 using siRNA (together and separately) and assessed the effects on lipid synthesis using ^{14}C-glucose incorporation into triglycerides (Figure 2.9). Similar to the experiments using rapamycin, these experiments showed that Map4k4 depletion requires Srebp-1 expression to increase lipid synthesis, as less ^{14}C-glucose incorporation into triglycerides was observed if Map4k4 and Srebp-1 were co-depleted (Figure 2.9). Overall, I interpreted these results to suggest that Map4k4 depletion requires both mTORC1 function and Srebp-1 expression to affect lipid synthesis. Although these results suggest that Map4k4 suppresses lipid synthesis in an Ampk, mTORC1, and Srebp-1-dependent mechanism in cultured adipocytes, we still lack mechanistic details determining how Map4k4 affects these signaling pathways. Since Map4k4 is a protein kinase, I hypothesize that Map4k4 alters the activity of substrates via direct phosphorylation events and these targets may in

turn, directly inhibit Ampk/mTORC1/Srebp-1 to affect lipid synthesis. Thus, future studies aimed at identifying Map4k4 substrates will be highly informative.

Obesity is paradoxically associated with a reduction in adipose lipid synthesis (105). Various animal models have suggested that enhanced adipose lipogenesis can have two important effects in whole-body metabolism: 1) enhanced adipose lipogenesis can be beneficial as the adipose sequesters lipids to prevent deleterious accumulation of these lipids in muscle and liver, and 2) adipose lipogenesis can generate endogenous lipid ligands that promote insulin sensitivity (158). Since obese and insulin resistant patients display reduced lipid synthesis that is associated with increased Map4k4 expression (105, 271), and based on the data I presented in Chapter II on Map4k4 repressing lipid synthesis, I hypothesized that Map4k4 adipose-specific depletion would result in improved metabolic health in obese mice. I therefore interbred Map4k4 floxed mice to adiponecticn-cre transgenic mice to delete Map4k4 in adipocytes *in vivo.* I fed these mice a high-fat diet to induce metabolic disease and assessed the differences between control and adipose-Map4k4 KO mice. Adipose-specific Map4k4 knockout mice did not display any detectable metabolic changes in lean or obese states as assessed by various tests including GTT, ITT, and fasting insulin and NEFAs levels. (Figure 3.4). Thus, although *ex vivo* lipid synthesis is slightly enhanced in these animals (data not shown), consistent with the notion that Map4k4 represses lipid synthesis (Chapter II), impairment of insulin sensitivity in the obese state was not prevented, contrary to our initial hypothesis. One possibility that explains these results is that the magnitude of the increased lipid synthesis

mediated by Map4k4 deletion *in vivo* is insufficient to alter whole-body metabolism. It is important to realize that regulation of lipid synthesis *in vivo* is subject to complex inter-organ endocrine control as well as conditions of changing nutrient flux (*i.e.* fasting vs feeding) that are not present in cell culture models. Furthermore, there may be redundancy in adipose tissue *in vivo* with other related Ste20 kinases such as Tnik and Mink, which would lessen the influence of Map4k4 deletion. Because of the lack of metabolic phenotypes in the adiponectin-cre (as well as albumin-cre model), I did not pursue further studies to verify whether Map4k4 impacts signaling pathways identified as targets in cultured cells (*i.e.* Ampk, mTORC1, and Srebp-1); however, this could be an area of interest in future studies.

The metabolic functions of Map4k4 *in vivo*

This section will address my interpretations, potential pitfalls, and future directions of the studies presented in Chapter III. In Chapter II (*in vitro* studies), I found that Map4k4 repressed lipid synthesis in cultured adipocytes. These results were consistent with previous literature, which suggested that Map4k4 inhibits insulin action in adipocytes, myocytes, and β-cells (212, 232, 233). Since obesity is associated with insulin resistance and *in vitro* studies suggest Map4k4 inhibits insulin action (212, 232, 233), I sought to determine whether Map4k4 plays a role in metabolic disease. To do so, I interbred mice carrying Map4k4 floxed alleles to mice with an inducible cre recombinase that is expressed systemically. I chose this model for two reasons: 1) to bypass embryonic development as global Map4k4 knockout mice display embryonic lethality (214) and 2)

mimic the systemic inhibition of Map4k4 activity that would result from a small molecule inhibitor. I confirmed Map4k4 depletion by mRNA and protein expression in various tissues including adipose tissue, liver, and skeletal muscle (Figure 3.1). Using this model, I induced metabolic disease and assessed metabolic function using various metabolic tests including GTTs and ITTs. These experiments demonstrated that mice with inducible systemic Map4k4 depletion displayed improved insulin tolerance when obese (Figure 3.3). Furthermore, these results were associated with improved insulin signaling to Akt in the adipose tissue and the liver as assessed by enhanced phospho-Akt in these tissues (Figure 3.3). Based on these experiments, I concluded that systemic Map4k4 depletion is beneficial in the setting of metabolic disease.

To further elucidate the role of Map4k4 in insulin-responsive tissues in the context of metabolic disease, I interbred Map4k4 floxed mice to either adiponectin-cre transgenics or albumin-cre transgenics to obtain tissue-specific knockout mice for the adipose tissue or the liver. These mice were challenged with a high-fat diet and metabolic tests were performed. However, neither adipose-Map4k4 KO mice nor liver-Map4k4 KO mice displayed any metabolic changes compared to appropriate controls (Figure 3.4 and Figure 3.5). It should be noted that these metabolic tests were also performed using a 45% high fat diet (compared to 60% high fat diet) for various time points including 8wks, 16wks, and 20wks of high-fat diets with similar results (data not shown). Furthermore, liver-specific Map4k4 depletion slightly enhanced hepatic steatosis, as was anticipated based on results described in Chapter II; however, this slight increase was neither statistically

significant nor sufficient to alter metabolic profiles of liver-Map4k4 knockout mice (Figure 3.5). I interpreted these results to suggest that the improved insulin signaling in the adipose tissue and the liver of iMap4k4-KO mice is not a cell autonomous effect and therefore, these results may be mediated by other resident cell types present in these tissues such as immune cells or a secreted factor may be altered in iMap4k4-KO mice enhancing insulin responsiveness in the adipose tissue and liver.

Next, I interbred Map4k4 floxed mice to Myf5-cre mice to deplete Map4k4 in the skeletal muscle.. These animals were challenged with a high-fat diet and metabolic disease assessed. Based on significant improvements in glucose tolerance and insulin sensitivity (as assessed by GTTs and ITTs, respectively), I concluded that mice with Map4k4 deletion in Myf5-positive cells (*i.e.* skeletal muscle) displayed improvements in metabolic disease despite equal obesity. Because systemic inducible Map4k4 KO mice also displayed metabolic improvements despite equal obesity, I interpreted these results to suggest that Myf5-Map4k4 KO mice largely recapitulated the effects observed upon systemic Map4k4 ablation, ameliorating obesity-induced metabolic dysfunction (Figure 3.6). I further assessed peripheral insulin sensitivity in Myf5-Map4k4 KO mice and observed a significant increase in insulin sensitivity in the visceral adipose tissue (VAT), but not in the liver or the skeletal muscle (Figure 3.7). Because VAT reportedly displays a low number of Myf5-positive cells (300-302) and Map4k4 expression in this tissue is not altered, I interpreted these results to suggest a

circulating factor(s) from Myf5-positive cells with Map4k4 deletion (*i.e.* skeletal muscle) affected Myf5-negative tissues (VAT) to improve whole-body metabolism.

There are several potential pitfalls with the Myf5-cre study. First, it has been reported that the Myf5 is expressed in muscle and adipose progenitors(300-302). Consistent with this literature, Map4k4 expression was depleted in skeletal muscles, BAT, and certain WAT depots (300, 302, 303). I chose this cre model because a previous colleague in the Czech laboratory reported that Map4k4 inhibits the early stages of muscle differentiation in C2C12 cells (234). Because adipose-Map4k4 KO mice did not show improvements in metabolic disease, I attributed the improvements in metabolic health observed in Myf5-Map4k4 KO mice to non-adipose Myf5-positive cells (*i.e.* skeletal muscle). To prove this, however, I need to interbreed Map4k4 floxed mice with skeletal-muscle specific KO mice (*i.e.* α-actin-cre or MCK-cre) and show similar improvements in metabolic disease.

Second, because Myf5-cre mice also potently deplete Map4k4 expression in the BAT, it could be postulated that the metabolic improvements in Myf5-Map4k4 KO mice are mediated by alternations in BAT. Since adipose-Map4k4 KO, which also display Map4k4 depletion in BAT, do not display any metabolic changes; and BAT histology and BAT-specific gene expression was unaltered in Myf5-Map4k4 KO mice (data not shown), I interpreted these results to suggest that the metabolic effects observed in the Myf5-Map4k4 KO mice are not mediated by effects of Map4k4 in BAT. However, to

confirm this conclusion, BAT-specific KO mice (*i.e* UCP1-Map4k4 KO mice) need to be tested. Alternatively, the BAT can be de-activated via denervation and the effects of Myf5-Map4k4 KO mice on metabolic disease tested. If my interpretation is correct that the BAT does not play a role in the metabolic phenotypes observed in Myf5-Map4k4 KO mice, then denervation of the BAT should not alter the metabolic benefits observed by Map4k4 deletion using Myf5-cre.

Third, because the VAT contains a low population of Myf5-positive cells (303) and Myf5-Map4k4 KO mice display increased insulin sensitivity in this tissue (Figure 3.7), I interpreted these results to suggest that there is communication between Myf5-positive Map4k4 KO cells and Myf5-negative cells, potentially via the secretion of as of yet unidentified factor(s). This unidentified secreted factor(s) could be secreted into the circulation to enhance insulin sensitivity in the adipose tissue. Another plausible hypothesis is that this communication occurs in the VAT via secretion of local factors within the adipose tissue that sensitizes the whole tissue to the effects of insulin. One way to prove a circulating factor is secreted into the circulation of Myf5-Map4k4 KO mice to enhance insulin sensitivity of the VAT is to perform a parabiosis experiment where a control mouse shares the circulatory system of a Myf5-Map4k4 KO mouse. If my interpretation is correct, I would expect to observe metabolic improvements in both control and Myf5-Map4k4 KO mice.

Although we have yet to find the identity of such factor, we hypothesize that such factor may directly or indirectly impact insulin signaling to Akt. For example, signaling downstream of such a factor could attenuate the activity of negative regulators of the insulin-signaling pathway such that Akt activation can be enhanced. Map4k4 has been previously shown to alter Signal transducer and activator of transcription 3 (Stat3) phosphorylation levels, resulting in reduced Stat3 transcriptional activity (215). I have preliminary evidence to suggest that Stat3 is downregulated in VAT of Myf5-Map4k4 KO mice. Thus, it is tempting to speculate that Stat3 downregulation potentiates insulin signaling to Akt in the adipose tissue as Stat3 is responsive to various growth factors and it drives the expression of Suppressor of cytokine signaling 3 (Socs3), a negative regulator of the insulin-signaling pathway (312). More work is needed to identify the secreted factor and its role in promoting insulin sensitivity in Myf5-negative adipose cells.

The data presented in this thesis provide evidence for a role of Map4k4 in metabolic disease. Global Map4k4 suppression improves obesity-induced metabolic dysfunction by enhancing systemic insulin sensitivity and lowering fasting glucose levels (Figure 3.3). These results are mediated, at least in part, by Map4k4 signaling in Myf5-positive tissues, which include all skeletal muscles, and not by Map4k4 signaling in the adipose tissue or liver. Since Myf5-Map4k4 KO mice display significant improvements in obesity-induced metabolic disease (Figure 3.6) and enhanced insulin signaling to Akt in the adipose tissue (Figure 3.7), a tissue with few Myf5-progenitor cells, we have uncovered an interesting

cross-talk between Myf5-positive and Myf5-negative tissues that regulate systemic insulin sensitivity and Map4k4 signaling is essential in this process (Figure 3.7).

In summary, there are three main implications from this thesis that have advanced the field:

1) Both *in vitro* (Chapter II) and *in vivo* (Chapter III) studies presented in this thesis are entirely consistent with the notion that Map4k4 can have deleterious effects on insulin action in the context of inflammation and excess nutrient supply, both of which are important mediators of metabolic disease. These results are also in agreement with previously published *in vitro* studies from our laboratory as well as others (212, 231-233). Based on the results in Chapter II, I expected Map4k4 to inhibit insulin action via its effects on adipose lipid synthesis. I found that Map4k4 also inhibits the effects of insulin *in vivo*, however, this is apparently not mediated by increased lipid synthesis in the adipose tissue. Nonetheless, the beneficial metabolic effects of Map4k4 ablation in obese adult mice confirms the potential of Map4k4 as a valid target of therapies for metabolic disease.
2) Results from Chapter III and Appendix I show that Map4k4 can have different tissue-specific roles in metabolic disease. For example, while Map4k4 represses whole-body glucose homeostasis in Myf5-positive cells, Map4k4 in the pancreas may be required for proper insulin secretion. Furthermore, *in vivo* studies strongly suggest a potentially novel crosstalk between skeletal muscle and adipose tissue.

Discovering the factor(s) responsible for this crosstalk as well as mechanisms of Map4k4 action in β-cells are likely to be fruitful areas of future research.

3) Finally, although our understanding of Map4k4 signaling is as yet far from complete, work in this thesis has advanced this understanding in several ways. I have refuted the reported role of Map4k4 as a positive regulator of the Jnk signaling pathway. Furthermore, I have also revealed novel roles for Map4k4 in the regulation of Ampk and Srebp-1 in cultured adipocytes.

APPENDIX I:

Map4k4 promotes obesity-induced hyperinsulinemia.

Author Contributions:

These studies represent co-authored work performed in conjunction with Rachel J. Roth Flach, Czech Lab.

Glucose-Stimulated insulin secretion
Agata Jurczyk, UMASS Medical School, Figure AI-1 D-E.

Introduction

Proper glucose regulation is essential for mammalian survival; therefore, highly controlled inter-organ networks exist to achieve euglycemia (1). In the fed state, glucose is absorbed from ingested foods and delivered via blood circulation to all tissues. Pancreatic β-cells sense this glucose surge and, in turn, secrete insulin (68). Insulin signals to peripheral tissues to normalize glucose levels by promoting glucose uptake in the muscle and adipose tissue while suppressing hepatic glucose production (313). During fasting conditions, low glucose levels promote glucagon secretion from pancreatic α-cells (5). Glucagon normalizes glucose levels by signaling to the liver to promote glycogen breakdown and glucose production (5). Therefore, circulating glucose levels reflect a balance between hepatic glucose production and peripheral (adipose tissue and skeletal muscle) glucose uptake and utilization, and proper pancreatic endocrine function is essential in this regulation.

Obesity can be associated with peripheral insulin resistance, whereby released insulin fails to promote skeletal muscle and adipose glucose uptake as well as suppress hepatic glucose production, resulting in hyperglycemic conditions (11). Hyperglycemia, in turn, induces a compensatory adaptation in the pancreas, which is manifested by an increase in β-cell mass and function, resulting in insulin hypersecretion to restore euglycemia (12, 13). Obese and insulin resistant patients eventually display β-cell dysfunction and failure, resulting in type-2 diabetes (T2D) (12, 14). Therefore, T2D is a condition with reduced

peripheral insulin action and gradual β-cell loss, which accounts for a 60% decrease in β-cell mass observed in type-2 diabetics (12).

T2D currently affects 9% of the population worldwide, however its incidence is predicted to dramatically increase as T2D-predisposing conditions such as obesity and insulin resistance continue to rise (7). It is of paramount importance to therapeutically manage insulin resistance and T2D as these diseases are commonly linked to other deadly co-morbidities including cardiovascular disease and certain cancers (7). Current therapies aim to suppress hepatic glucose production (metformin) or potentiate insulin secretion (insulin secretagogues), however further intervention is often required (15). Interestingly, recent evidence suggests that although insulin resistance-induced hyperinsulinemic conditions are required to restore euglycemia, they can be detrimental in further promoting adiposity and insulin resistance (17). Thus, peripheral insulin resistance promotes insulin hypersecretion and hyperinsulinemia, which in turn, can further promote insulin resistance, creating a vicious feed-forward cycle that results in T2D (17). Thus, drug therapies that simultaneously improve the underlying peripheral insulin resistance and lower hyperinsulinemic conditions would prove useful in developing therapies for T2D (17).

In finding novel regulators of insulin action, our laboratory identified the protein kinase Map4k4 as a negative regulator of insulin-mediated glucose transport (212). Studies *in vitro* suggest Map4k4 inhibits metabolic function (220). In cultured adipocytes, Map4k4

represses glucose transport and lipid synthesis (Chapter II) (236); in muscle cells, Map4k4 promotes Tnf-α-induced insulin resistance (232); and in β-cells, Map4k4 promotes Tnf-α inhibition of glucose-stimulated insulin secretion (GSIS) (233). Recent studies *in vivo* extend our understanding of Map4k4 and suggest Map4k4 regulates systemic insulin sensitivity (Chapter III). Inducible global Map4k4 depletion restores obesity-induced insulin resistance and improves fasting glucose levels (Chapter III, Figure 3.3). However, despite enhanced insulin sensitivity, inducible Map4k4 global knockouts do not display changes in glucose clearance (Chapter III, Figure 3.3). Furthermore, global Map4k4 knockout mice show a significant reduction in fasting insulin levels (Chapter III, Figure 3.3). We therefore aimed to assess the role of Map4k4 in β-cell insulin secretion. These studies extend our understanding of the role of Map4k4 in metabolic dysfunction and further suggest Map4k4 as a therapeutic target for metabolic disease.

Materials and Methods

Animal Studies

All of the studies performed were approved by the Institutional Animal Care and Use Committee (IACUC) of the University of Massachusetts Medical School. Animals were maintained in a 12hr light/dark cycle. Map4k4$^{flox/flox}$ (control) and Map4k4-$^{flox/flox}$-UBC-cre ERT2 (iMap4k4) mice were fed standard chow (Lab diet 5P76) and injected with 30 μ g tamoxifen/40g body weight dissolved in corn oil for 5 consecutive days. 2wks after the 1st tamoxifen injection, mice were fed high-fat diet (HFD) (12492i Harlan) for 16wks.

For *in vivo* insulin secretion, mice were fasted for 16hrs and IP injected with 1g/kg glucose dissolved in PBS. Blood samples were withdrawn from the tail vein before and 30 minutes after glucose injection.

RNA Isolation and RT-qPCR

Total RNA was isolated from isolated islets using TriPure isolation reagent (Roche) and following manufacturer's instructions. Isolated RNA was DNAse treated (DNA-free, Life Technologies), and cDNA was synthesized using iScript cDNA synthesis kit (BioRad). RT-qPCR was performed using iQ SybrGreen supermix. Primer sequences used are as follows: Rplp0 (5'–TCCAGGCTTTGGGCATCA–3', 3'–CTTTATCAGCTGCACATCACTCAGA–5'); Map4k4 (5'-CATCTCCAGGGAAATCCTCAGG-3', 3'-TTCTGTAGTCGTAAGTGGCGTCTG-5'); Insulin 1 (5'-CCATCAGCAAGCAGGTCATTG-3', 3'-TGTGTAGAAGAAGCCACGCTCC-5'); Insulin 2 (5'-CAGAAACCATCAGCAAGCAGG-3', 3'-TTGACAAAAGCCTGGGTGGG-5'); Glucagon (5'-GAGGAACCGGAACAACATTGC-3', 3'-GCAATGAATTCCTTTGCTGCC-5'); Glut2 (5'-TGCTGCTGGATAAATTCGCC-3', 3'-TCAGCAACCATGAACCAAGG-3'); MafA (5'-AGGAGGAGGTCATCCGACTG-3', 3'-CTTCTCGCTCTCCAGAATGTG-5'); MafB (5'-AGGACCTGTACTGGATGGC-3', 3'-CACTACGGAAGCCGTCGAAG-5'); Nkx6.1 (5'-CTTCTGGCCCGGAGTGATG-3', 3'-GGGTCTGGTGTGTTTTCTCTTC-5'); Pdx-1 (5'-GAGGTGCTTACACAGCGGAA-3', 3'-GGGGCCGGGAGATGTATTT-5').

Plasma analysis

Mice were fasted overnight (16hrs), and plasma was collected via the tail vein. Serum insulin, C-peptide, and glucagon measurements were performed using an Insulin ELISA kit (Millipore), C-peptide ELISA kit (ALPCO), and Glucagon ELISA kit (R&D systems) according to the manufacturer's instructions.

Histology

Mouse pancreatic tissue was isolated, arranged in one block, and fixed in 10% formalin for 4hrs. Blocks were paraffin embedded, sectioned, and stained with hematoxylin and eosin (H&E), insulin (ab7842), glucagon (ab10988), or Ki67 (BD biosciences). The UMass Morphology Core performed the embedding, sectioning, and staining. To obtain β-cell mass, the ratio of β-cell area to total pancreas area was calculated and multiplied by the wet weight of the pancreas.

Islet isolation and insulin secretion

Islets were isolated from similarly weighted animals by ductal collagenase injection and Ficoll separation as previously described (314). Glucose-stimulated insulin secretion was measured using a perifusion system whereby 25 similarly shaped and sized islets were hand-selected using a microscope. Islets were incubated in 3mM glucose for 20 minutes then stimulated with a high concentration of glucose (20mM). Media was collected every 1-3 minutes to assess the bi-phasic nature of insulin secretion. Secreted insulin in response to glucose was normalized to KCl secreted insulin.

Statistics

Results are described as the mean ± SEM. Significance was assessed using a two-tailed Student's t-test.

Results and Discussion

iMap4k4-KO mice display reduced insulin secretion

Inducible systemic Map4k4 depletion (iMap4k4-KO) improves obesity-induced insulin resistance without altering glucose clearance (Chapter II). We hypothesized that reduced insulin secretion in iMap4k4-KO mice may mask potential effects on glucose clearance. To assess whether Map4k4 regulates insulin secretion, we collected plasma of HFD-fed tamoxifen-injected Map4k4$^{flox/flox}$ (control) and Map4k4-$^{flox/flox}$-UBC-cre ERT^{2} (iMap4k4-KO) mice after an overnight fast as well as 30 minutes after an intraperitoneal (IP) glucose injection. As predicted, an exogenous glucose surge promotes insulin secretion as assessed by increased circulating insulin levels 30 minutes after the glucose injection (Figure AI-1, A). iMap4k4-KO mice, however, displayed reduced insulin levels both basally and after glucose injection (Figure AI-1, A). These results suggest that iMap4k4-KO mice have reduced circulating insulin levels either due to altered insulin secretion or enhanced insulin turnover. Because proinsulin is packaged into vesicles before the connecting peptide (C-peptide) is removed, measurements of circulating C-peptide levels are a direct measure of insulin secretion (315). Using the same conditions, we measured circulating C-peptide levels before and 30 minutes after a glucose injection, and observed that iMap4k4-KO mice displayed lower C-peptide levels (Figure AI-1, B). These data suggest Map4k4 depletion disrupts insulin secretion. We also measured circulating glucagon levels and detected no statistical differences between groups; thus, altered secretory effects are β-cell specific (Figure AI-1, C.). To assess whether the altered insulin secretion was mediated by a cell-autonomous effect or merely a result of

enhanced peripheral insulin sensitivity, we isolated islets from HFD-fed control and iMap4k4-KO mice and performed glucose-stimulated insulin secretion experiments (GSIS). Using a perifusion model, media was collected every few minutes and insulin secretion was measured either basally (3mM glucose) or with the addition of 20mM glucose or 20mM KCl. As expected, increasing glucose concentrations enhances insulin secretion in a biphasic manner, with the 1st wave of insulin secretion occurring approximately 5 minutes after the glucose surge and the 2nd wave of insulin secretion occurring 30 minutes after initial glucose surge. Interestingly, iMap4k4-KO mice displayed a significant reduction in the 1st wave of insulin secretion (Figure AI-1, D-E). We confirmed Map4k4 expression was significantly depleted in islets from iMap4k4-KO mice with a concomitant trend to reduced Insulin-1 and Insulin-2 gene expression (Figure AI-1, F). Consistent with a role of Map4k4 affecting in β-cell function, gene expression analysis of islet specification genes including Pancreatic and duodenal homeobox 1 (Pdx-1), v-maf musculoaponeurotic fibrosarcoma oncogene family, protein A (MafA), and v-maf musculoaponeurotic fibrosarcoma oncogene family, protein B (MafB) were significantly decreased in HFD-fed iMap4k4-KO islets (Figure AI-1, G). These results suggest that Map4k4 promotes obesity-induced hyperinsulinemia.

Figure AI-1. Map4k4 promotes HFD-induced hyperinsulinemia.

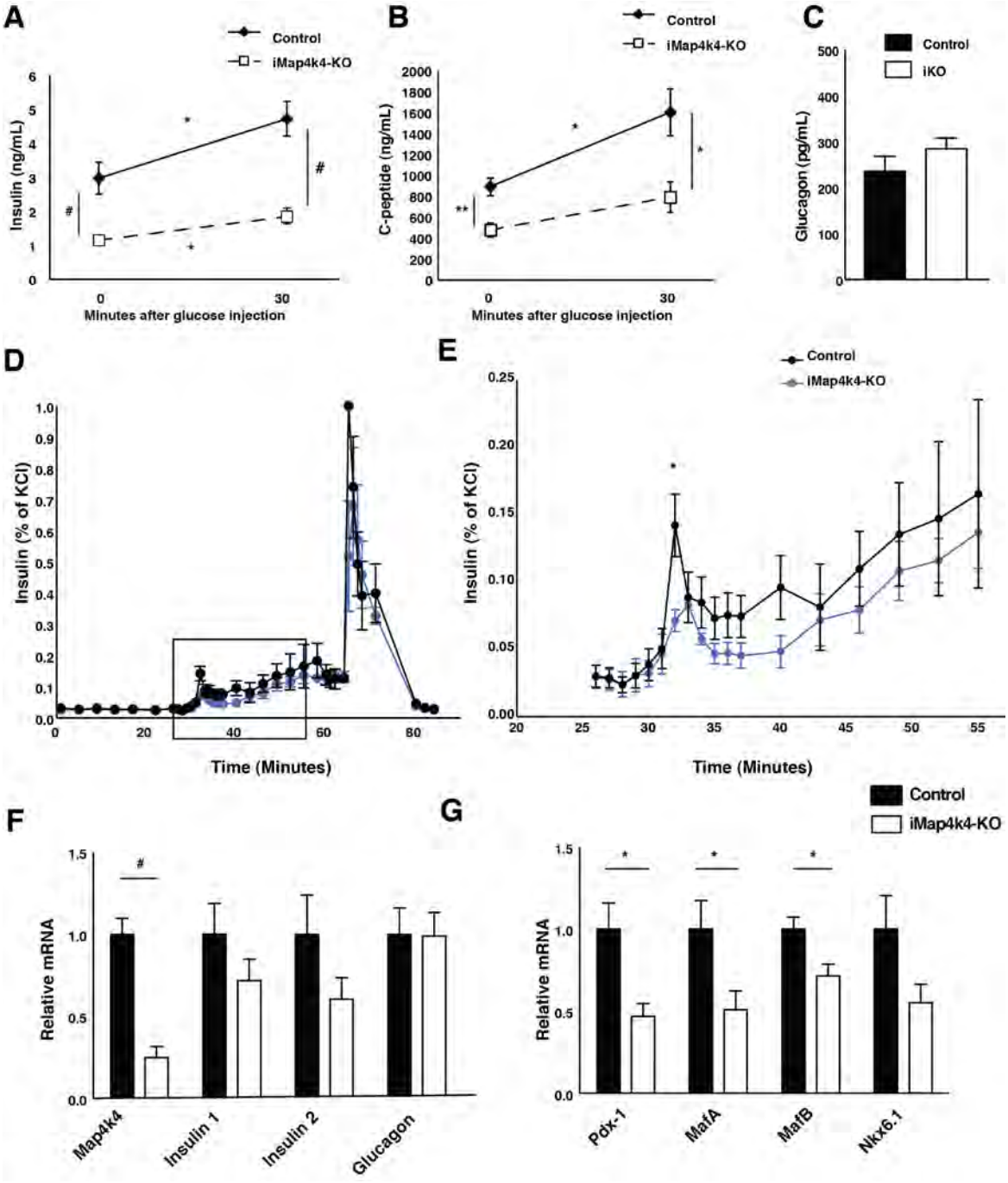

Figure AI-1. Map4k4 promotes HFD-induced hyperinsulinemia. (A-G) Both control and iMap4k4-KO mice were fed a high-fat diet for 16wks. **(A)** Fasting Insulin levels before and 30 minutes after glucose injection (* $P<0.05$, # $P<0.0005$, N=6-10). **(B)** Fasting C-peptide levels before and 30 minutes after glucose injection (* $P<0.05$, ** $P<0.005$, N=6-7). **(C)** Circulating fasting glucagon levels (N=6-8). (**D-E)** Glucose-stimulated insulin secretion performed in isolated islets as described in Materials and Methods. **D**. Islets were incubated in 3mM glucose then stimulated with 20mM glucose was administered at 30 minutes KCl was administered at 65 minutes. **E**. Higher magnification of data within box from **D** (*; $p<0.05$, N=4). **(F-G)** Relative gene expression in isolated islets. Results represent the mean ± SEM (* $P < 0.05$ N=10).

iMap4k4-KO mice display normal islet morphology with a concomitant reduction in islet mass

To assess whether islet morphology was altered in iMap4k4-KO mice, leading to changes in insulin secretion, we isolated whole pancreas from HFD-fed control and iMap4k4-KO mice and determined islet morphology using immunofluorescent stains for β-cells (insulin) and α-cells (glucagon) (Figure AI-2, A). Although iMap4k4-KO mice display reduced insulin secretion, islet size and shape were similar between groups (Figure AI-2, A). Despite normal islet morphology, however, histological examination of the entire pancreas revealed a significant reduction in islet mass and number (Figure AI-2, B-C). Because obesity-induced insulin resistance is associated with an increase in β-cell number and mass that is partly mediated by enhanced β-cell proliferation (313), we measured β-cell proliferation rates using immunofluorescent stains for β-cells (insulin) and proliferating cells (Ki67) (Figure AI-2, D-E). HFD-fed iMap4k4-KO mice displayed a significant reduction in proliferation rates compared to control mice, consistent with a reduction in islet number and mass. These results suggest Map4k4 promotes HFD-induced β-cell expansion by regulating β-cell proliferation.

Figure AI-2. Map4k4 depletion attenuates β-cell expansion.

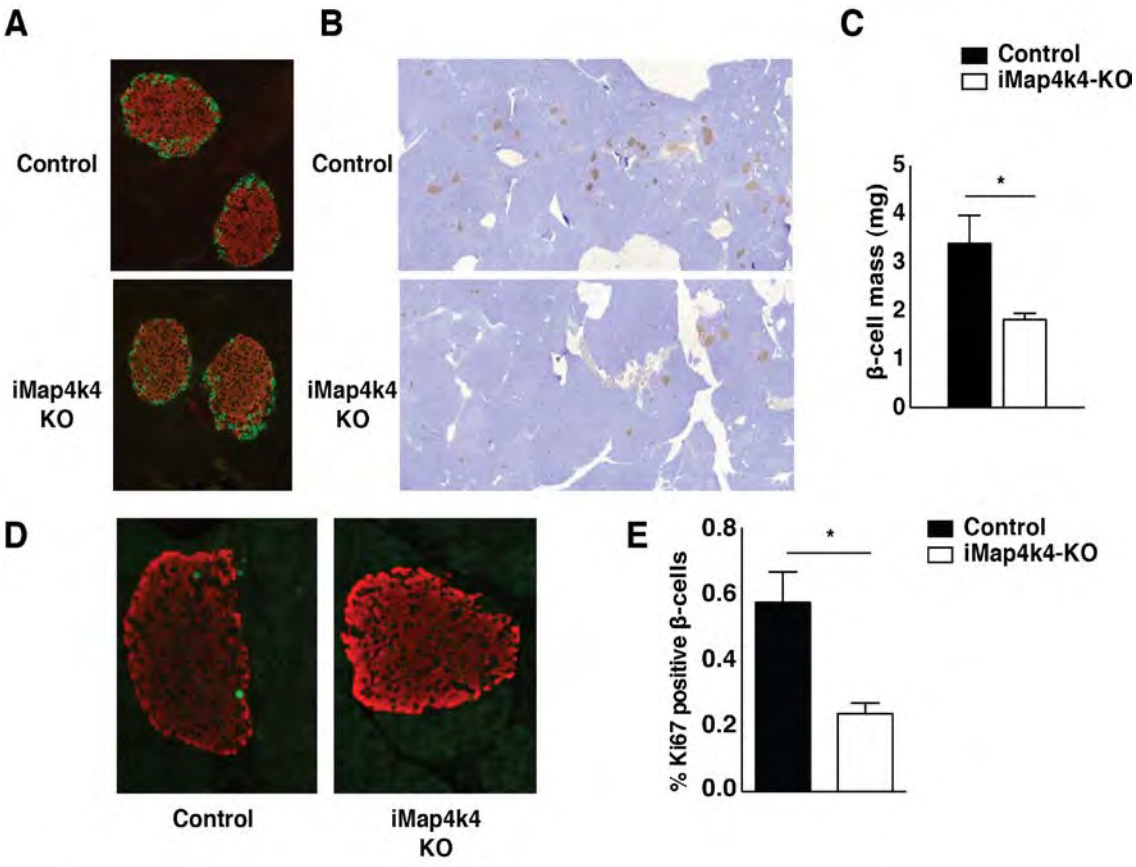

Figure AI-2. Map4k4 depletion attenuates β-cell expansion. (A-E) Both control and iMap4k4-KO mice were fed a HFD for 16 wks. **(A)** Representative images of islets doubled stained with insulin (red) and glucagon (green). **(B)** Representative images of H&E stained pancreata. **(C)** β-cell mass quantification. The ratio of β-cell area to total pancreas was calculated and multiplied by wet weight of pancreas (* $P<0.05$, N=9-12). **(D)** Representative images of islets doubled stained for insulin (red) and Ki67 (green). **(E)** β-cell proliferation was determined by counting the number of Ki67 positive β-cells divided by the total number of β-cells. Results represent the mean ± SEM (* $P < 0.05$, N=4-5).

These results suggest Map4k4 may have dual pancreatic functions, promoting insulin secretion and β-cell expansion. First, Map4k4 is a positive regulator of insulin secretion; specifically Map4k4 depletion disrupts the 1st wave of insulin release. Insulin is released in a biphasic manner, with the 1st wave of insulin secretion occurring 5 minutes after glucose surge and the 2nd wave occurring 30 minutes after initial glucose surge. During the 1st wave of insulin secretion, glucose is metabolized, increasing the ATP:ADP ratio, which causes a closure of K_{ATP} channels (82). K_{ATP} channels closure causes a depolarization of the plasma membrane and opening of voltage-activated Ca^{2+} channels, allowing Ca^{2+} influx, and insulin vesicle exocytosis (82). Fewer mechanistic details are known about the 2nd wave of insulin secretion; however, it is hypothesized to be independent of K_{ATP} channels (84). Interestingly, previous studies suggest Map4k4 directly binds and phosphorylates the Na^{+}-H^{+} exchanger (Nhe1) (316). Nhe1 is a plasma membrane ion exchanger involved in regulation of intracellular pH (317). Nhe1 is highly expressed in β-cells and protects from intracellular acidification (317). Although Nhe1 is not causally involved in insulin secretion, suppression of Nhe1 augments insulin secretion via cytosolic acidification, closure of K_{ATP} channels, and insulin (318). We hypothesize that Map4k4 inhibits Nhe1 via direct phosphorylation; thus, Map4k4 depletion enhances Nhe1 activity and results in less β-cell cytosolic acidification and less insulin release. Second, Map4k4 promotes β-cell expansion by regulating β-cell proliferation. HFD-fed iMap4k4-KO mice displayed reduced β-cell proliferation, which was associated with a reduction β-cell number and mass. These results suggest Map4k4

may be a novel therapeutic target improving peripheral insulin resistance and lowering hyperinsulinemic conditions that occur in obesity-induced insulin resistance.

References

1. **Cryer PE.** 1981. Glucose counterregulation in man. Diabetes **30:**261-264.
2. **Zierler K.** 1999. Whole body glucose metabolism. Am J Physiol **276:**E409-426.
3. **Zammitt NN, Frier BM.** 2005. Hypoglycemia in type 2 diabetes: pathophysiology, frequency, and effects of different treatment modalities. Diabetes Care **28:**2948-2961.
4. **Reaven GM, Hollenbeck C, Jeng CY, Wu MS, Chen YD.** 1988. Measurement of plasma glucose, free fatty acid, lactate, and insulin for 24 h in patients with NIDDM. Diabetes **37:**1020-1024.
5. **Jiang G, Zhang BB.** 2003. Glucagon and regulation of glucose metabolism. Am J Physiol Endocrinol Metab **284:**E671-678.
6. **Kowall B, Rathmann W.** 2013. HbA1c for diagnosis of type 2 diabetes. Is there an optimal cut point to assess high risk of diabetes complications, and how well does the 6.5% cutoff perform? Diabetes Metab Syndr Obes **6:**477-491.
7. **Ryu TY, Park J, Scherer PE.** 2014. Hyperglycemia as a risk factor for cancer progression. Diabetes Metab J **38:**330-336.
8. **Weisberg SP, McCann D, Desai M, Rosenbaum M, Leibel RL, Ferrante AW, Jr.** 2003. Obesity is associated with macrophage accumulation in adipose tissue. J Clin Invest **112:**1796-1808.
9. **Wellen KE, Hotamisligil GS.** 2003. Obesity-induced inflammatory changes in adipose tissue. J Clin Invest **112:**1785-1788.
10. **Xu H, Barnes GT, Yang Q, Tan G, Yang D, Chou CJ, Sole J, Nichols A, Ross JS, Tartaglia LA, Chen H.** 2003. Chronic inflammation in fat plays a crucial role in the development of obesity-related insulin resistance. J Clin Invest **112:**1821-1830.
11. **Saltiel AR, Kahn CR.** 2001. Insulin signalling and the regulation of glucose and lipid metabolism. Nature **414:**799-806.
12. **Butler AE, Janson J, Bonner-Weir S, Ritzel R, Rizza RA, Butler PC.** 2003. Beta-cell deficit and increased beta-cell apoptosis in humans with type 2 diabetes. Diabetes **52:**102-110.
13. **DeFronzo RA.** 1997. Insulin resistance: a multifaceted syndrome responsible for NIDDM, obesity, hypertension, dyslipidaemia and atherosclerosis. Neth J Med **50:**191-197.
14. **Pfeifer MA, Halter JB, Porte D, Jr.** 1981. Insulin secretion in diabetes mellitus. Am J Med **70:**579-588.
15. **Meneghini LF.** 2013. Intensifying insulin therapy: what options are available to patients with type 2 diabetes? Am J Med **126:**S28-37.
16. **Mansour M.** 2014. The roles of peroxisome proliferator-activated receptors in the metabolic syndrome. Prog Mol Biol Transl Sci **121:**217-266.

17. **Soccio RE, Chen ER, Lazar MA.** 2014. Thiazolidinediones and the promise of insulin sensitization in type 2 diabetes. Cell Metab **20:**573-591.
18. **Biddinger SB, Kahn CR.** 2006. From mice to men: insights into the insulin resistance syndromes. Annu Rev Physiol **68:**123-158.
19. **Patti ME, Kahn CR.** 1998. The insulin receptor--a critical link in glucose homeostasis and insulin action. J Basic Clin Physiol Pharmacol **9:**89-109.
20. **Ullrich A, Schlessinger J.** 1990. Signal transduction by receptors with tyrosine kinase activity. Cell **61:**203-212.
21. **White MF.** 1998. The IRS-signalling system: a network of docking proteins that mediate insulin action. Mol Cell Biochem **182:**3-11.
22. **Taniguchi CM, Emanuelli B, Kahn CR.** 2006. Critical nodes in signalling pathways: insights into insulin action. Nat Rev Mol Cell Biol **7:**85-96.
23. **Lietzke SE, Bose S, Cronin T, Klarlund J, Chawla A, Czech MP, Lambright DG.** 2000. Structural basis of 3-phosphoinositide recognition by pleckstrin homology domains. Mol Cell **6:**385-394.
24. **Sarbassov DD, Guertin DA, Ali SM, Sabatini DM.** 2005. Phosphorylation and regulation of Akt/PKB by the rictor-mTOR complex. Science **307:**1098-1101.
25. **Shepherd PR, Withers DJ, Siddle K.** 1998. Phosphoinositide 3-kinase: the key switch mechanism in insulin signalling. Biochem J **333 (Pt 3):**471-490.
26. **Shepherd PR, Kahn BB.** 1999. Glucose transporters and insulin action--implications for insulin resistance and diabetes mellitus. N Engl J Med **341:**248-257.
27. **Leney SE, Tavare JM.** 2009. The molecular basis of insulin-stimulated glucose uptake: signalling, trafficking and potential drug targets. J Endocrinol **203:**1-18.
28. **Stenbit AE, Tsao TS, Li J, Burcelin R, Geenen DL, Factor SM, Houseknecht K, Katz EB, Charron MJ.** 1997. GLUT4 heterozygous knockout mice develop muscle insulin resistance and diabetes. Nat Med **3:**1096-1101.
29. **Laplante M, Sabatini DM.** 2012. mTOR signaling in growth control and disease. Cell **149:**274-293.
30. **Sancak Y, Thoreen CC, Peterson TR, Lindquist RA, Kang SA, Spooner E, Carr SA, Sabatini DM.** 2007. PRAS40 is an insulin-regulated inhibitor of the mTORC1 protein kinase. Mol Cell **25:**903-915.
31. **Thedieck K, Polak P, Kim ML, Molle KD, Cohen A, Jeno P, Arrieumerlou C, Hall MN.** 2007. PRAS40 and PRR5-like protein are new mTOR interactors that regulate apoptosis. PLoS One **2:**e1217.
32. **Vander Haar E, Lee SI, Bandhakavi S, Griffin TJ, Kim DH.** 2007. Insulin signalling to mTOR mediated by the Akt/PKB substrate PRAS40. Nat Cell Biol **9:**316-323.
33. **Wang L, Harris TE, Roth RA, Lawrence JC, Jr.** 2007. PRAS40 regulates mTORC1 kinase activity by functioning as a direct inhibitor of substrate binding. J Biol Chem **282:**20036-20044.

34. **Inoki K, Li Y, Xu T, Guan KL.** 2003. Rheb GTPase is a direct target of TSC2 GAP activity and regulates mTOR signaling. Genes Dev **17:**1829-1834.
35. **Tee AR, Manning BD, Roux PP, Cantley LC, Blenis J.** 2003. Tuberous sclerosis complex gene products, Tuberin and Hamartin, control mTOR signaling by acting as a GTPase-activating protein complex toward Rheb. Curr Biol **13:**1259-1268.
36. **Inoki K, Li Y, Zhu T, Wu J, Guan KL.** 2002. TSC2 is phosphorylated and inhibited by Akt and suppresses mTOR signalling. Nat Cell Biol **4:**648-657.
37. **Manning BD, Tee AR, Logsdon MN, Blenis J, Cantley LC.** 2002. Identification of the tuberous sclerosis complex-2 tumor suppressor gene product tuberin as a target of the phosphoinositide 3-kinase/akt pathway. Mol Cell **10:**151-162.
38. **Potter CJ, Pedraza LG, Xu T.** 2002. Akt regulates growth by directly phosphorylating Tsc2. Nat Cell Biol **4:**658-665.
39. **Ma XM, Blenis J.** 2009. Molecular mechanisms of mTOR-mediated translational control. Nat Rev Mol Cell Biol **10:**307-318.
40. **Martin KA, Blenis J.** 2002. Coordinate regulation of translation by the PI 3-kinase and mTOR pathways. Adv Cancer Res **86:**1-39.
41. **Richter JD, Sonenberg N.** 2005. Regulation of cap-dependent translation by eIF4E inhibitory proteins. Nature **433:**477-480.
42. **Laplante M, Sabatini DM.** 2009. An emerging role of mTOR in lipid biosynthesis. Curr Biol **19:**R1046-1052.
43. **Nicholson KM, Anderson NG.** 2002. The protein kinase B/Akt signalling pathway in human malignancy. Cell Signal **14:**381-395.
44. **Vivanco I, Sawyers CL.** 2002. The phosphatidylinositol 3-Kinase AKT pathway in human cancer. Nat Rev Cancer **2:**489-501.
45. **Hotamisligil GS, Peraldi P, Budavari A, Ellis R, White MF, Spiegelman BM.** 1996. IRS-1-mediated inhibition of insulin receptor tyrosine kinase activity in TNF-alpha- and obesity-induced insulin resistance. Science **271:**665-668.
46. **Qiao LY, Goldberg JL, Russell JC, Sun XJ.** 1999. Identification of enhanced serine kinase activity in insulin resistance. J Biol Chem **274:**10625-10632.
47. **Draznin B.** 2006. Molecular mechanisms of insulin resistance: serine phosphorylation of insulin receptor substrate-1 and increased expression of p85alpha: the two sides of a coin. Diabetes **55:**2392-2397.
48. **Copps KD, Hancer NJ, Opare-Ado L, Qiu W, Walsh C, White MF.** 2010. Irs1 serine 307 promotes insulin sensitivity in mice. Cell Metab **11:**84-92.
49. **Elchebly M, Payette P, Michaliszyn E, Cromlish W, Collins S, Loy AL, Normandin D, Cheng A, Himms-Hagen J, Chan CC, Ramachandran C, Gresser MJ, Tremblay ML, Kennedy BP.** 1999. Increased insulin sensitivity and obesity resistance in mice lacking the protein tyrosine phosphatase-1B gene. Science **283:**1544-1548.

50. **Ueki K, Kondo T, Kahn CR.** 2004. Suppressor of cytokine signaling 1 (SOCS-1) and SOCS-3 cause insulin resistance through inhibition of tyrosine phosphorylation of insulin receptor substrate proteins by discrete mechanisms. Mol Cell Biol **24:**5434-5446.
51. **Emanuelli B, Peraldi P, Filloux C, Chavey C, Freidinger K, Hilton DJ, Hotamisligil GS, Van Obberghen E.** 2001. SOCS-3 inhibits insulin signaling and is up-regulated in response to tumor necrosis factor-alpha in the adipose tissue of obese mice. J Biol Chem **276:**47944-47949.
52. **Rui L, Yuan M, Frantz D, Shoelson S, White MF.** 2002. SOCS-1 and SOCS-3 block insulin signaling by ubiquitin-mediated degradation of IRS1 and IRS2. J Biol Chem **277:**42394-42398.
53. **Maehama T, Dixon JE.** 1998. The tumor suppressor, PTEN/MMAC1, dephosphorylates the lipid second messenger, phosphatidylinositol 3,4,5-trisphosphate. J Biol Chem **273:**13375-13378.
54. **Wishart MJ, Dixon JE.** 2002. PTEN and myotubularin phosphatases: from 3-phosphoinositide dephosphorylation to disease. Trends Cell Biol **12:**579-585.
55. **Bluher M.** 2013. Adipose tissue dysfunction contributes to obesity related metabolic diseases. Best Pract Res Clin Endocrinol Metab **27:**163-177.
56. **Guilherme A, Virbasius JV, Puri V, Czech MP.** 2008. Adipocyte dysfunctions linking obesity to insulin resistance and type 2 diabetes. Nat Rev Mol Cell Biol **9:**367-377.
57. **Liu L, Mei M, Yang S, Li Q.** 2014. Roles of chronic low-grade inflammation in the development of ectopic fat deposition. Mediators Inflamm **2014:**418185.
58. **Aguirre V, Uchida T, Yenush L, Davis R, White MF.** 2000. The c-Jun NH(2)-terminal kinase promotes insulin resistance during association with insulin receptor substrate-1 and phosphorylation of Ser(307). J Biol Chem **275:**9047-9054.
59. **Hirosumi J, Tuncman G, Chang L, Gorgun CZ, Uysal KT, Maeda K, Karin M, Hotamisligil GS.** 2002. A central role for JNK in obesity and insulin resistance. Nature **420:**333-336.
60. **Shi H, Kokoeva MV, Inouye K, Tzameli I, Yin H, Flier JS.** 2006. TLR4 links innate immunity and fatty acid-induced insulin resistance. J Clin Invest **116:**3015-3025.
61. **Griffin ME, Marcucci MJ, Cline GW, Bell K, Barucci N, Lee D, Goodyear LJ, Kraegen EW, White MF, Shulman GI.** 1999. Free fatty acid-induced insulin resistance is associated with activation of protein kinase C theta and alterations in the insulin signaling cascade. Diabetes **48:**1270-1274.
62. **Hajduch E, Balendran A, Batty IH, Litherland GJ, Blair AS, Downes CP, Hundal HS.** 2001. Ceramide impairs the insulin-dependent membrane recruitment of protein kinase B leading to a loss in downstream signalling in L6 skeletal muscle cells. Diabetologia **44:**173-183.
63. **Summers SA.** 2006. Ceramides in insulin resistance and lipotoxicity. Prog Lipid Res **45:**42-72.

64. **Herman MA, Kahn BB.** 2006. Glucose transport and sensing in the maintenance of glucose homeostasis and metabolic harmony. J Clin Invest **116:**1767-1775.
65. **Carey M, Kehlenbrink S, Hawkins M.** 2013. Evidence for central regulation of glucose metabolism. J Biol Chem **288:**34981-34988.
66. **Brelje TC, Scharp DW, Sorenson RL.** 1989. Three-dimensional imaging of intact isolated islets of Langerhans with confocal microscopy. Diabetes **38:**808-814.
67. **Gromada J, Bokvist K, Ding WG, Barg S, Buschard K, Renstrom E, Rorsman P.** 1997. Adrenaline stimulates glucagon secretion in pancreatic A-cells by increasing the Ca2+ current and the number of granules close to the L-type Ca2+ channels. J Gen Physiol **110:**217-228.
68. **Quesada I, Tuduri E, Ripoll C, Nadal A.** 2008. Physiology of the pancreatic alpha-cell and glucagon secretion: role in glucose homeostasis and diabetes. J Endocrinol **199:**5-19.
69. **Furuta M, Zhou A, Webb G, Carroll R, Ravazzola M, Orci L, Steiner DF.** 2001. Severe defect in proglucagon processing in islet A-cells of prohormone convertase 2 null mice. J Biol Chem **276:**27197-27202.
70. **Rouille Y, Bianchi M, Irminger JC, Halban PA.** 1997. Role of the prohormone convertase PC2 in the processing of proglucagon to glucagon. FEBS Lett **413:**119-123.
71. **Furuta M, Yano H, Zhou A, Rouille Y, Holst JJ, Carroll R, Ravazzola M, Orci L, Furuta H, Steiner DF.** 1997. Defective prohormone processing and altered pancreatic islet morphology in mice lacking active SPC2. Proc Natl Acad Sci U S A **94:**6646-6651.
72. **Webb GC, Akbar MS, Zhao C, Swift HH, Steiner DF.** 2002. Glucagon replacement via micro-osmotic pump corrects hypoglycemia and alpha-cell hyperplasia in prohormone convertase 2 knockout mice. Diabetes **51:**398-405.
73. **Johansson H, Gylfe E, Hellman B.** 1987. The actions of arginine and glucose on glucagon secretion are mediated by opposite effects on cytoplasmic Ca2+. Biochem Biophys Res Commun **147:**309-314.
74. **Pipeleers DG, Schuit FC, Van Schravendijk CF, Van de Winkel M.** 1985. Interplay of nutrients and hormones in the regulation of glucagon release. Endocrinology **117:**817-823.
75. **Unger RH.** 1985. [New findings on the mechanisms of secretion of glucagon]. Recenti Prog Med **76:**284-286.
76. **Franklin I, Gromada J, Gjinovci A, Theander S, Wollheim CB.** 2005. Beta-cell secretory products activate alpha-cell ATP-dependent potassium channels to inhibit glucagon release. Diabetes **54:**1808-1815.
77. **Leung YM, Ahmed I, Sheu L, Gao X, Hara M, Tsushima RG, Diamant NE, Gaisano HY.** 2006. Insulin regulates islet alpha-cell function by reducing

KATP channel sensitivity to adenosine 5'-triphosphate inhibition. Endocrinology **147:**2155-2162.

78. **Rorsman P, Berggren PO, Bokvist K, Ericson H, Mohler H, Ostenson CG, Smith PA.** 1989. Glucose-inhibition of glucagon secretion involves activation of GABAA-receptor chloride channels. Nature **341:**233-236.
79. **Shi Y, Kanaani J, Menard-Rose V, Ma YH, Chang PY, Hanahan D, Tobin A, Grodsky G, Baekkeskov S.** 2000. Increased expression of GAD65 and GABA in pancreatic beta-cells impairs first-phase insulin secretion. Am J Physiol Endocrinol Metab **279:**E684-694.
80. **Sorenson RL, Garry DG, Brelje TC.** 1991. Structural and functional considerations of GABA in islets of Langerhans. Beta-cells and nerves. Diabetes **40:**1365-1374.
81. **Goodner CJ, Walike BC, Koerker DJ, Ensinck JW, Brown AC, Chideckel EW, Palmer J, Kalnasy L.** 1977. Insulin, glucagon, and glucose exhibit synchronous, sustained oscillations in fasting monkeys. Science **195:**177-179.
82. **Ashcroft FM, Rorsman P.** 1989. Electrophysiology of the pancreatic beta-cell. Prog Biophys Mol Biol **54:**87-143.
83. **Nesher R, Cerasi E.** 2002. Modeling phasic insulin release: immediate and time-dependent effects of glucose. Diabetes **51 Suppl 1:**S53-59.
84. **Gembal M, Gilon P, Henquin JC.** 1992. Evidence that glucose can control insulin release independently from its action on ATP-sensitive K+ channels in mouse B cells. J Clin Invest **89:**1288-1295.
85. **Muoio DM, Newgard CB.** 2008. Mechanisms of disease:Molecular and metabolic mechanisms of insulin resistance and beta-cell failure in type 2 diabetes. Nat Rev Mol Cell Biol **9:**193-205.
86. **Sakuraba H, Mizukami H, Yagihashi N, Wada R, Hanyu C, Yagihashi S.** 2002. Reduced beta-cell mass and expression of oxidative stress-related DNA damage in the islet of Japanese Type II diabetic patients. Diabetologia **45:**85-96.
87. **Scheuner D, Song B, McEwen E, Liu C, Laybutt R, Gillespie P, Saunders T, Bonner-Weir S, Kaufman RJ.** 2001. Translational control is required for the unfolded protein response and in vivo glucose homeostasis. Mol Cell **7:**1165-1176.
88. **Scheuner D, Vander Mierde D, Song B, Flamez D, Creemers JW, Tsukamoto K, Ribick M, Schuit FC, Kaufman RJ.** 2005. Control of mRNA translation preserves endoplasmic reticulum function in beta cells and maintains glucose homeostasis. Nat Med **11:**757-764.
89. **Rossetti L, Giaccari A, DeFronzo RA.** 1990. Glucose toxicity. Diabetes Care **13:**610-630.
90. **Johnson KH, O'Brien TD, Betsholtz C, Westermark P.** 1989. Islet amyloid, islet-amyloid polypeptide, and diabetes mellitus. N Engl J Med **321:**513-518.

91. **Westermark P.** 1972. Occurrence of amyloid deposits in the skin in secondary systemic amyloidosis. Acta Pathol Microbiol Scand A **80:**718-720.
92. **Donath MY, Maedler K, Sergeev P, Dyntar D, Thomas D, Spinas GA.** 2002. [The pathogenesis of type 2 diabetes--new aspects and clinical consequences]. Ther Umsch **59:**381-385.
93. **Donath MY, Shoelson SE.** 2011. Type 2 diabetes as an inflammatory disease. Nat Rev Immunol **11:**98-107.
94. **Wellen KE, Hotamisligil GS.** 2005. Inflammation, stress, and diabetes. J Clin Invest **115:**1111-1119.
95. **Ehses JA, Perren A, Eppler E, Ribaux P, Pospisilik JA, Maor-Cahn R, Gueripel X, Ellingsgaard H, Schneider MK, Biollaz G, Fontana A, Reinecke M, Homo-Delarche F, Donath MY.** 2007. Increased number of islet-associated macrophages in type 2 diabetes. Diabetes **56:**2356-2370.
96. **Loweth AC, Williams GT, James RF, Scarpello JH, Morgan NG.** 1998. Human islets of Langerhans express Fas ligand and undergo apoptosis in response to interleukin-1beta and Fas ligation. Diabetes **47:**727-732.
97. **Spinas GA, Hansen BS, Linde S, Kastern W, Molvig J, Mandrup-Poulsen T, Dinarello CA, Nielsen JH, Nerup J.** 1987. Interleukin 1 dose-dependently affects the biosynthesis of (pro)insulin in isolated rat islets of Langerhans. Diabetologia **30:**474-480.
98. **Brownlee M.** 2001. Biochemistry and molecular cell biology of diabetic complications. Nature **414:**813-820.
99. **Tiedge M, Lortz S, Drinkgern J, Lenzen S.** 1997. Relation between antioxidant enzyme gene expression and antioxidative defense status of insulin-producing cells. Diabetes **46:**1733-1742.
100. **Gustafson B, Gogg S, Hedjazifar S, Jenndahl L, Hammarstedt A, Smith U.** 2009. Inflammation and impaired adipogenesis in hypertrophic obesity in man. Am J Physiol Endocrinol Metab **297:**E999-E1003.
101. **Lafontan M.** 2014. Adipose tissue and adipocyte dysregulation. Diabetes Metab **40:**16-28.
102. **Sam S, Mazzone T.** 2014. Adipose tissue changes in obesity and the impact on metabolic function. Transl Res **164:**284-292.
103. **Huang-Doran I, Sleigh A, Rochford JJ, O'Rahilly S, Savage DB.** 2010. Lipodystrophy: metabolic insights from a rare disorder. J Endocrinol **207:**245-255.
104. **Simha V, Garg A.** 2006. Lipodystrophy: lessons in lipid and energy metabolism. Curr Opin Lipidol **17:**162-169.
105. **Unger RH, Scherer PE.** 2010. Gluttony, sloth and the metabolic syndrome: a roadmap to lipotoxicity. Trends Endocrinol Metab **21:**345-352.
106. **Kim JK, Gavrilova O, Chen Y, Reitman ML, Shulman GI.** 2000. Mechanism of insulin resistance in A-ZIP/F-1 fatless mice. J Biol Chem **275:**8456-8460.
107. **Barrnett RJ, Ball EG.** 1960. Metabolic and ultrastructural changes induced in adipose tissue by insulin. J Biophys Biochem Cytol **8:**83-101.

108. **Dimitriadis G, Mitrou P, Lambadiari V, Maratou E, Raptis SA.** 2011. Insulin effects in muscle and adipose tissue. Diabetes Res Clin Pract **93 Suppl 1:**S52-59.
109. **Kane S, Sano H, Liu SC, Asara JM, Lane WS, Garner CC, Lienhard GE.** 2002. A method to identify serine kinase substrates. Akt phosphorylates a novel adipocyte protein with a Rab GTPase-activating protein (GAP) domain. J Biol Chem **277:**22115-22118.
110. **Roach WG, Chavez JA, Miinea CP, Lienhard GE.** 2007. Substrate specificity and effect on GLUT4 translocation of the Rab GTPase-activating protein Tbc1d1. Biochem J **403:**353-358.
111. **Sakamoto K, Holman GD.** 2008. Emerging role for AS160/TBC1D4 and TBC1D1 in the regulation of GLUT4 traffic. Am J Physiol Endocrinol Metab **295:**E29-37.
112. **Ong JM, Kirchgessner TG, Schotz MC, Kern PA.** 1988. Insulin increases the synthetic rate and messenger RNA level of lipoprotein lipase in isolated rat adipocytes. J Biol Chem **263:**12933-12938.
113. **Picard F, Naimi N, Richard D, Deshaies Y.** 1999. Response of adipose tissue lipoprotein lipase to the cephalic phase of insulin secretion. Diabetes **48:**452-459.
114. **Foretz M, Guichard C, Ferre P, Foufelle F.** 1999. Sterol regulatory element binding protein-1c is a major mediator of insulin action on the hepatic expression of glucokinase and lipogenesis-related genes. Proc Natl Acad Sci U S A **96:**12737-12742.
115. **Shimomura I, Matsuda M, Hammer RE, Bashmakov Y, Brown MS, Goldstein JL.** 2000. Decreased IRS-2 and increased SREBP-1c lead to mixed insulin resistance and sensitivity in livers of lipodystrophic and ob/ob mice. Mol Cell **6:**77-86.
116. **Yamashita H, Takenoshita M, Sakurai M, Bruick RK, Henzel WJ, Shillinglaw W, Arnot D, Uyeda K.** 2001. A glucose-responsive transcription factor that regulates carbohydrate metabolism in the liver. Proc Natl Acad Sci U S A **98:**9116-9121.
117. **Jeon TI, Osborne TF.** 2011. SREBPs: metabolic integrators in physiology and metabolism. Trends Endocrinol Metab **23:**65-72.
118. **Postic C, Dentin R, Denechaud PD, Girard J.** 2007. ChREBP, a transcriptional regulator of glucose and lipid metabolism. Annu Rev Nutr **27:**179-192.
119. **Shimomura I, Bashmakov Y, Ikemoto S, Horton JD, Brown MS, Goldstein JL.** 1999. Insulin selectively increases SREBP-1c mRNA in the livers of rats with streptozotocin-induced diabetes. Proc Natl Acad Sci U S A **96:**13656-13661.
120. **Uyeda K, Repa JJ.** 2006. Carbohydrate response element binding protein, ChREBP, a transcription factor coupling hepatic glucose utilization and lipid synthesis. Cell Metab **4:**107-110.

121. **Shepherd PR, Gnudi L, Tozzo E, Yang H, Leach F, Kahn BB.** 1993. Adipose cell hyperplasia and enhanced glucose disposal in transgenic mice overexpressing GLUT4 selectively in adipose tissue. J Biol Chem **268:**22243-22246.
122. **Liu ML, Gibbs EM, McCoid SC, Milici AJ, Stukenbrok HA, McPherson RK, Treadway JL, Pessin JE.** 1993. Transgenic mice expressing the human GLUT4/muscle-fat facilitative glucose transporter protein exhibit efficient glycemic control. Proc Natl Acad Sci U S A **90:**11346-11350.
123. **Kim JY, van de Wall E, Laplante M, Azzara A, Trujillo ME, Hofmann SM, Schraw T, Durand JL, Li H, Li G, Jelicks LA, Mehler MF, Hui DY, Deshaies Y, Shulman GI, Schwartz GJ, Scherer PE.** 2007. Obesity-associated improvements in metabolic profile through expansion of adipose tissue. J Clin Invest **117:**2621-2637.
124. **Sugii S, Olson P, Sears DD, Saberi M, Atkins AR, Barish GD, Hong SH, Castro GL, Yin YQ, Nelson MC, Hsiao G, Greaves DR, Downes M, Yu RT, Olefsky JM, Evans RM.** 2009. PPARgamma activation in adipocytes is sufficient for systemic insulin sensitization. Proc Natl Acad Sci U S A **106:**22504-22509.
125. **Dallman MF, Strack AM, Akana SF, Bradbury MJ, Hanson ES, Scribner KA, Smith M.** 1993. Feast and famine: critical role of glucocorticoids with insulin in daily energy flow. Front Neuroendocrinol **14:**303-347.
126. **Kumon A, Hara T, Takahashi A.** 1976. Effects of catecholamines on the lipolysis of two kinds of fat cells from adult rabbit. J Lipid Res **17:**559-564.
127. **Carey GB.** 1998. Mechanisms regulating adipocyte lipolysis. Adv Exp Med Biol **441:**157-170.
128. **Lafontan M, Berlan M.** 1993. Fat cell adrenergic receptors and the control of white and brown fat cell function. J Lipid Res **34:**1057-1091.
129. **Lafontan M, Sengenes C, Galitzky J, Berlan M, De Glisezinski I, Crampes F, Stich V, Langin D, Barbe P, Riviere D.** 2000. Recent developments on lipolysis regulation in humans and discovery of a new lipolytic pathway. Int J Obes Relat Metab Disord **24 Suppl 4:**S47-52.
130. **Langin D, Lucas S, Lafontan M.** 2000. Millennium fat-cell lipolysis reveals unsuspected novel tracks. Horm Metab Res **32:**443-452.
131. **Greenberg AS, Egan JJ, Wek SA, Garty NB, Blanchette-Mackie EJ, Londos C.** 1991. Perilipin, a major hormonally regulated adipocyte-specific phosphoprotein associated with the periphery of lipid storage droplets. J Biol Chem **266:**11341-11346.
132. **Stralfors P, Belfrage P.** 1983. Phosphorylation of hormone-sensitive lipase by cyclic AMP-dependent protein kinase. J Biol Chem **258:**15146-15152.
133. **Holm C.** 2003. Molecular mechanisms regulating hormone-sensitive lipase and lipolysis. Biochem Soc Trans **31:**1120-1124.
134. **Large V, Peroni O, Letexier D, Ray H, Beylot M.** 2004. Metabolism of lipids in human white adipocyte. Diabetes Metab **30:**294-309.

135. **Degerman E, Belfrage P, Manganiello VC.** 1997. Structure, localization, and regulation of cGMP-inhibited phosphodiesterase (PDE3). J Biol Chem **272:**6823-6826.
136. **Kitamura T, Kitamura Y, Kuroda S, Hino Y, Ando M, Kotani K, Konishi H, Matsuzaki H, Kikkawa U, Ogawa W, Kasuga M.** 1999. Insulin-induced phosphorylation and activation of cyclic nucleotide phosphodiesterase 3B by the serine-threonine kinase Akt. Mol Cell Biol **19:**6286-6296.
137. **Olsson H, Belfrage P.** 1987. The regulatory and basal phosphorylation sites of hormone-sensitive lipase are dephosphorylated by protein phosphatase-1, 2A and 2C but not by protein phosphatase-2B. Eur J Biochem **168:**399-405.
138. **Olsson H, Belfrage P.** 1988. Phosphorylation and dephosphorylation of hormone-sensitive lipase. Interactions between the regulatory and basal phosphorylation sites. FEBS Lett **232:**78-82.
139. **Pham K, Langlais P, Zhang X, Chao A, Zingsheim M, Yi Z.** 2012. Insulin-stimulated phosphorylation of protein phosphatase 1 regulatory subunit 12B revealed by HPLC-ESI-MS/MS. Proteome Sci **10:**52.
140. **Bergman RN.** 1997. New concepts in extracellular signaling for insulin action: the single gateway hypothesis. Recent Prog Horm Res **52:**359-385; discussion 385-357.
141. **Aguilar-Valles A, Inoue W, Rummel C, Luheshi GN.** 2015. Obesity, adipokines and neuroinflammation. Neuropharmacology doi:10.1016/j.neuropharm.2014.12.023.
142. **Flier JS.** 2004. Obesity wars: molecular progress confronts an expanding epidemic. Cell **116:**337-350.
143. **Romacho T, Elsen M, Rohrborn D, Eckel J.** 2014. Adipose tissue and its role in organ crosstalk. Acta Physiol (Oxf) **210:**733-753.
144. **Halaas JL, Gajiwala KS, Maffei M, Cohen SL, Chait BT, Rabinowitz D, Lallone RL, Burley SK, Friedman JM.** 1995. Weight-reducing effects of the plasma protein encoded by the obese gene. Science **269:**543-546.
145. **Maffei M, Fei H, Lee GH, Dani C, Leroy P, Zhang Y, Proenca R, Negrel R, Ailhaud G, Friedman JM.** 1995. Increased expression in adipocytes of ob RNA in mice with lesions of the hypothalamus and with mutations at the db locus. Proc Natl Acad Sci U S A **92:**6957-6960.
146. **Considine RV, Sinha MK, Heiman ML, Kriauciunas A, Stephens TW, Nyce MR, Ohannesian JP, Marco CC, McKee LJ, Bauer TL, et al.** 1996. Serum immunoreactive-leptin concentrations in normal-weight and obese humans. N Engl J Med **334:**292-295.
147. **Margetic S, Gazzola C, Pegg GG, Hill RA.** 2002. Leptin: a review of its peripheral actions and interactions. Int J Obes Relat Metab Disord **26:**1407-1433.
148. **Zhang Y, Proenca R, Maffei M, Barone M, Leopold L, Friedman JM.** 1994. Positional cloning of the mouse obese gene and its human homologue. Nature **372:**425-432.

149. **Berg AH, Combs TP, Du X, Brownlee M, Scherer PE.** 2001. The adipocyte-secreted protein Acrp30 enhances hepatic insulin action. Nat Med **7:**947-953.
150. **Fruebis J, Tsao TS, Javorschi S, Ebbets-Reed D, Erickson MR, Yen FT, Bihain BE, Lodish HF.** 2001. Proteolytic cleavage product of 30-kDa adipocyte complement-related protein increases fatty acid oxidation in muscle and causes weight loss in mice. Proc Natl Acad Sci U S A **98:**2005-2010.
151. **Yamauchi T, Kamon J, Waki H, Terauchi Y, Kubota N, Hara K, Mori Y, Ide T, Murakami K, Tsuboyama-Kasaoka N, Ezaki O, Akanuma Y, Gavrilova O, Vinson C, Reitman ML, Kagechika H, Shudo K, Yoda M, Nakano Y, Tobe K, Nagai R, Kimura S, Tomita M, Froguel P, Kadowaki T.** 2001. The fat-derived hormone adiponectin reverses insulin resistance associated with both lipoatrophy and obesity. Nat Med **7:**941-946.
152. **Arita Y, Kihara S, Ouchi N, Takahashi M, Maeda K, Miyagawa J, Hotta K, Shimomura I, Nakamura T, Miyaoka K, Kuriyama H, Nishida M, Yamashita S, Okubo K, Matsubara K, Muraguchi M, Ohmoto Y, Funahashi T, Matsuzawa Y.** 1999. Paradoxical decrease of an adipose-specific protein, adiponectin, in obesity. Biochem Biophys Res Commun **257:**79-83.
153. **Yatagai T, Nagasaka S, Taniguchi A, Fukushima M, Nakamura T, Kuroe A, Nakai Y, Ishibashi S.** 2003. Hypoadiponectinemia is associated with visceral fat accumulation and insulin resistance in Japanese men with type 2 diabetes mellitus. Metabolism **52:**1274-1278.
154. **Kadowaki T, Yamauchi T, Kubota N, Hara K, Ueki K, Tobe K.** 2006. Adiponectin and adiponectin receptors in insulin resistance, diabetes, and the metabolic syndrome. J Clin Invest **116:**1784-1792.
155. **Kubota N, Terauchi Y, Yamauchi T, Kubota T, Moroi M, Matsui J, Eto K, Yamashita T, Kamon J, Satoh H, Yano W, Froguel P, Nagai R, Kimura S, Kadowaki T, Noda T.** 2002. Disruption of adiponectin causes insulin resistance and neointimal formation. J Biol Chem **277:**25863-25866.
156. **Maeda N, Shimomura I, Kishida K, Nishizawa H, Matsuda M, Nagaretani H, Furuyama N, Kondo H, Takahashi M, Arita Y, Komuro R, Ouchi N, Kihara S, Tochino Y, Okutomi K, Horie M, Takeda S, Aoyama T, Funahashi T, Matsuzawa Y.** 2002. Diet-induced insulin resistance in mice lacking adiponectin/ACRP30. Nat Med **8:**731-737.
157. **Nawrocki AR, Rajala MW, Tomas E, Pajvani UB, Saha AK, Trumbauer ME, Pang Z, Chen AS, Ruderman NB, Chen H, Rossetti L, Scherer PE.** 2006. Mice lacking adiponectin show decreased hepatic insulin sensitivity and reduced responsiveness to peroxisome proliferator-activated receptor gamma agonists. J Biol Chem **281:**2654-2660.
158. **Lodhi IJ, Wei X, Semenkovich CF.** 2011. Lipoexpediency: de novo lipogenesis as a metabolic signal transmitter. Trends Endocrinol Metab **22:**1-8.

159. **Cao H, Gerhold K, Mayers JR, Wiest MM, Watkins SM, Hotamisligil GS.** 2008. Identification of a lipokine, a lipid hormone linking adipose tissue to systemic metabolism. Cell **134:**933-944.
160. **Arner P.** 1999. Catecholamine-induced lipolysis in obesity. Int J Obes Relat Metab Disord **23 Suppl 1:**10-13.
161. **Shulman GI.** 2000. Cellular mechanisms of insulin resistance. J Clin Invest **106:**171-176.
162. **Kawasaki N, Asada R, Saito A, Kanemoto S, Imaizumi K.** 2012. Obesity-induced endoplasmic reticulum stress causes chronic inflammation in adipose tissue. Sci Rep **2:**799.
163. **Ozcan U, Cao Q, Yilmaz E, Lee AH, Iwakoshi NN, Ozdelen E, Tuncman G, Gorgun C, Glimcher LH, Hotamisligil GS.** 2004. Endoplasmic reticulum stress links obesity, insulin action, and type 2 diabetes. Science **306:**457-461.
164. **Cinti S, Mitchell G, Barbatelli G, Murano I, Ceresi E, Faloia E, Wang S, Fortier M, Greenberg AS, Obin MS.** 2005. Adipocyte death defines macrophage localization and function in adipose tissue of obese mice and humans. J Lipid Res **46:**2347-2355.
165. **Hosogai N, Fukuhara A, Oshima K, Miyata Y, Tanaka S, Segawa K, Furukawa S, Tochino Y, Komuro R, Matsuda M, Shimomura I.** 2007. Adipose tissue hypoxia in obesity and its impact on adipocytokine dysregulation. Diabetes **56:**901-911.
166. **Exley MA, Hand L, O'Shea D, Lynch L.** 2014. Interplay between the immune system and adipose tissue in obesity. J Endocrinol **223:**R41-48.
167. **Wang P, Wu P, Siegel MI, Egan RW, Billah MM.** 1995. Interleukin (IL)-10 inhibits nuclear factor kappa B (NF kappa B) activation in human monocytes. IL-10 and IL-4 suppress cytokine synthesis by different mechanisms. J Biol Chem **270:**9558-9563.
168. **Lee J.** 2013. Adipose tissue macrophages in the development of obesity-induced inflammation, insulin resistance and type 2 diabetes. Arch Pharm Res **36:**208-222.
169. **Nordlie RC, Foster JD, Lange AJ.** 1999. Regulation of glucose production by the liver. Annu Rev Nutr **19:**379-406.
170. **Cohen JC, Horton JD, Hobbs HH.** 2011. Human fatty liver disease: old questions and new insights. Science **332:**1519-1523.
171. **Ramnanan CJ, Edgerton DS, Kraft G, Cherrington AD.** 2011. Physiologic action of glucagon on liver glucose metabolism. Diabetes Obes Metab **13 Suppl 1:**118-125.
172. **Oh KJ, Han HS, Kim MJ, Koo SH.** 2013. CREB and FoxO1: two transcription factors for the regulation of hepatic gluconeogenesis. BMB Rep **46:**567-574.
173. **Altarejos JY, Montminy M.** 2011. CREB and the CRTC co-activators: sensors for hormonal and metabolic signals. Nat Rev Mol Cell Biol **12:**141-151.
174. **Biggs WH, 3rd, Meisenhelder J, Hunter T, Cavenee WK, Arden KC.** 1999. Protein kinase B/Akt-mediated phosphorylation promotes nuclear exclusion

of the winged helix transcription factor FKHR1. Proc Natl Acad Sci U S A **96:**7421-7426.

175. **Brunet A, Bonni A, Zigmond MJ, Lin MZ, Juo P, Hu LS, Anderson MJ, Arden KC, Blenis J, Greenberg ME.** 1999. Akt promotes cell survival by phosphorylating and inhibiting a Forkhead transcription factor. Cell **96:**857-868.
176. **Nakae J, Park BC, Accili D.** 1999. Insulin stimulates phosphorylation of the forkhead transcription factor FKHR on serine 253 through a Wortmannin-sensitive pathway. J Biol Chem **274:**15982-15985.
177. **Castano JG, Nieto A, Feliu JE.** 1979. Inactivation of phosphofructokinase by glucagon in rat hepatocytes. J Biol Chem **254:**5576-5579.
178. **Kurland IJ, Pilkis SJ.** 1995. Covalent control of 6-phosphofructo-2-kinase/fructose-2,6-bisphosphatase: insights into autoregulation of a bifunctional enzyme. Protein Sci **4:**1023-1037.
179. **Okar DA, Lange AJ.** 1999. Fructose-2,6-bisphosphate and control of carbohydrate metabolism in eukaryotes. Biofactors **10:**1-14.
180. **Akatsuka A, Singh TJ, Nakabayashi H, Lin MC, Huang KP.** 1985. Glucagon-stimulated phosphorylation of rat liver glycogen synthase in isolated hepatocytes. J Biol Chem **260:**3239-3242.
181. **Ciudad C, Camici M, Ahmad Z, Wang Y, DePaoli-Roach AA, Roach PJ.** 1984. Control of glycogen synthase phosphorylation in isolated rat hepatocytes by epinephrine, vasopressin and glucagon. Eur J Biochem **142:**511-520.
182. **Kersten S.** 2001. Mechanisms of nutritional and hormonal regulation of lipogenesis. EMBO Rep **2:**282-286.
183. **Cohen P.** 1993. Dissection of the protein phosphorylation cascades involved in insulin and growth factor action. Biochem Soc Trans **21 (Pt 3):**555-567.
184. **Parker PJ, Caudwell FB, Cohen P.** 1983. Glycogen synthase from rabbit skeletal muscle; effect of insulin on the state of phosphorylation of the seven phosphoserine residues in vivo. Eur J Biochem **130:**227-234.
185. **Villar-Palasi C, Larner J.** 1960. Insulin-mediated effect on the activity of UDPG-glycogen transglucosylase of muscle. Biochim Biophys Acta **39:**171-173.
186. **Roach PJ.** 2002. Glycogen and its metabolism. Curr Mol Med **2:**101-120.
187. **Parker PJ, Embi N, Caudwell FB, Cohen P.** 1982. Glycogen synthase from rabbit skeletal muscle. State of phosphorylation of the seven phosphoserine residues in vivo in the presence and absence of adrenaline. Eur J Biochem **124:**47-55.
188. **Rylatt DB, Aitken A, Bilham T, Condon GD, Embi N, Cohen P.** 1980. Glycogen synthase from rabbit skeletal muscle. Amino acid sequence at the sites phosphorylated by glycogen synthase kinase-3, and extension of the N-terminal sequence containing the site phosphorylated by phosphorylase kinase. Eur J Biochem **107:**529-537.

189. **Cross DA, Alessi DR, Cohen P, Andjelkovich M, Hemmings BA.** 1995. Inhibition of glycogen synthase kinase-3 by insulin mediated by protein kinase B. Nature **378:**785-789.
190. **Nakae J, Kitamura T, Silver DL, Accili D.** 2001. The forkhead transcription factor Foxo1 (Fkhr) confers insulin sensitivity onto glucose-6-phosphatase expression. J Clin Invest **108:**1359-1367.
191. **Meshkani R, Adeli K.** 2009. Hepatic insulin resistance, metabolic syndrome and cardiovascular disease. Clin Biochem **42:**1331-1346.
192. **Lamming DW, Sabatini DM.** 2013. A Central role for mTOR in lipid homeostasis. Cell Metab **18:**465-469.
193. **Ferre P, Foufelle F.** 2007. SREBP-1c transcription factor and lipid homeostasis: clinical perspective. Horm Res **68:**72-82.
194. **Brown MS, Goldstein JL.** 2008. Selective versus total insulin resistance: a pathogenic paradox. Cell Metab **7:**95-96.
195. **Moon YA, Liang G, Xie X, Frank-Kamenetsky M, Fitzgerald K, Koteliansky V, Brown MS, Goldstein JL, Horton JD.** 2012. The Scap/SREBP pathway is essential for developing diabetic fatty liver and carbohydrate-induced hypertriglyceridemia in animals. Cell Metab **15:**240-246.
196. **Horton JD, Goldstein JL, Brown MS.** 2002. SREBPs: activators of the complete program of cholesterol and fatty acid synthesis in the liver. J Clin Invest **109:**1125-1131.
197. **Rolfe DF, Brown GC.** 1997. Cellular energy utilization and molecular origin of standard metabolic rate in mammals. Physiol Rev **77:**731-758.
198. **Shulman GI, Rothman DL, Jue T, Stein P, DeFronzo RA, Shulman RG.** 1990. Quantitation of muscle glycogen synthesis in normal subjects and subjects with non-insulin-dependent diabetes by 13C nuclear magnetic resonance spectroscopy. N Engl J Med **322:**223-228.
199. **Klip A, Paquet MR.** 1990. Glucose transport and glucose transporters in muscle and their metabolic regulation. Diabetes Care **13:**228-243.
200. **Ozawa E.** 2011. Regulation of phosphorylase kinase by low concentrations of Ca ions upon muscle contraction: the connection between metabolism and muscle contraction and the connection between muscle physiology and Ca-dependent signal transduction. Proc Jpn Acad Ser B Phys Biol Sci **87:**486-508.
201. **Wasserman DH, Kang L, Ayala JE, Fueger PT, Lee-Young RS.** 2011. The physiological regulation of glucose flux into muscle in vivo. J Exp Biol **214:**254-262.
202. **Leturque A, Loizeau M, Vaulont S, Salminen M, Girard J.** 1996. Improvement of insulin action in diabetic transgenic mice selectively overexpressing GLUT4 in skeletal muscle. Diabetes **45:**23-27.
203. **Tsao TS, Burcelin R, Katz EB, Huang L, Charron MJ.** 1996. Enhanced insulin action due to targeted GLUT4 overexpression exclusively in muscle. Diabetes **45:**28-36.

204. **Gulve EA, Ren JM, Marshall BA, Gao J, Hansen PA, Holloszy JO, Mueckler M.** 1994. Glucose transport activity in skeletal muscles from transgenic mice overexpressing GLUT1. Increased basal transport is associated with a defective response to diverse stimuli that activate GLUT4. J Biol Chem **269:**18366-18370.
205. **Kelley DE, Mandarino LJ.** 1990. Hyperglycemia normalizes insulin-stimulated skeletal muscle glucose oxidation and storage in noninsulin-dependent diabetes mellitus. J Clin Invest **86:**1999-2007.
206. **Frame S, Cohen P.** 2001. GSK3 takes centre stage more than 20 years after its discovery. Biochem J **359:**1-16.
207. **Eckardt K, Gorgens SW, Raschke S, Eckel J.** 2014. Myokines in insulin resistance and type 2 diabetes. Diabetologia **57:**1087-1099.
208. **Lin Z, Tian H, Lam KS, Lin S, Hoo RC, Konishi M, Itoh N, Wang Y, Bornstein SR, Xu A, Li X.** 2013. Adiponectin mediates the metabolic effects of FGF21 on glucose homeostasis and insulin sensitivity in mice. Cell Metab **17:**779-789.
209. **Bostrom P, Wu J, Jedrychowski MP, Korde A, Ye L, Lo JC, Rasbach KA, Bostrom EA, Choi JH, Long JZ, Kajimura S, Zingaretti MC, Vind BF, Tu H, Cinti S, Hojlund K, Gygi SP, Spiegelman BM.** 2012. A PGC1-alpha-dependent myokine that drives brown-fat-like development of white fat and thermogenesis. Nature **481:**463-468.
210. **Matthews VB, Astrom MB, Chan MH, Bruce CR, Krabbe KS, Prelovsek O, Akerstrom T, Yfanti C, Broholm C, Mortensen OH, Penkowa M, Hojman P, Zankari A, Watt MJ, Bruunsgaard H, Pedersen BK, Febbraio MA.** 2009. Brain-derived neurotrophic factor is produced by skeletal muscle cells in response to contraction and enhances fat oxidation via activation of AMP-activated protein kinase. Diabetologia **52:**1409-1418.
211. **Boden G.** 2008. Obesity and free fatty acids. Endocrinol Metab Clin North Am **37:**635-646, viii-ix.
212. **Tang X, Guilherme A, Chakladar A, Powelka AM, Konda S, Virbasius JV, Nicoloro SM, Straubhaar J, Czech MP.** 2006. An RNA interference-based screen identifies MAP4K4/NIK as a negative regulator of PPARgamma, adipogenesis, and insulin-responsive hexose transport. Proc Natl Acad Sci U S A **103:**2087-2092.
213. **Bruning JC, Michael MD, Winnay JN, Hayashi T, Horsch D, Accili D, Goodyear LJ, Kahn CR.** 1998. A muscle-specific insulin receptor knockout exhibits features of the metabolic syndrome of NIDDM without altering glucose tolerance. Mol Cell **2:**559-569.
214. **Xue Y, Wang X, Li Z, Gotoh N, Chapman D, Skolnik EY.** 2001. Mesodermal patterning defect in mice lacking the Ste20 NCK interacting kinase (NIK). Development **128:**1559-1572.
215. **Wright JH, Wang X, Manning G, LaMere BJ, Le P, Zhu S, Khatry D, Flanagan PM, Buckley SD, Whyte DB, Howlett AR, Bischoff JR, Lipson KE,**

Jallal B. 2003. The STE20 kinase HGK is broadly expressed in human tumor cells and can modulate cellular transformation, invasion, and adhesion. Mol Cell Biol **23:**2068-2082.
216. **Delpire E.** 2009. The mammalian family of sterile 20p-like protein kinases. Pflugers Arch **458:**953-967.
217. **Dan I, Watanabe NM, Kusumi A.** 2001. The Ste20 group kinases as regulators of MAP kinase cascades. Trends Cell Biol **11:**220-230.
218. **Strange K, Denton J, Nehrke K.** 2006. Ste20-type kinases: evolutionarily conserved regulators of ion transport and cell volume. Physiology (Bethesda) **21:**61-68.
219. **Kyriakis JM.** 1999. Signaling by the germinal center kinase family of protein kinases. J Biol Chem **274:**5259-5262.
220. **Puri V, Virbasius JV, Guilherme A, Czech MP.** 2008. RNAi screens reveal novel metabolic regulators: RIP140, MAP4k4 and the lipid droplet associated fat specific protein (FSP) 27. Acta Physiol (Oxf) **192:**103-115.
221. **Chapman JO, Li H, Lundquist EA.** 2008. The MIG-15 NIK kinase acts cell-autonomously in neuroblast polarization and migration in C. elegans. Dev Biol **324:**245-257.
222. **Poinat P, De Arcangelis A, Sookhareea S, Zhu X, Hedgecock EM, Labouesse M, Georges-Labouesse E.** 2002. A conserved interaction between beta1 integrin/PAT-3 and Nck-interacting kinase/MIG-15 that mediates commissural axon navigation in C. elegans. Curr Biol **12:**622-631.
223. **Cobreros-Reguera L, Fernandez-Minan A, Fernandez-Espartero CH, Lopez-Schier H, Gonzalez-Reyes A, Martin-Bermudo MD.** 2010. The Ste20 kinase misshapen is essential for the invasive behaviour of ovarian epithelial cells in Drosophila. EMBO Rep **11:**943-949.
224. **Houalla T, Hien Vuong D, Ruan W, Suter B, Rao Y.** 2005. The Ste20-like kinase misshapen functions together with Bicaudal-D and dynein in driving nuclear migration in the developing drosophila eye. Mech Dev **122:**97-108.
225. **Su YC, Maurel-Zaffran C, Treisman JE, Skolnik EY.** 2000. The Ste20 kinase misshapen regulates both photoreceptor axon targeting and dorsal closure, acting downstream of distinct signals. Mol Cell Biol **20:**4736-4744.
226. **Liang JJ, Wang H, Rashid A, Tan TH, Hwang RF, Hamilton SR, Abbruzzese JL, Evans DB, Wang H.** 2008. Expression of MAP4K4 is associated with worse prognosis in patients with stage II pancreatic ductal adenocarcinoma. Clin Cancer Res **14:**7043-7049.
227. **Qiu MH, Qian YM, Zhao XL, Wang SM, Feng XJ, Chen XF, Zhang SH.** 2012. Expression and prognostic significance of MAP4K4 in lung adenocarcinoma. Pathol Res Pract **208:**541-548.
228. **Rizzardi AE, Rosener NK, Koopmeiners JS, Isaksson Vogel R, Metzger GJ, Forster CL, Marston LO, Tiffany JR, McCarthy JB, Turley EA, Warlick CA, Henriksen JC, Schmechel SC.** 2014. Evaluation of protein biomarkers of prostate cancer aggressiveness. BMC Cancer **14:**244.

229. **LeClaire LL, Rana M, Baumgartner M, Barber DL.** 2015. The Nck-interacting kinase NIK increases Arp2/3 complex activity by phosphorylating the Arp2 subunit. J Cell Biol **208:**161-170.
230. **Yue J, Xie M, Gou X, Lee P, Schneider MD, Wu X.** 2014. Microtubules regulate focal adhesion dynamics through MAP4K4. Dev Cell **31:**572-585.
231. **Aouadi M, Tesz GJ, Nicoloro SM, Wang M, Chouinard M, Soto E, Ostroff GR, Czech MP.** 2009. Orally delivered siRNA targeting macrophage Map4k4 suppresses systemic inflammation. Nature **458:**1180-1184.
232. **Austin RL, Rune A, Bouzakri K, Zierath JR, Krook A.** 2008. siRNA-mediated reduction of inhibitor of nuclear factor-kappaB kinase prevents tumor necrosis factor-alpha-induced insulin resistance in human skeletal muscle. Diabetes **57:**2066-2073.
233. **Bouzakri K, Ribaux P, Halban PA.** 2009. Silencing mitogen-activated protein 4 kinase 4 (MAP4K4) protects beta cells from tumor necrosis factor-alpha-induced decrease of IRS-2 and inhibition of glucose-stimulated insulin secretion. J Biol Chem **284:**27892-27898.
234. **Wang M, Amano SU, Flach RJ, Chawla A, Aouadi M, Czech MP.** 2013. Identification of Map4k4 as a novel suppressor of skeletal muscle differentiation. Mol Cell Biol **33:**678-687.
235. **Chuang HC, Sheu WH, Lin YT, Tsai CY, Yang CY, Cheng YJ, Huang PY, Li JP, Chiu LL, Wang X, Xie M, Schneider MD, Tan TH.** 2014. HGK/MAP4K4 deficiency induces TRAF2 stabilization and Th17 differentiation leading to insulin resistance. Nat Commun **5:**4602.
236. **Danai LV, Guilherme A, Guntur KV, Straubhaar J, Nicoloro SM, Czech MP.** 2013. Map4k4 suppresses Srebp-1 and adipocyte lipogenesis independent of JNK signaling. J Lipid Res **54:**2697-2707.
237. **Diraison F, Dusserre E, Vidal H, Sothier M, Beylot M.** 2002. Increased hepatic lipogenesis but decreased expression of lipogenic gene in adipose tissue in human obesity. Am J Physiol Endocrinol Metab **282:**E46-51.
238. **Roberts R, Hodson L, Dennis AL, Neville MJ, Humphreys SM, Harnden KE, Micklem KJ, Frayn KN.** 2009. Markers of de novo lipogenesis in adipose tissue: associations with small adipocytes and insulin sensitivity in humans. Diabetologia **52:**882-890.
239. **Ranganathan G, Unal R, Pokrovskaya I, Yao-Borengasser A, Phanavanh B, Lecka-Czernik B, Rasouli N, Kern PA.** 2006. The lipogenic enzymes DGAT1, FAS, and LPL in adipose tissue: effects of obesity, insulin resistance, and TZD treatment. J Lipid Res **47:**2444-2450.
240. **Herman MA, Peroni OD, Villoria J, Schon MR, Abumrad NA, Bluher M, Klein S, Kahn BB.** 2012. A novel ChREBP isoform in adipose tissue regulates systemic glucose metabolism. Nature **484:**333-338.
241. **Hurtado del Pozo C, Vesperinas-Garcia G, Rubio MA, Corripio-Sanchez R, Torres-Garcia AJ, Obregon MJ, Calvo RM.** 2011. ChREBP expression in the

liver, adipose tissue and differentiated preadipocytes in human obesity. Biochim Biophys Acta **1811:**1194-1200.

242. **Richardson DK, Czech MP.** 1978. Primary role of decreased fatty acid synthesis in insulin resistance of large rat adipocytes. Am J Physiol **234:**E182-189.
243. **Czech MP, Richardson DK, Smith CJ.** 1977. Biochemical basis of fat cell insulin resistance in obese rodents and man. Metabolism **26:**1057-1078.
244. **Czech MP.** 1976. Cellular basis of insulin insensitivity in large rat adipocytes. J Clin Invest **57:**1523-1532.
245. **Im SS, Kwon SK, Kang SY, Kim TH, Kim HI, Hur MW, Kim KS, Ahn YH.** 2006. Regulation of GLUT4 gene expression by SREBP-1c in adipocytes. Biochem J **399:**131-139.
246. **Sato R, Okamoto A, Inoue J, Miyamoto W, Sakai Y, Emoto N, Shimano H, Maeda M.** 2000. Transcriptional regulation of the ATP citrate-lyase gene by sterol regulatory element-binding proteins. J Biol Chem **275:**12497-12502.
247. **Lopez JM, Bennett MK, Sanchez HB, Rosenfeld JM, Osborne TF.** 1996. Sterol regulation of acetyl coenzyme A carboxylase: a mechanism for coordinate control of cellular lipid. Proc Natl Acad Sci U S A **93:**1049-1053.
248. **Griffin MJ, Wong RH, Pandya N, Sul HS.** 2007. Direct interaction between USF and SREBP-1c mediates synergistic activation of the fatty-acid synthase promoter. J Biol Chem **282:**5453-5467.
249. **Boizard M, Le Liepvre X, Lemarchand P, Foufelle F, Ferre P, Dugail I.** 1998. Obesity-related overexpression of fatty-acid synthase gene in adipose tissue involves sterol regulatory element-binding protein transcription factors. J Biol Chem **273:**29164-29171.
250. **Mauvoisin D, Rocque G, Arfa O, Radenne A, Boissier P, Mounier C.** 2007. Role of the PI3-kinase/mTor pathway in the regulation of the stearoyl CoA desaturase (SCD1) gene expression by insulin in liver. J Cell Commun Signal **1:**113-125.
251. **Ericsson J, Jackson SM, Kim JB, Spiegelman BM, Edwards PA.** 1997. Identification of glycerol-3-phosphate acyltransferase as an adipocyte determination and differentiation factor 1- and sterol regulatory element-binding protein-responsive gene. J Biol Chem **272:**7298-7305.
252. **Kim JB, Spiegelman BM.** 1996. ADD1/SREBP1 promotes adipocyte differentiation and gene expression linked to fatty acid metabolism. Genes Dev **10:**1096-1107.
253. **Fajas L, Schoonjans K, Gelman L, Kim JB, Najib J, Martin G, Fruchart JC, Briggs M, Spiegelman BM, Auwerx J.** 1999. Regulation of peroxisome proliferator-activated receptor gamma expression by adipocyte differentiation and determination factor 1/sterol regulatory element binding protein 1: implications for adipocyte differentiation and metabolism. Mol Cell Biol **19:**5495-5503.

254. **Takashima M, Ogawa W, Emi A, Kasuga M.** 2009. Regulation of SREBP1c expression by mTOR signaling in hepatocytes. Kobe J Med Sci **55:**E45-52.
255. **Peterson TR, Sengupta SS, Harris TE, Carmack AE, Kang SA, Balderas E, Guertin DA, Madden KL, Carpenter AE, Finck BN, Sabatini DM.** 2011. mTOR complex 1 regulates lipin 1 localization to control the SREBP pathway. Cell **146:**408-420.
256. **Li S, Brown MS, Goldstein JL.** 2010. Bifurcation of insulin signaling pathway in rat liver: mTORC1 required for stimulation of lipogenesis, but not inhibition of gluconeogenesis. Proc Natl Acad Sci U S A **107:**3441-3446.
257. **Bakan I, Laplante M.** 2012. Connecting mTORC1 signaling to SREBP-1 activation. Curr Opin Lipidol **23:**226-234.
258. **Gwinn DM, Shackelford DB, Egan DF, Mihaylova MM, Mery A, Vasquez DS, Turk BE, Shaw RJ.** 2008. AMPK phosphorylation of raptor mediates a metabolic checkpoint. Mol Cell **30:**214-226.
259. **Li Y, Xu S, Mihaylova MM, Zheng B, Hou X, Jiang B, Park O, Luo Z, Lefai E, Shyy JY, Gao B, Wierzbicki M, Verbeuren TJ, Shaw RJ, Cohen RA, Zang M.** 2011. AMPK phosphorylates and inhibits SREBP activity to attenuate hepatic steatosis and atherosclerosis in diet-induced insulin-resistant mice. Cell Metab **13:**376-388.
260. **Shaw RJ.** 2009. LKB1 and AMP-activated protein kinase control of mTOR signalling and growth. Acta Physiol (Oxf) **196:**65-80.
261. **Guntur KV, Guilherme A, Xue L, Chawla A, Czech MP.** 2010. Map4k4 negatively regulates peroxisome proliferator-activated receptor (PPAR) gamma protein translation by suppressing the mammalian target of rapamycin (mTOR) signaling pathway in cultured adipocytes. J Biol Chem **285:**6595-6603.
262. **Kersten S.** 2002. Peroxisome proliferator activated receptors and obesity. Eur J Pharmacol **440:**223-234.
263. **Kim JE, Chen J.** 2004. regulation of peroxisome proliferator-activated receptor-gamma activity by mammalian target of rapamycin and amino acids in adipogenesis. Diabetes **53:**2748-2756.
264. **Houde VP, Brule S, Festuccia WT, Blanchard PG, Bellmann K, Deshaies Y, Marette A.** 2010. Chronic rapamycin treatment causes glucose intolerance and hyperlipidemia by upregulating hepatic gluconeogenesis and impairing lipid deposition in adipose tissue. Diabetes **59:**1338-1348.
265. **Chakrabarti P, English T, Shi J, Smas CM, Kandror KV.** 2010. Mammalian target of rapamycin complex 1 suppresses lipolysis, stimulates lipogenesis, and promotes fat storage. Diabetes **59:**775-781.
266. **Porstmann T, Santos CR, Lewis C, Griffiths B, Schulze A.** 2009. A new player in the orchestra of cell growth: SREBP activity is regulated by mTORC1 and contributes to the regulation of cell and organ size. Biochem Soc Trans **37:**278-283.

267. **Yao Z, Zhou G, Wang XS, Brown A, Diener K, Gan H, Tan TH.** 1999. A novel human STE20-related protein kinase, HGK, that specifically activates the c-Jun N-terminal kinase signaling pathway. J Biol Chem **274:**2118-2125.
268. **Su YC, Han J, Xu S, Cobb M, Skolnik EY.** 1997. NIK is a new Ste20-related kinase that binds NCK and MEKK1 and activates the SAPK/JNK cascade via a conserved regulatory domain. EMBO J **16:**1279-1290.
269. **Liu H, Su YC, Becker E, Treisman J, Skolnik EY.** 1999. A Drosophila TNF-receptor-associated factor (TRAF) binds the ste20 kinase Misshapen and activates Jun kinase. Curr Biol **9:**101-104.
270. **Cobb MH, Xu S, Hepler JE, Hutchison M, Frost J, Robbins DJ.** 1994. Regulation of the MAP kinase cascade. Cell Mol Biol Res **40:**253-256.
271. **Isakson P, Hammarstedt A, Gustafson B, Smith U.** 2009. Impaired preadipocyte differentiation in human abdominal obesity: role of Wnt, tumor necrosis factor-alpha, and inflammation. Diabetes **58:**1550-1557.
272. **Derijard B, Hibi M, Wu IH, Barrett T, Su B, Deng T, Karin M, Davis RJ.** 1994. JNK1: a protein kinase stimulated by UV light and Ha-Ras that binds and phosphorylates the c-Jun activation domain. Cell **76:**1025-1037.
273. **Sluss HK, Barrett T, Derijard B, Davis RJ.** 1994. Signal transduction by tumor necrosis factor mediated by JNK protein kinases. Mol Cell Biol **14:**8376-8384.
274. **Jiang ZY, Zhou QL, Coleman KA, Chouinard M, Boese Q, Czech MP.** 2003. Insulin signaling through Akt/protein kinase B analyzed by small interfering RNA-mediated gene silencing. Proc Natl Acad Sci U S A **100:**7569-7574.
275. **Schmittgen TD, Livak KJ.** 2008. Analyzing real-time PCR data by the comparative C(T) method. Nat Protoc **3:**1101-1108.
276. **Livak KJ, Schmittgen TD.** 2001. Analysis of relative gene expression data using real-time quantitative PCR and the 2(-Delta Delta C(T)) Method. Methods **25:**402-408.
277. **Rodbell M.** 1964. Metabolism of Isolated Fat Cells. I. Effects of Hormones on Glucose Metabolism and Lipolysis. J Biol Chem **239:**375-380.
278. **Dole VP.** 1956. A relation between non-esterified fatty acids in plasma and the metabolism of glucose. J Clin Invest **35:**150-154.
279. **Seki E, Brenner DA, Karin M.** 2012. A Liver Full of JNK: Signaling in Regulation of Cell Function and Disease Pathogenesis, and Clinical Approaches. Gastroenterology doi:S0016-5085(12)00820-7 [pii]
10.1053/j.gastro.2012.06.004.
280. **Brown NF, Stefanovic-Racic M, Sipula IJ, Perdomo G.** 2007. The mammalian target of rapamycin regulates lipid metabolism in primary cultures of rat hepatocytes. Metabolism **56:**1500-1507.
281. **Baumgartner M, Sillman AL, Blackwood EM, Srivastava J, Madson N, Schilling JW, Wright JH, Barber DL.** 2006. The Nck-interacting kinase phosphorylates ERM proteins for formation of lamellipodium by growth factors. Proc Natl Acad Sci U S A **103:**13391-13396.

282. **Xie M, Zhang D, Dyck JR, Li Y, Zhang H, Morishima M, Mann DL, Taffet GE, Baldini A, Khoury DS, Schneider MD.** 2006. A pivotal role for endogenous TGF-beta-activated kinase-1 in the LKB1/AMP-activated protein kinase energy-sensor pathway. Proc Natl Acad Sci U S A **103:**17378-17383.
283. **Yu XX, Murray SF, Watts L, Booten SL, Tokorcheck J, Monia BP, Bhanot S.** 2008. Reduction of JNK1 expression with antisense oligonucleotide improves adiposity in obese mice. Am J Physiol Endocrinol Metab **295:**E436-445.
284. **Chang Y, Wang J, Lu X, Thewke DP, Mason RJ.** 2005. KGF induces lipogenic genes through a PI3K and JNK/SREBP-1 pathway in H292 cells. J Lipid Res **46:**2624-2635.
285. **Ito M, Nagasawa M, Omae N, Tsunoda M, Ishiyama J, Ide T, Akasaka Y, Murakami K.** 2013. A novel JNK2/SREBP-1c pathway involved in insulin-induced fatty acid synthesis in human adipocytes. J Lipid Res **54:**1531-1540.
286. **Kotzka J, Knebel B, Haas J, Kremer L, Jacob S, Hartwig S, Nitzgen U, Muller-Wieland D.** 2012. Preventing phosphorylation of sterol regulatory element-binding protein 1a by MAP-kinases protects mice from fatty liver and visceral obesity. PLoS One **7:**e32609.
287. **Shimano H, Yahagi N, Amemiya-Kudo M, Hasty AH, Osuga J, Tamura Y, Shionoiri F, Iizuka Y, Ohashi K, Harada K, Gotoda T, Ishibashi S, Yamada N.** 1999. Sterol regulatory element-binding protein-1 as a key transcription factor for nutritional induction of lipogenic enzyme genes. J Biol Chem **274:**35832-35839.
288. **Shimano H, Shimomura I, Hammer RE, Herz J, Goldstein JL, Brown MS, Horton JD.** 1997. Elevated levels of SREBP-2 and cholesterol synthesis in livers of mice homozygous for a targeted disruption of the SREBP-1 gene. J Clin Invest **100:**2115-2124.
289. **Shimomura I, Hammer RE, Richardson JA, Ikemoto S, Bashmakov Y, Goldstein JL, Brown MS.** 1998. Insulin resistance and diabetes mellitus in transgenic mice expressing nuclear SREBP-1c in adipose tissue: model for congenital generalized lipodystrophy. Genes Dev **12:**3182-3194.
290. **Horton JD, Shimomura I, Ikemoto S, Bashmakov Y, Hammer RE.** 2003. Overexpression of sterol regulatory element-binding protein-1a in mouse adipose tissue produces adipocyte hypertrophy, increased fatty acid secretion, and fatty liver. J Biol Chem **278:**36652-36660.
291. **Kuriyama H, Liang G, Engelking LJ, Horton JD, Goldstein JL, Brown MS.** 2005. Compensatory increase in fatty acid synthesis in adipose tissue of mice with conditional deficiency of SCAP in liver. Cell Metab **1:**41-51.
292. **Boucher J, Kleinridders A, Kahn CR.** 2014. Insulin receptor signaling in normal and insulin-resistant states. Cold Spring Harb Perspect Biol **6**.
293. **Sartorius T, Staiger H, Ketterer C, Heni M, Machicao F, Guilherme A, Grallert H, Schulze MB, Boeing H, Stefan N, Fritsche A, Czech MP, Haring HU.** 2012. Association of common genetic variants in the MAP4K4 locus with prediabetic traits in humans. PLoS One **7:**e47647.

294. **Elbein SC, Das SK, Hallman DM, Hanis CL, Hasstedt SJ.** 2009. Genome-wide linkage and admixture mapping of type 2 diabetes in African American families from the American Diabetes Association GENNID (Genetics of NIDDM) Study Cohort. Diabetes **58:**268-274.
295. **Li Q, Li S, Mana-Capelli S, Roth Flach RJ, Danai LV, Amcheslavsky A, Nie Y, Kaneko S, Yao X, Chen X, Cotton JL, Mao J, McCollum D, Jiang J, Czech MP, Xu L, Ip YT.** 2014. The conserved misshapen-warts-yorkie pathway acts in enteroblasts to regulate intestinal stem cells in Drosophila. Dev Cell **31:**291-304.
296. **Berry MN, Friend DS.** 1969. High-yield preparation of isolated rat liver parenchymal cells: a biochemical and fine structural study. J Cell Biol **43:**506-520.
297. **Folch J LM, Sloane Stanley GH.** 1957. A simple method for the isolation and purification of total lipides from animal tissues The Journal of Biological Chemistry **226:**497-509.
298. **Roth Flach R, Matevossian A, Akie TE, Negrin KA, Paul MT, Czech MP.** 2013. b3-Adrenergic receptor stimulation induces E-selectin-mediated adipose tissue inflammation. The Journal of Biological Chemistry **288:**2882-2892.
299. **Farese RV, Jr., Zechner R, Newgard CB, Walther TC.** 2012. The problem of establishing relationships between hepatic steatosis and hepatic insulin resistance. Cell Metab **15:**570-573.
300. **Atit R, Sgaier SK, Mohamed OA, Taketo MM, Dufort D, Joyner AL, Niswander L, Conlon RA.** 2006. Beta-catenin activation is necessary and sufficient to specify the dorsal dermal fate in the mouse. Dev Biol **296:**164-176.
301. **Sanchez-Gurmaches J, Hung CM, Sparks CA, Tang Y, Li H, Guertin DA.** 2012. PTEN loss in the Myf5 lineage redistributes body fat and reveals subsets of white adipocytes that arise from Myf5 precursors. Cell Metab **16:**348-362.
302. **Seale P, Bjork B, Yang W, Kajimura S, Chin S, Kuang S, Scime A, Devarakonda S, Conroe HM, Erdjument-Bromage H, Tempst P, Rudnicki MA, Beier DR, Spiegelman BM.** 2008. PRDM16 controls a brown fat/skeletal muscle switch. Nature **454:**961-967.
303. **Sanchez-Gurmaches J, Guertin DA.** 2014. Adipocyte lineages: tracing back the origins of fat. Biochim Biophys Acta **1842:**340-351.
304. **Li LO, Grevengoed TJ, Paul DS, Ilkayeva O, Koves TR, Pascual F, Newgard CB, Muoio DM, Coleman RA.** 2014. Compartmentalized acyl-CoA metabolism in skeletal muscle regulates systemic glucose homeostasis. Diabetes doi:10.2337/db13-1070.
305. **Peterson JM, Seldin MM, Tan SY, Wong GW.** 2014. CTRP2 overexpression improves insulin and lipid tolerance in diet-induced obese mice. PLoS One **9:**e88535.

306. **Chakraborty A, Koldobskiy MA, Bello NT, Maxwell M, Potter JJ, Juluri KR, Maag D, Kim S, Huang AS, Dailey MJ, Saleh M, Snowman AM, Moran TH, Mezey E, Snyder SH.** 2010. Inositol pyrophosphates inhibit Akt signaling, thereby regulating insulin sensitivity and weight gain. Cell **143:**897-910.
307. **Gensch N, Borchardt T, Schneider A, Riethmacher D, Braun T.** 2008. Different autonomous myogenic cell populations revealed by ablation of Myf5-expressing cells during mouse embryogenesis. Development **135:**1597-1604.
308. **Tallquist MD, Weismann KE, Hellstrom M, Soriano P.** 2000. Early myotome specification regulates PDGFA expression and axial skeleton development. Development **127:**5059-5070.
309. **Waddell JN, Zhang P, Wen Y, Gupta SK, Yevtodiyenko A, Schmidt JV, Bidwell CA, Kumar A, Kuang S.** 2010. Dlk1 is necessary for proper skeletal muscle development and regeneration. PLoS One **5:**e15055.
310. **Kyriakis JM, Avruch J.** 2012. Mammalian MAPK signal transduction pathways activated by stress and inflammation: a 10-year update. Physiol Rev **92:**689-737.
311. **Ruderman NB, Carling D, Prentki M, Cacicedo JM.** 2013. AMPK, insulin resistance, and the metabolic syndrome. J Clin Invest **123:**2764-2772.
312. **Galic S, Sachithanandan N, Kay TW, Steinberg GR.** 2014. Suppressor of cytokine signalling (SOCS) proteins as guardians of inflammatory responses critical for regulating insulin sensitivity. Biochem J **461:**177-188.
313. **DeFronzo RA.** 2004. Pathogenesis of type 2 diabetes mellitus. Med Clin North Am **88:**787-835, ix.
314. **Pascoe J, Hollern D, Stamateris R, Abbasi M, Romano LC, Zou B, O'Donnell CP, Garcia-Ocana A, Alonso LC.** 2012. Free fatty acids block glucose-induced beta-cell proliferation in mice by inducing cell cycle inhibitors p16 and p18. Diabetes **61:**632-641.
315. **Block MB, Mako ME, Steiner DF, Rubenstein AH.** 1972. Circulating C-peptide immunoreactivity. Studies in normals and diabetic patients. Diabetes **21:**1013-1026.
316. **Yan W, Nehrke K, Choi J, Barber DL.** 2001. The Nck-interacting kinase (NIK) phosphorylates the Na+-H+ exchanger NHE1 and regulates NHE1 activation by platelet-derived growth factor. J Biol Chem **276:**31349-31356.
317. **Deisl C, Albano G, Fuster DG.** 2014. Role of Na/H exchange in insulin secretion by islet cells. Curr Opin Nephrol Hypertens **23:**406-410.
318. **Stiernet P, Nenquin M, Moulin P, Jonas JC, Henquin JC.** 2007. Glucose-induced cytosolic pH changes in beta-cells and insulin secretion are not causally related: studies in islets lacking the Na+/H+ exchangeR NHE1. J Biol Chem **282:**24538-24546.